NOTE TO USERS

Page(s) missing in number only; text follows. Page(s) were scanned as received.

97

This reproduction is the best copy available.

UMI®

DISSERTATION

THE DUAL ROLES OF DNA-PKcs, NBS1, AND TRF2 PROTEINS IN DNA REPAIR AND TELOMERE END-CAPPING

Submitted by

Eli Stowe Williams

Graduate Degree Program in Cell and Molecular Biology

In partial fulfillment of the requirements

For the Degree of Doctor of Philosophy

Colorado State University

Fort Collins, CO

Fall 2007

COLORADO STATE UNIVERSITY

July 30, 2007

WE HEREBY RECOMMEND THAT THE **DISSERTATION** PREPARED UNDER OUR SUPERVISION BY ***ELI STOWE WILLIAMS*** ENTITLED ***"THE DUAL ROLES OF DNA-PKCS, NBS1, AND TRF2 IN DNA REPAIR AND TELOMERE END-CAPPING"*** BE ACCEPTED AS FULFILLING IN PART REQUIREMENTS FOR THE DEGREE OF DOCTOR OF PHILOSOPHY.

Committee on Graduate Work

Susan M. Bailey, Ph.D.

Joel S. Bedford, D. Phil.

Michael N. Cornforth, Ph.D.

Rajinder S. Ranu, Ph.D., D.V.M.

Adviser: Robert L. Ullrich, Ph.D.

Department Head: Norman P. Curthoys, Ph.D.

ABSTRACT OF DISSERTATION

THE DUAL ROLES OF DNA-PKcs, NBS1, AND TRF2 PROTEINS IN DNA REPAIR AND TELOMERE END-CAPPING

Telomeres are the nucleoprotein structures located at the ends of linear chromosomes that distinguish naturally occurring chromosome ends from DNA double-strand breaks (DSBs). The ability to properly distinguish telomeres as such is critical to long term cellular survival as failure to do so can result in genomic instability and favor the progression towards cancer, cellular senescence or apoptosis. Cells unable to efficiently cap their chromosome ends are recognized cytogenetically as dicentric chromosomes which maintain telomere sequence at the point of fusion (telomere fusions). It has been shown that deficiencies in Telomere Repeat Binding Factor 2 (TRF2), a telomere binding protein, results in massive telomere dysfunction characterized by high numbers of telomere fusions, thus establishing TRF2 as an essential telomere end-capping protein. Surprisingly, TRF2 is rapidly and abundantly recruited to laser microbeam-induced damage, implicating this telomere protein in the early cellular response to DNA damage. We demonstrate that TRF2 is, in fact, not recruited to localized IR- or UV-induced DNA damage, arguing against a role for TRF2 in the DNA damage response, as well as illustrating important differences between damage produced by laser microbeams, as compared to other types of radiation.

An abundance of evidence, however, confirms significant overlap between DNA repair proteins and telomeres. Most strikingly, deficiencies of key proteins involved in the cellular response to DNA damage, particularly the catalytic subunit of the DNA dependent protein kinase (DNA-PKcs), also lead to the formation of telomere fusions, suggesting a role for these proteins in telomere end-capping. We show here that auto-phosphorylation of

DNA-PKcs is critical for its function at telomeres, as well as establish the utility of the BALB/c mouse in investigating the contribution of telomere dysfunction in driving genomic instability. NBS1, a homologous recombination (HR) protein critical in the cell's initial response to damage, has also been implicated in telomere end-capping. We demonstrate that cells depleted of NBS1 show an increase in telomere associations. Overall, this study helps to further clarify the complex interplay between DNA repair proteins and telomeres.

Eli Stowe Williams
Graduate Degree Program in Cell and Molecular Biology
Colorado State University
Fort Collins, CO 80523
Fall 2007

ACKNOWLEDGEMENTS

There are many people to whom I am indebted for their assistance, guidance, encouragement and patience throughout my graduate career. The following is certainly not an exhaustive list, and there are many who have contributed, in one way or another, to the last five years of my life who are not listed here. Ideally, I could list everyone who has made my graduate study a success, but various factors, primarily my memory, prevent this from happening.

I would like to thank:

My advisor, Dr. Bob Ullrich, for providing me with wonderful opportunities and putting me in a position to succeed

Dr. Susan Bailey for her infectious love of telomeres and whose open door policy I often abused

The rest of my academic committee, Dr. Joel Bedford, Dr. Michael Cornforth, and Dr. Rajinder Ranu, for their guidance and helpful suggestions along the way

My collaborators and ambassadors to the Netherlands, Dr. Jacob Aten, whose excitement for science and life invigorated my interest in science, and Jan Stap, with whom I went on several wandering cycling trips trough Dutch countryside and whose attention to detail was second to none

Drs. Howard Liber, Ying Zhang, and Ming Zhang for fruitful collaborations

Drs. Brian Ponnaiya and Charles Geard for their invaluable assistance and insights to the Columbia charged particle microbeam

Chrissy Battaglia for knowing how to keep a large lab in shape and being a wonderful friend to my wife.

Dr. Andy Ray for providing structure and guidance in the lab, especially as I was starting out

Tanner Hagelstrom and Steve Keyser for discussions du jour, most of them science related

Dr. Mike Fox for his enthusiasm for teaching

Beka for isolating and growing the mammary epithelial cells

Dr. Scott Pearson for making sure I had the most recent papers

Matt Callan for assistance with Westerns and LabBall

All the members of the Ullrich/Bailey lab; I think it is rare to find such a large group of people working together with such little drama

Paul Kim, Kristin Askin, Kristi McClellan, and the rest of the gang for late night study sessions in the early years

Dr. Taka Kato for being at school almost every time I was, no matter what

Norma Bulera for making me feel at home as soon as I arrived in Fort Collins

The ERHS administrative staff, particularly Julie Asmus and Mary Pridgen, whose attention to detail prevented many oversights on my part

Lori Williams for making sure that all the deadlines and logistics for my graduation were meet and completed

Dr. Hatsumi Nagasaki, who cytogenetic expertise was invaluable and for letting us know when the liquid nitrogen freezer was "crying"

David Maranon whose willingness for scientific discussion and collaboration was refreshing

Dr. Paul Wilson for getting me started on the 4th floor fluorescent scope

Dr. John Zimbrick for his advice and accessibility

Mrs. Willard, my high school science teacher, whose microbiology class gave me the first taste of how cool laboratory science could be

Kathryn Stowe, for providing me with the tools I needed to make this a reality

My parents for their love and support

My wife, Anna, for everything she is and does

TABLE OF CONTENTS

LIST OF TABLES

LIST OF FIGURES

I. BACKGROUND

The notion of a structure that caps the ends of linear chromosomes was first proposed in the 1930s by the Drosophila geneticist Hermann J. Muller. He postulated that the "terminal gene must have a special function, that of sealing the end of the chromosome," and termed these structures telomeres, literally "end part" [1]. Experiments in maize by Barbara McClintock at about the same time showed that X-ray mutagenized maize chromosomes formed ring chromosomes through the fusing of the ends of a single chromosome [3]. These observations supported Muller's theory of a structure designed to prevent chromosome ends from fusing together and leading to gross chromosomal aberrations. The end-capping function of telomeres is now known to include a number of DNA repair proteins, a somewhat surprising observation given the importance of distinguishing telomeres from DNA damage. While understanding chromosome end-capping is fundamental to understanding the nature of telomeres, it is still not well understood.

Telomeres have garnered particular attention of late due to their profound involvement in cellular transformation and carcinogenesis. Telomeres have been shown to provide a measuring stick of cellular aging, as they shorten with successive replications. Overcoming this perpetual shortening confers immortality to the cell, and thus pushes the cell towards transformation. Indeed, telomere length maintenance has been designated a hallmark of cancer [5]. This crucial role in cellular proliferation, coupled with telomere's earliest identified function of preventing chromosome end-to-end fusions thereby preserving genomic integrity, demonstrate the need to elucidate the precise manner in which telomeres function, the proteins critical for this function, and the pathways by which telomere dysfunction can lead to cellular transformation.

Telomeres are complex, dynamic structures that interact with a large and diverse complement of proteins including those involved in DNA repair, DNA replication and gene silencing. This study examines the dual nature of two known DNA repair proteins, the catalytic subunit of the DNA-dependent protein kinase (DNA-PKcs) and Nijmegen Breakage Syndrome 1 (NBS1), in DNA repair and telomere end-capping. Further, we examine the possible role for telomere repeat binding factor 2 (TRF2) in the early response to DNA damage.

TELOMERES

In the vast majority of eukaryotic organisms telomeric DNA consists of tandem arrays of repetitive G-rich sequence. Human telomeres are characterized by 3 to 15 kilobases (kb) of TTAGGG hexamer oriented 5' to 3' towards the end of the chromosome, ending in a G-rich 3' single-stranded overhang [6-9]. The G-rich overhang is a common feature of telomeres in many species and evidence suggests it plays an important role in distinguishing telomeres as natural chromosomal termini [10]. The unique position of telomeres at the beginning and end of every linear chromosome poses several unique problems to the cell, including telomere replication and telomere recognition.

Semi-conservative DNA replication utilizes a DNA polymerase that is able to replicate only in a 5' to 3' direction necessitating the use of multiple RNA primers for synthesis of the lagging strand [11,12]. However, no primer can be placed at the very end of the chromosome, resulting in the inability to replicate the most terminal DNA sequences and the continual shortening of the daughter telomere with each round of replication

(**Figure 1.1**). This phenomenon, known as the "end-replication problem" [13,14], provides the cell with a "mitotic clock" or counting mechanism for cellular age and induces replicative senescence when a critically short length is reached [15].

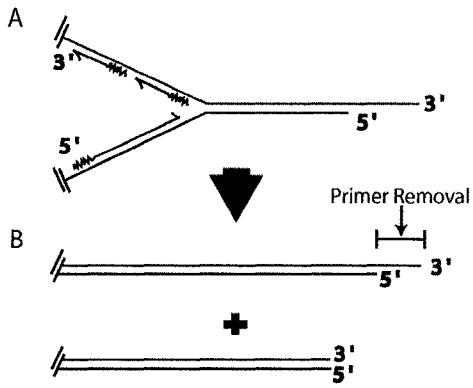

Figure 1.1: The End-Replication Problem. (A) Replication fork moving towards the DNA terminus. (B) Replication products. Removal of the Okazaki fragment (represented by a zigzag line) from the lagging strand generates a 3' overhang (upper product). Leading-strand synthesis generates a blunt end (lower product) that may be further processed to generate a 3' single-strand overhang.

The rate of telomere shortening has been estimated in human cells to range from 50 to 200 basepairs (bp) per cell division. This variation is due to placement of the terminal RNA primer, as well as the degree of end-processing following replication. Telomeric end-processing generates the G-rich overhang, a single-stranded tail extending fifty to several hundred nucleotides from the end of the duplex telomeric DNA [8,16,17]. Telomeres formed by lagging-strand synthesis naturally possess this overhang as a result of the footprint left by the removal of the terminal RNA primer. Leading strand telomeres are presumed to be blunt-ended *in vivo,* as they have shown to be *in vitro,* and therefore must be processed to form the G-rich overhang [18,19]. The extent of telomeric end-processing in human cells, as well as the nucleases and helicases responsible for this processing, has been the subject of much research and some debate.

Makarov et al. [8] estimated that more than 80% of telomeres possess long (processed) G-rich overhangs, whereas Wright et al. [20] observed that only half of the telomeres had long G-rich overhangs. Recent evidence from the Wright [21] lab indicates

that leading and lagging strand telomeres do possess different G-overhang lengths with longer overhangs at lagging strands, lending credence to their earlier observations, as well as suggesting a difference in processing of leading and lagging strand telomeres. The Mre11/Rad50/NBS1 (MRN) complex is a prime candidate for telomeric processing, as it possesses nuclease activity and is present at telomeres during or immediately following replication [22]. Furthermore, RNA interference (RNAi) knockdown of either Mre11 or NBS1 results in significantly shorter G-rich overhangs [23]. However, G-rich overhang length returns in time despite persistent knockdown of Mre11 suggesting that other proteins can compensate for its action in G-rich overhang processing.

The G-rich overhang is critical for properly distinguishing telomeres from DNA double-strand breaks (DSBs). Masking telomeres from improper DNA repair is a vital function in long term cellular survival as failure to do so can result in genomic instability, favoring the progression towards cancer, or cellular senescence and apoptosis. Evidence from electron microscopy studies suggest that telomeres may remodel into higher order structures known as telomere loops (t-loops) and G-quadruplexes, and the presence of G-rich overhangs is obligatory for both structures [4,24]. This reconfiguration also depends on a large and varied complement of proteins, the core of which is a six protein complex originally termed the telosome [25], more recently renamed named "shelterin" [26].

The Shelterin Complex

Shelterin is composed of a six protein complex that is responsible for regulating essential telomere processes such as replication, length regulation, and end-capping [26]. These proteins orchestrate the assembly of themselves and other telomere accessory proteins

onto telomeres, in order to efficiently perform these processes. Three shelterin proteins, Telomere Repeat binding Factors 1 and 2 (TRF1 and 2) [27,28] and Protection of Telomeres 1 (POT1) [29-31], bind directly to telomeric DNA with high specificity. The remaining three proteins, TRF1 Interacting Nuclear protein 2 (TIN2) [32], TPP1 (formerly named TINT1/PTOP/ PIP1) [33-35] and repressor activator protein (Rap1) [36], interact with TRF1, TRF2 and/or POT1 to complete the shelterin complex.

The proteins TRF1 and TRF2 are able to specifically bind duplex telomeric DNA via a protein domain known as the "telobox" [37] present on both proteins. The telobox of TRF1 and TRF2 share approximately 58% homology [27,37]; not surprisingly, TRF1 and TRF2 bind the same consensus sequence of TAGGGTT [38]. Both proteins also contain a central dimerization domain, though hetero-dimerization of TRF1 and TRF2 does not occur [27,39]. Pre-formed TRF1 and TRF2 homodimers are the functional units of each protein and constitute the vast majority of protein found in the cell [27,40,41]. Despite these similarities, these two proteins have evolved distinct functions at the telomeres, and this distinction is partly attributed to the divergence of their N-terminal region. TRF1 contains an acidic N-terminal domain and is primarily known for its role in telomerase-dependent telomere length regulation [42-45]. TRF2 is associated with telomeric end-capping [46]. The N-terminus of TRF2 is basic and has recently been suggested to participate in its essential role in the formation of the t-loop [47], a structure discussed in the next section. Both proteins are negative regulators of telomere length as over-expression results in telomere shortening [44,48].

POT1 has the unique ability to bind single-stranded G-rich telomeric DNA with high specificity, thus localizing POT1 to the G-rich overhang [29,30,49]. Accordingly,

POT1 plays important roles in both telomerase accessibility and end-capping [31,50]. POT1 forms a complex with another shelterin component, TPP1, which regulates the recruitment of POT1 to telomeric ends [34]. Together, these two proteins share a high degree of homology with the only known protozoan telomere end-binding proteins, TEBP-α and TEBP-β [51,52]. This high degree of evolutionary conservation has provided important clues to their function at telomeres, particularly in telomerase regulation, as will be discussed later.

The functions of the two remaining proteins of the shelterin complex are less clear. TIN2 associates with telomeres by virtue of its interactions with TRF1 and TRF2 [32,53]. It is believed that TIN2 exerts regulatory effects on TRF1 by promoting conformational changes of TRF1 [54]. It may also help stabilize TRF2 binding at telomeres by tethering TRF1 and TRF2 complexes [53,55]. Finally, TIN2 can recruit and secure the POT1/TPP1 complex to telomeres and has been proposed to play a role in shifting POT1/TPP1 from the G-overhang to duplex telomeric DNA, thereby allowing telomerase accessibility [34,35]. Human Rap1 (hRap1) has not been extensively studied, but it is known to interact specifically with TRF2, and like TRF2, is a negative regulator of telomere length [56].

The shelterin complex dictates the form and function of telomeres through the direct actions of its individual components and through the recruitment of accessory telomere proteins. The precise manner in which these proteins interact is an area of active investigation; the current studies will provide important clues into the mechanism of telomere replication, telomere end-capping, and telomere length maintenance.

Telomere End-Capping: T-loops & G-quadruplexes

A principle function of the shelterin complex, particularly TRF2, is to provide a mechanism by which the cellular end-processing machinery can distinguish telomeres from DNA DSBs. Cells deprived of TRF2—either by expression of a dominant-negative form of the protein or by generating conditional mutants—results in massive telomere dysfunction [46,57]. This dysfunction is easily recognizable cytogenetically as chromosome end-to-end fusions maintaining telomere sequence at the point of fusion (telomere fusions). The presence of telomeric DNA at the point of fusion is important, as it indicates these fusions events are not a result of critical telomere shortening, but instead represent failure to form a functional telomere end-cap. Telomeric end-capping must occur following each round of replication, as any end-capping structure must be resolved to allow the passage of the replication fork. Interestingly, it has been proposed that telomeres must induce a DNA damage signal following replication in order protect themselves from subsequent processing [58]. Several DNA repair, replication, and recombination proteins have been implicated in telomere end-capping, including DNA-PKcs and the Ku heterodimer [59-62], Rad51D [63], the MRN complex [22,58,64] and the RecQ helicases, WRN and BLM [65-67]. Whether these proteins function at telomeres as they do in their repair or recombination roles is not known. Two models for telomere end-capping, t-loops and G-quadruplexes, have been proposed, both supported by experimental evidence [4]. The contributions of each model *in vivo*, particularly at mammalian telomeres, remains to be clearly delineated.

Experimental evidence for the existence of t-loops in mammalian cells was first provided by electron microscopy studies of linear telomeric DNA incubated with TRF2 [4]. The linear DNA was found to form large lasso-like structures in 38% of the substrates, and

this looping was dependent on the presence of TRF2, but not TRF1 (**Figure 1.2**). The presence of the G-rich overhang was also an absolute requirement for loop formation. These observations prompted the authors to propose that the telomere was restructured by TRF2 so that the G-rich overhang loops back, invading the duplex telomeric DNA and forming a stable, short single-stranded Displacement Loop (D-loop).

The similarities between the proposed t-loop structure and Holliday junctions, a homologous recombination intermediate, leads to speculation about the requirements for the RAD51 family of proteins for t-loop formation. Indeed the RAD51 paralog, RAD51D, has been shown to be essential for telomere end-capping. Cells deficient in RAD51D show an increased incidence of telomere fusions and telomere loss compared to wild-type cells [63]. Recent evidence has suggested a direct role for TRF2 in the formation of the t-loop, showing that TRF2 can positively supercoil DNA around itself *in vitro*, unwinding neighboring DNA and thereby promoting strand-invasion [47]. Other *in vitro* tests have supported the t-loop model (reviewed in [26]) making it an attractive candidate for telomere

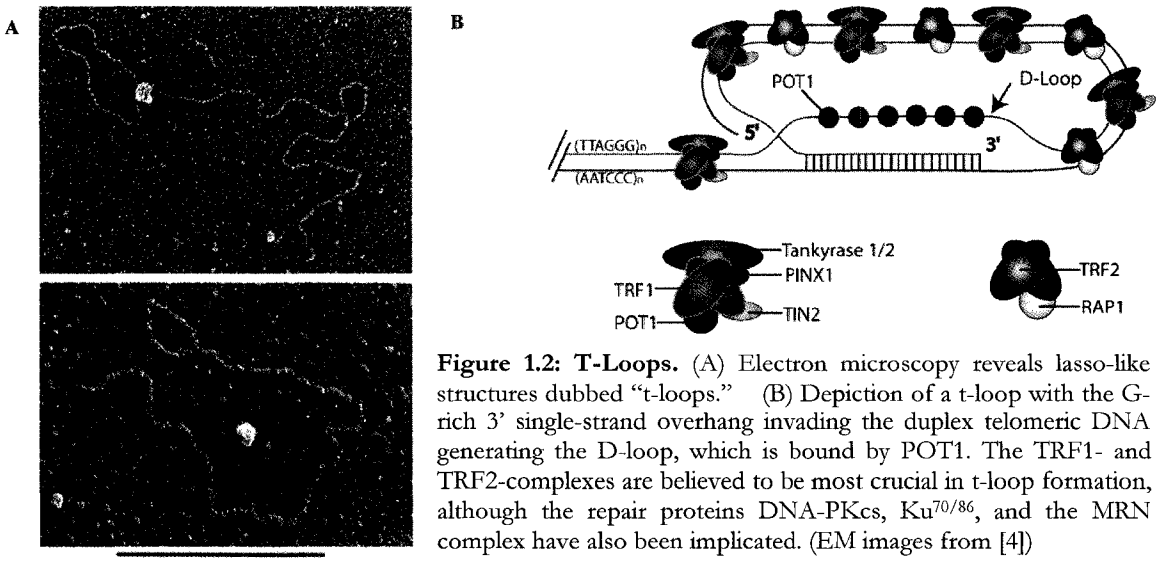

Figure 1.2: T-Loops. (A) Electron microscopy reveals lasso-like structures dubbed "t-loops." (B) Depiction of a t-loop with the G-rich 3' single-strand overhang invading the duplex telomeric DNA generating the D-loop, which is bound by POT1. The TRF1- and TRF2-complexes are believed to be most crucial in t-loop formation, although the repair proteins DNA-PKcs, $Ku^{70/86}$, and the MRN complex have also been implicated. (EM images from [4])

end-capping. It accounts for the abundance of the DNA recombination and repair proteins found at telomeres; however, it is a seemingly complex mechanism. The complexity of this restructuring raises questions as to how frequent t-loops are formed *in vivo*, especially given the ease of G-quadruplex formation under physiological conditions.

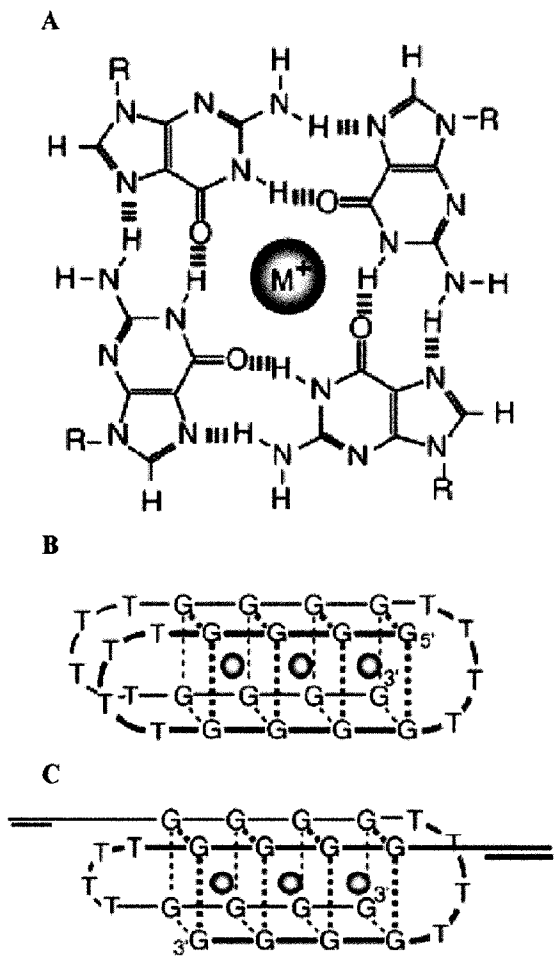

Figure 1.3: Structures formed by G-rich DNA. (A) The G-quartet is a square, planar arrangement of four guanine bases that each donates and accepts two hydrogen bonds. Vertical stacking of G-quartets in the presence of monovalent ions leads to the formation of G-quadruplexes in (B) a single telomere or (C) a stable complex of two (or more) telomeres [2].

The nearly universal presence of the G-rich overhang along with the aforementioned ease of formation of G-G base pairing, a requirement of G-quadruplex formation, has made G-quadruplexes a viable *in vivo* model. Short G-rich oligonucleotides can fold into a compact arrangement of square planar arrays of four hydrogen-bonded guanines (G-quartets, **Figure 1.3A**) [24,68]. The formation of G-quadruplexes occurs when the G-quartets are vertically stacked in the presence of a monovalent ion (**Figure 1.3B,C**) [24,68]. Most work in this field has been done in the ciliated protozoa stichotrichous, whose macronuclei contain millions of gene-sized chromosomes, complete with telomeres, providing an abundance of telomeric DNA and telomere-associated proteins [69]. The

G-rich overhangs of ciliate telomeres can form the four-stranded G-quadruplexes by virtue of interaction of one, two, or four telomeres, thus enabling end-capping of multiple telomeres with one structure (reviewed in [70]). Support for this hypothesis comes from the generation of an antibody against G-quadruplex DNA. This antibody reacts specifically with the macronuclei of ciliate nuclei, lending credence to the hypothesis that G-quadruplexes form at telomeres *in vivo* [71].

The relative simplicity of telomeric G-quadruplex formation, coupled with evidence of their existence *in vivo,* reinforces this structure as a viable option in end-capping. However, this model doesn't account for the ever increasing number of DNA repair, recombination, and replication proteins found at the telomere. On the contrary, the t-loop can neatly fit the presence of these proteins into a working model which has withstood numerous *in vitro* challenges; however it has yet to be directly shown that t-loops exist *in vivo.* Likely, telomere end-capping uses a combination of both of these models, and perhaps other as-yet unidentified mechanisms, to effectively distinguish telomeres from DNA DSBs.

Telomere Length Maintenance

Telomere length has been closely linked to cellular survival, as those cells with extremely short telomeres, resulting from either the chronic effects of the end-replication problem or from stochastic telomere loss, trigger senescence [72]. Cells able to maintain sufficient telomere length through a telomere length maintenance mechanism, such as activation of telomerase, are effectively rendered immortal and have a practically infinite replicative potential. Not surprisingly, telomere length maintenance is a hallmark of tumorigenesis, and telomerase is positively expressed in over 90% of human cancers [73]. The remainders of cancers are thought to employ Alternate Lengthening of Telomeres

(ALT) mechanisms, which is based on recombination between telomeric sequences (discussed below).

Telomerase is a specialized DNA polymerase consisting of an RNA template (TERC) and a catalytic subunit (TERT) that is able to synthesize and elongate telomeres [43,74-76]. Expression of TERC is independent of telomerase activity and is highly expressed in all tissue types [77], whereas the expression of TERT is minimal in most cell types, with human somatic cells estimated to contain less than five copies [78]. Telomerase activity in normal human somatic cells is restricted to developmental stages after which telomerase is down-regulated in most tissues; notable exceptions include male germ line cells, activated lymphocytes and certain stem cell populations [73,79,80]. The tight regulation of TERT in normal somatic cells, and its up-regulation during immortalization and carcinogenesis, indicate the catalytic subunit as the primary determinant in regulating telomerase activity [73,79,81].

The shelterin complex plays a critical role in telomerase-dependent telomere extension. Telomeres exist in two proposed states in the cell: a non-extendable state in which telomeres are protected from the action of telomerase regardless of TERT expression and activity and an extendible state [82]. Evidence strongly suggests that the arrangement of the shelterin complex, most notably POT1 and TPP1, determines the ability of telomerase to access the end [51,52]. It has been known for some time that shelterin components can inhibit the access of telomerase to DNA ends through the formation of the t-loop or through direct contact with telomerase. For instance, TRF1 controls the action of telomerase at each telomere by inhibiting telomerase access in *cis*- [45]. POT1 can also directly inhibit telomerase accessibility to the telomere. *In vitro* studies show that when

POT1 is bound to the telomere 3' overhang, telomerase binding and telomere extension is prohibited [51], thus providing multiple modes of shelterin-dependent telomerase-inhibition.

Reciprocally, recent evidence has strengthened the notion that shelterin can promote telomerase activity. TPP1 has now been shown to be the first shelterin protein to interact with telomerase and stimulate telomerase's enzymatic activity and processivity [51,52]. TPP1 does not bind DNA directly, rather it is tethered to telomeric DNA through association with POT1 [51,52]. An appealing model for POT1/TPP1 control of telomerase is that binding of POT1/TPP1 to the 3' single strand overhang prohibits telomerase access. Here, if POT1/TPP1 shifts slightly upstream to bind the duplex telomere tract through interactions with TIN2, telomerase would be able to access and extend telomeres. The manner in which this transition takes place, as well as the true molecular nature of the non-extendable and extendable telomere states, has yet to be determined.

The ALT pathway of telomere length maintenance occurs much less frequently than telomerase activation, and it is only activated in cancer cells or immortalized cell lines [83-85]. Approximately 10% of human cancers use ALT for telomere maintenance, though some cancers are especially enriched for ALT [73]. Human osteosarcomas, for example, display ALT in over 60% of cases and ALT-positive osteosarcomas display a more favorable clinical prognosis than telomerase positive osteosarcomas [86,87].

The presence of significant telomere length heterogeneity and ALT-specific nuclear bodies facilitate the identification of ALT-positive cells. Telomere lengths in ALT cells can range from less than 3 kb to over 50 kb, and the onset of this phenotype corresponds well with the activation of ALT [83,84,88,89]. ALT-positive cells also display ALT-associated PML bodies (APBs) which are subnuclear structures containing the promyelocytic leukemia

(PML) protein, telomeric DNA, the core telomeric proteins TRF1 and TRF2, as well as proteins involved in DNA recombination and replication [89]. The HR proteins RAD51, RAD52, MRE11, RAD50, NBS1, as well as the RecQ helicases BLM and WRN are present in APBs [22,89-91]. The suggestion of a recombination-based telomere length mechanism was proposed over a decade ago by John Murnane and colleagues [88] and the two characteristic phenotypes of ALT—heterogenous telomere lengths and APBs—support this hypothesis, though the precise mechanism has yet to be elucidated.

DNA Damage Response and Repair

The cell must constantly monitor the integrity of its DNA and repair any lesions that arise, as DNA damage occurs continuously from a variety of endogenous processes or exogenous agents. Most notably, ionizing radiation (IR) is known to produce a particularly deleterious type of DNA damage, the DNA DSB. There are many consequences of DSBs, depending on whether or not they are repaired and how accurately they are repaired. Two primary pathways are employed by the cell to cope with DNA DSBs, non-homologous end-joining (NHEJ) and homologous recombination (HR). NHEJ is believed to operate throughout the cell cycle and serves as the primary pathway employed by mammalian cells to repair IR-induced DNA DSBs [92]. Cells deficient in HR proteins show defects primarily in S/G2, consistent with the idea that HR occurs primarily between sequences of sister chromatids [92].

Small deletions at the point of ligation have been reported following NHEJ [93], promoting the belief that NHEJ is an error-prone process. However, NHEJ allows cells to

quickly re-enter the cell cycle, as essentially all damage is removed within six hours with the majority of breaks repaired within 30 minutes [94]. In genomes such as that of humans, which possess a high percentage of non-coding DNA sequence, these types of small deletions can be tolerated with no ill effects. Nevertheless, NHEJ can mis-join broken ends from two chromosomes resulting in aberrations such as dicentric chromosomes or chromosome translocations. These rearrangements can be quite harmful to the cell and can promote further mutations or lead to apoptosis [95]. HR repairs DNA DSBs with high fidelity by using a homologous template, although adverse cellular effects, such as loss of heterozygosity (LOH) may also occur.

The principle proteins involved in each of these pathways have been identified, yet precisely how these proteins interact to effectively repair DSBs remains unclear. The ataxia telangiectasia mutated (ATM) kinase is known to be an apical kinase in the cellular response to exogenous DNA damage. ATM initiates a signaling cascade that activates DNA repair pathways and cell cycle checkpoint pathways. Key cell cycle regulators, such as p53 and Chk2, are phosphorylated by ATM, leading to cell cycle arrest following DNA damage [96-98]. The MRN complex has been shown to be a key mediator of ATM phosphorylation facilitating ATM binding to downstream targets [99,100]. The MRN complex localizes to the sites of damage through a direct interaction with another ATM target, the histone variant H2AX [101,102].

The phosphorylated form of H2AX, γ-H2AX, is detectable extremely rapidly following exposure to ionizing radiation (IR), and is among the first proteins to be detectable at a break site. The recruitment and retention of 53BP1, mediator of damage checkpoint protein 1 (MDC1), breast cancer protein 1 (BRCA1), and the aforementioned MRN

complex are dependent on interactions with γ-H2AX [101,103-105]. Though γ-H2AX is not strictly required for DNA repair, γ-H2AX deficient cells are sensitive to IR [104,106]. The robustness of H2AX phosphorylation, which encompass between 500 to 1000 kilobases of DNA surrounding the break [107,108], has made immunofluorescent staining an attractive marker for detecting and locating DNA DSBs. However, care must be taken when interpreting results, as all γ-H2AX foci are not created equal. While it is generally agreed that 1 Gy of IR produces 30 to 40 DSBs, different qualities of radiation have been shown to generate different size γ-H2AX foci appearing with different kinetics [109]. Other agents can also contribute to foci formation, including DNA replication processes, ultraviolet (UV) exposure, or even on-going genomic instability [110-112].

Some proteins are recruited to DNA DSBs due to their affinity for free DNA ends. Thus, a large complement of proteins is present at damage sites via direct protein-DNA interactions, as well as through protein-protein interaction as described above. It has still not been directly shown how the cell decides whether to use NHEJ or HR in the repair of DSBs. Certainly competition for free DNA ends plays a part in this decision making process, as does the presence/absence of a homologous template. The MRN complex has been shown to be involved in early processing of DNA to produce a repairable DNA end [100]. HR is mediated primarily by the Rad51 paralogs, and by Rad54. These proteins search for homologous regions of DNA and promote strand invasion (reviewed in [113]). NHEJ is initiated by the binding of the Ku heterodimer to duplex DNA, and the subsequent recruitment of DNA-PKcs [114,115] . The necessity of DNA-PKcs in NHEJ and the importance of DNA-PKcs in telomere function warrant a brief overview of the current model of this DNA DSB repair pathway.

Non-Homologous End Joining

NHEJ is the predominant pathway employed to repair DNA DSBs and functions by recognizing, processing, and fusing any two broken DNA duplexes. The Ku70/Ku80 heterodimer, a component of the essential end-joining protein DNA-PK, binds duplex DNA rapidly and with high affinity, thereby initiating NHEJ [114,115]. The binding of DNA by the Ku heterodimer also facilitates the recruitment and activation of the catalytic subunit of DNA-PK, DNA-PKcs [114]. Both the kinase activity and the physical presence of DNA-PKcs have been shown to be important in NHEJ [116]. DNA-PKcs phosphorylates numerous proteins involved in NHEJ including the Ku heterodimer, X-ray complementing Chinese hamster 4 (XRCC4), and Artemis [117-119]. Perhaps the most important target of DNA-PKcs is itself. DNA-PKcs possesses two clusters of auto-phosphorylation sites whose phosphorylation has been shown to alter the accessibility of end processing proteins, most likely through a conformational change in DNA-PKcs [120-122].

The physical presence of DNA-PKcs at break ends is required for the recruitment of XRCC4 and DNA Ligase IV, likely a result of direct protein-protein interaction [123]. Two groups have recently identified a new partner in the XRCC4/Ligase IV complex, named Cernunnos or XRCC4-like factor (XLF) [124,125]. Cells deficient of Cernunnos/XLF show phenotypes characteristic of NHEJ defects such as increased radiosensitivity, as well as defective V(D)J recombination and DNA-end joining [124,125]. Cernunnos/XLF has also been shown to promote ligation in the absence of processing factors [126]. Processing of broken ends has been proposed to involve several different nucleases including Artemis and MRE11 [127-129]. It remains to be seen whether Artemis and MRE11 are responsible for

the resolution of a specific subset of damage, or if another mechanism is responsible for determining nuclease activity at the break site. Artemis has been implicated specifically in the resolution of complex end-structures, such as hairpins, lending credence to the idea that different nucleases may be specific for different damage structures. DNA Ligase IV is necessary for the pathway's final step, re-establishing the phosphodiester linkages of the two broken DNA ends [130].

Like many early events of the DNA damage response and repair pathways, NHEJ specifics as to protein loading and activation remain to be discovered. A clearer understanding of the role of DNA-PK will provide many clues to the series of steps necessary to rapidly re-join broken chromosome ends. The identification of required targets for *in vivo* DNA-PKcs phosphorylation, including auto-phosphorylation, has proven useful in our understanding of how end accessibility is regulated. Several NHEJ proteins localize to telomeres and play roles in telomere metabolism, including DNA-PK and Artmeis. The interactions between NHEJ and telomeres will also be vital in revealing the way in which DNA ends are distinguished and processed to maintain genomic integrity.

TRF2

de Lange's work in the early 1990's lead to the identification of a vertebrate telomere binding protein, named telomere repeat binding factor (TRF, later TRF1), which bound specifically to human chromosome ends [131]. The ability of TRF1 to bind specifically to duplex telomeric repeats through a specialized Myb-type DNA binding domain, named the "telobox," prompted the search for other telobox-associated proteins. Indeed, work out of

two labs independently confirmed the presence of a second telobox containing protein, appropriately dubbed TRF2 [27,37]. TRF2 shares significant homology with TRF1, particularly in the telobox domain; however, divergence of the N-terminal domains of the two proteins has lead to different telomere functions of TRF1 and TRF2, as discussed previously.

The TRF2 protein is encoded by the gene *TERF2*, which has been mapped to human chromosome 16q22.1 (mouse chromosome 8) [132]. TRF2 is more highly conserved between mouse and humans (85% homology) compared to the rapid divergence of TRF1 (65% homology) [27]. *TERF2* encompasses 30,338 bases and encodes a 10 exon transcript with a size of 2907 bp [27,132,133]. The TRF2 protein is 500 amino acids in length and is composed of three major functional domains, the N-terminal basic domain, the central dimerization domain, and the C-terminal DNA binding domain [27,37]. The dimerization and the DNA binding domains function to, as their names imply, form TRF2 homodimers and bind telomeric DNA, respectively. The function of the basic N-terminal domain remains elusive, although recent evidence has provided clues. Deletion of this domain has no effect on TRF2's ability to localize to telomeres or bind DNA [134]; however it does result in stochastic telomere deletions and senescence. The basic N-terminal domain is also required for recruitment of TRF2 to sites of laser-microbeam induced damage [135], as well as TRF2 binding to replication intermediates [136]. It remains to be seen whether the non-telomeric binding functions of the TRF2 N-terminal domain have *in vivo* significance.

The primary function of TRF2 is to enable the formation of an effective telomere end-capping structure. Inability of TRF2 to bind to telomeres, e.g., following introduction of the dominant negative form $TRF2^{\Delta B \Delta M}$, leads to the rapid formation of abundant telomere

fusions [46]. Similar to the phenotype seen with DNA-PKcs deficiency, these fusions do not result from telomere loss, but rather from a defect in the end-capping mechanism. Recent evidence has indicated that TRF2 can positively supercoil DNA around TRF2 homodimers resulting in negative supercoiling in the overall DNA strand [47]. This tension must be relieved through either further DNA looping or separation of the DNA duplex, presenting an opportunity for DNA strand invasion, producing an attractive model for T-loop formation. TRF2 also interacts with a wide variety of proteins which are believed to be required for end-capping. In addition to other shelterin components, TRF2 has been shown to interact with the DNA DSB repair proteins ATM [137], MRE11, RAD50, NBS1 [22], the nucleotide excision repair protein XPF/ERCC1 [138], and the RecQ helicases BLM and WRN [67,139,140].

The interactions between TRF2 and repair, replication, and recombination proteins are presumed to be involved in forming a functional end-cap and evidence supports this presumption. For instance, Karlseder et al. [137] demonstrated that TRF2 inhibits activation of ATM following IR, and dampens downstream ATM effects such as the induction of p53 and phosphorylation of NBS1. This group utilized chromatin immunoprecipitation to show that ATM complexes with TRF2. This evidence points to a role for TRF2 in inhibiting ATM activation at telomeres, thereby avoiding an improper DNA damage response to proper chromosome ends. Members of the MRN complex MRE11 and RAD50 are present at telomeres in a cell cycle independent fashion [22]. NBS1, the regulatory subunit of the MRN complex, associates with TRF2 only in S/G2 phase when end-capping is presumed to occur, implicating the MRN complex in telomere end-processing and capping functions [22]. In addition to the extensive evidence showing that the interactions between repair proteins

and TRF2 are for end-capping functions, there is also some support for the more controversial notion that TRF2 is involved in DNA repair.

One study looked directly at a role for TRF2 in DNA repair. Bradshaw et al. [135] showed that TRF2 is rapidly and abundantly recruited to sites of DNA damage induced by a high intensity laser microbeams, and that this recruitment depended on the basic N-terminal domain. From this observation, the authors suggest that TRF2 is recruited to sites of DNA damage and plays an early role in cellular response to DNA DSBs damage. Our study directly addresses this assertion, and raises issue to the utility of laser microbeam-induced damage in this context. One additional study used to argue in favor of a role for TRF2 in the DNA DSB response is the observation that TRF2 is phosphorylated in response to IR exposure, similar to many repair proteins, including ATM, DNA-PKcs, and NBS1 [141]. This phosphorylation occurs on a highly conserved PIKK residue, threonine-188. However, the purpose of this phosphorylation could be telomere related. Taken together with concerns over the specificity of the phosphorylated-TRF2 antibody (T. de Lange, personal communication), the conclusion that TRF2 phosphorylation has a role in the early DSB damage response may be premature.

THE DNA-DEPENDENT PROTEIN KINASE (DNA-PK)

DNA-PK is a heterotrimeric protein composed of the Ku70/Ku80 heterodimer, and the catalytic subunit (DNA-PKcs). DNA-PK is primarily known for its involvement in three important cellular processes: NHEJ, telomere end-capping, and V(D)J recombination. Many of the specifics of DNA-PK functioning, particularly in NHEJ and telomere function, have

remained enigmatic due in part to the huge size of the catalytic subunit (460 kDa), as well as the protein's robust *in vitro* kinase activity.

The Ku Heterodimer

Two subunits, Ku70 and Ku80, so named because of their approximate size (70 and 83 kDa, respectively) form a stable heterodimer which comprises the regulatory subunit of DNA-PK [142,143]. The donut-shaped complex binds and fully encircles duplex DNA ends [144]. Protein charge and shape are believed to be responsible for the Ku heterodimer binding of DNA as little direct interaction occurs between protein and DNA [144]. This characteristic allows the Ku heterodimer to bind all DNA ends and to migrate along the DNA.

The Ku heterodimer, specifically the C-terminus of Ku80, is essential for the recruitment of DNA-PKcs to DNA ends [145], although the precise manner in which this recruitment occurs remains to be elucidated. Ku can be phosphorylated by DNA-PKcs, promoting either translocation of the heterodimer [146] or disassembly of the complex [117,147,148]. Upon DNA-PKcs binding, the Ku heterodimer is displaced approximately 10 bp [149] followed by an additional 20 bp displacement in the presence of XRCC4/LigaseIV [150]. This translocation is ATP-dependent and required for the recruitment of XRCC4/LigaseIV.

Ku is a highly interactive protein with over 40 reported protein interactions involving a variety of proteins such as histone acetyltransferases (reviewed in [151]), the telomere proteins TRF1 and TRF2 [152,153], and the RecQ helicase WRN [154]. Presumably these interactions occur to facilitate DNA repair and/or telomere maintenance. For example, Ku stimulates the exonuclease activity of WRN helicase [155,156] which can then be inactivated

via DNA-PKcs phosphorylation [157,158], prompting the model whereby Ku recruits and stimulates WRN helicase to resolve complex DNA ends, followed by the phosphorylation of WRN helicase by DNA-PKcs, inactivating the enzymatic activity and allowing NHEJ to proceed. Ku has also been shown to enhance the ligation reaction of XRCC4/LigaseIV in NHEJ [147,150].

DNA-PKcs

The DNA-PKcs is a member of the phosphotidylinositol 3 (PI-3)-kinase related kinases family of proteins, whose members are primarily involved in cellular response to DNA damage from replication or exogenous agents, such as ionizing radiation. Other members include the ATM kinase, an apical kinase in DNA double strand break repair pathways, and ATM rad3-related (ATR) which initiates a cellular response to stalled replication forks. These proteins have no detectable activity towards lipids, distinguishing them from the PI-3 kinase family and leading to the nomenclature PI-3 kinase like kinases (PIKK) [159]. The gene encoding DNA-PKcs is named *Prkdc* and has been mapped to human chromosome 8q11 by fluorescence *in situ* hybridization (FISH) [160]. *Prkdc* encompasses 12,228 bp encoding 86 exons producing an especially large protein kinase of 4,127 amino acids with a molecular weight of approximately 470 kDa [159].

DNA-PKcs is required for DNA end-joining processes such as the DNA DSB repair pathway of NHEJ and V(D)J recombination in higher eukaryotes. It is known that the kinase activity of DNA-PKcs is required for the end-joining activities occurring in both of these processes [146,161], yet the *in vivo* targets of this phosphorylation have been difficult to discern. DNA-PKcs shows preference for phosphorylating threonine or serine residues

followed by a glutamine residue (SQ or TQ motifs) and has robust *in vitro* phosphorylation activity [162]. The Ku heterodimer [117] and XRCC4 [118], also involved in NHEJ, are phosphorylated by DNA-PKcs and are likely *in vivo* targets. Other proteins involved in repair and replication have been shown to be phosphorylated *in vitro* by DNA-PKcs, including the cell-cycle protein MDM2 (mouse double minute protein 2) [163], Replication Protein A (RPA) [164], and the transcription factor IFN Regulatory Factor 3 (IRF3) [165]. The *in vivo* effects of phosphorylation of these proteins remain to be determined. The only sites shown to be essential for NHEJ *in vivo* are phosphorylation sites on DNA-PKcs itself [120-122,166]. Two auto-phosphorylation sites on DNA-PKcs, one located at Serine residue 2056 (Ser-2056) and the second located at Threonine 2609 (Thr-2609), are believed to regulate the accessibility to the DNA end through changes in DNA-PKcs conformation.

Surrounding Ser-2056 and Thr-2609 exists two clusters of PIKK consensus sequences that are phosphorylated in response to DNA DSBs [167,168]. Auto-phosphorylation of DNA-PKcs dramatically reduces the kinase activity and causes changes in its association with the Ku heterodimer [169]. Protein sequencing of DNA-PKcs identified first the Thr-2609 cluster [120,168] followed by the Ser-2056 cluster [167,170]. Work began to mutate these sites with either alanines to prohibit phosphorylation, or with aspartic acid to mimic phosphorylation. This work clearly demonstrated a reciprocal function of these sites, as phosphorylation of the Thr-2609 site results in an accessible, "open" state at DNA ends, while phosphorylation of Ser-2056 results in a closed state [167,170,171]. The ATM kinase has been shown to significantly contribute to the phosphorylation of Thr-2609, thereby placing ATM directly into the NHEJ pathway [172].

A model emerges from these studies in which DNA-PKcs is recruited in an unphosphorylated state to Ku-bound DNA ends. Once bound, DNA-PKcs is activated, and also is believed to physically block DNA ends from unregulated processing. Auto-phosphorylation of the Thr-2609 cluster occurs in *trans-* by virtue of the two DNA-PKcs molecules bound to both DNA DSB ends [173], thereby promoting the open state allowing necessary processing of DNA ends. The action of the NHEJ nuclease Artemis is dependent upon auto-phosphorylation of the Thr-2609 cluster [174]. As mentioned, ATM can hetero-phosphorylate the Thr-2609 cluster; regulation of the phosphorylation of this cluster remains to be determined. Ser-2056 phosphorylation results in a closed state blocking further end-processing [170], although questions to the timing and importance of phosphorylation of this site remain. The *in vivo* mechanism of protein regulation by DNA-PKcs remains to be well defined, though this early work implicates DNA-PKcs as a key regulator of end-accessibility in NHEJ.

DNA-PKcs & Telomeres

DNA-PKcs is important for proper telomere function, as deficiencies in DNA-PKcs lead to telomere uncapping and end-to-end telomere fusion [60]. This phenotype, easily recognizable by telomeric FISH probes, maintains essentially full length telomeres at the point of fusion, indicating that loss of DNA-PKcs leads to disruption of the telomere end cap, and not stochastic loss of telomere sequence [60]. Chemical inhibition of the kinase activity results in the same telomere fusion phenotype seen in cells deficient in DNA-PKcs, indicating that DNA-PKcs plays an active role in telomere structure and is not simply a structural element, per se [59]. Additional clues as to the mechanism of action of DNA-

PKcs at telomeres comes from the observation that telomere fusions in DNA-PKcs deficient cells involve only telomeres generated via leading-strand DNA synthesis [175]. This suggests not only that DNA-PKcs acts preferentially on leading strand telomeres, presumably to generate the 3'single strand overhang absent following replication, but also that leading and lagging strand telomeres are processed differently following replication.

The frequency of these telomere fusions, however, has been shown to vary considerably depending on the cell type, immortalization status, DNA-PKcs mutation type, and experimental context; the contribution of each of these factors is an area of active investigation. The formation of telomere fusions is mediated by the NHEJ pathway, of which DNA-PKcs is an essential element, possibly explaining the variation in telomere fusion frequency depending on the specific mutation in DNA-PKcs, and therefore the efficiency of NHEJ. One line of evidence demonstrates a role for DNA-PKcs in maintenance of telomere length. Mouse cells doubly deficient for DNA-PKcs and the RNA component of telomerase, Terc, display increased telomere shortening compared to cells deficient in Terc alone [176]. This implies a role of DNA-PKcs in the telomere length maintenance pathway, though increased cellular turnover in this context cannot be excluded.

While it seems clear that DNA-PKcs plays important roles at telomeres, the impact of this interaction in organism survival and carcinogenesis remains controversial. Work from the Blasco lab has pointed to accelerated aging and tissue atrophy in mice doubly deficient for DNA-PKcs and Terc compared to those deficient in Terc alone, however no evidence for increased tumorigenesis was observed [177]. The doubly deficient mice showed decreased proliferation, but showed no affects on apoptotic pathways, a key inhibitor of the uncontrolled cell growth necessary for tumor formation. Bailey and colleagues have

demonstrated the ability of dysfunctional telomeres in DNA-PKcs deficient cells to fuse with DNA DSBs to produce chromosomal translocations, an aberration known to promote carcinogenesis in some situations [178]. However, the relatively low frequency of these telomere-DSB fusions (0.01 – 0.1 events per cell) compared to other chromosomal aberrations has led some to doubt the significance of this event in generating genomic instability. Our current studies address this issue by examining the contribution of telomere-DSB fusions in the delayed genomic instability observed in the DNA-PKcs deficient Balb/c mouse.

NBS1

The regulatory protein NBS1 is critical in normal cellular response to DSBs. Mutations in the *NBS1* gene are responsible for the rare autosomal recessive hereditary disorder Nijmegen breakage syndrome (NBS) whose patients are predisposed to develop malignancy at an early age, particularly lymphomas and leukemias [179,180]. Cells isolated from NBS patients are especially sensitive to IR, display abnormal cell-cycle checkpoints, and experience accelerated telomere shortening [181-184]. The complete ablation of the murine homologue of NBS1, NBN, is embryonic lethal [185].

The *NBS1* gene contains 16 exons encompassing 48,797 bp on human chromosome 8q21 [186-188]. The NBS1 gene product is a 95-kDa protein that, along with MRE11 and RAD50, forms the MRN complex [186,189]. The MRN complex plays essential roles in DNA DSB repair via the NHEJ and HR pathways, cell cycle checkpoints, telomere maintenance, as well being implicated in DNA replication. Alterations in any of these

processes could lead to the mutations necessary to promote the early-onset malignancy seen in NBS1 patients.

Three functional domains comprise the NBS1 protein. The N-terminus contains a fork head associated (FHA) and breast cancer C-terminal (BRCT) domain that directly binds phosphorylated histone variant H2AX, and, in so doing, recruits other members of the MRN complex to sites of DNA DSBs [101,102,190]. The central region of NBS1 contains two SQ motifs consistent with the consensus sequence of PIKK kinases. Specifically, the ATM kinase has been shown to phosphorylate serine residues 278 and 343 *in vitro* and *in vivo,* and such phosphorylation is essential for the intra-S phase checkpoint in response to IR [191-193]. The NBS1 C-terminal domain contains a well conserved MRE11 binding site, essential for MRN complex formation [194,195].

The other two members of the MRN complex, MRE11 and RAD50 localize primarily in the cytoplasm and relocate to the nucleus upon induction of DNA damage in a NBS1-dependent fashion [196]. MRE11 possesses a variety of biochemical activities which contribute to the multitude of functions carried out by the MRN complex. MRE11 displays ATP-dependent 3'– 5' exonuclease activity [197,198], but has also been shown to possess a number of other ATP-dependent properties, including 5'– 3' exonuclease activity [199], hairpin opening activity [197,200], DNA unwinding [201], as well as an ATP-independent ssDNA endonuclease [198,202,203].

RAD50 is a large coiled-coil protein belonging to the structural maintenance of chromosome (SMC) family with ATPase motifs at both its N- and C-terminus [203,204]. RAD50 is required for the nuclease activities of Mre11, and the long coiled-coil region that ends in a "zinc hook" is believed to bridge broken ends [201,205,206]. MRE11 and RAD50

are well conserved through evolution, while NBS1 (or yeast homolog Xrs2) is only found in eukaryotes and has significantly less sequence conservation among species [202,207-209]. Working together, the components of the MRN complex play critical roles in a variety of DNA replication, recombination and repair pathways.

The MRN complex is essential for the efficient processing of DNA DSBs, and there is much *in vitro* and *in vivo* evidence to support this. Surprisingly, however, much is still unknown about the role of the MRN complex in the repair process, and debate still exists as to whether it functions in NHEJ, HR, or both. *In vitro* end-joining assays in mammalian systems have demonstrated that MRN enhances DNA fragment joining [210,211]; however chicken DT40 cells with a targeted disruption of NBS1 show wild-type NHEJ [196]. Also, V(D)J recombination in NBS1 patients is comparable with wild type arguing against a role for NBS1 and the MRN complex in end joining processes *in vivo* [212]. The role of MRN in HR is more established, as NBS1-deficient DT40 cells show significantly decreased (100 fold) HR compared to wild-type, as well as reduced sister chromatid exchanges (an HR dependent event) following mitomycin-C treatment [196,213,214]. These data strongly point towards a role for NBS1 and the MRN complex in the HR pathway.

Cells from NBS patients undergo radiation-resistant DNA synthesis (RDS) indicating a failure of the intra-S phase checkpoint, although the phenotype is milder than that observed in AT patients, suggesting multiple braches to the ATM-triggered intra-S phase arrest [181,213,215]. Indeed, three parallel pathways have been shown to modulate this checkpoint in which ATM is the apical kinase (reviewed in [216]). NBS1 phophorylation on serine residues 278 and 343 by ATM is responsible for intra-S phase checkpoint control [192,217]. Several lines of evidence have revealed an intimate

relationship between ATM and NBS1, as interaction between these two proteins strongly stimulates the kinase activity of ATM and increases ATM's affinity for downstream targets such as p53, chk2, and H2AX [99,100,218,219]. A functional MRN complex is indispensible for ATM phosphorylation of chk2, a vital step in the intra-S phase checkpoint [99]. NBS1 and the MRN complex are also thought to have roles in G1 and G2, although different experimental systems produce conflicting results, and the redundancy of the checkpoint pathways have made it difficult to tease out a definitive role for NBS1 or MRN.

NBS1 & Telomeres

Cells from NBS patients display accelerated telomere shortening compared to wild type cells and this results in shorter proliferative life spans [183]. Introduction of the catalytic subunit of telomerase, TERT, allows longer proliferation of cells in culture, but this is insufficient to rescue the shortened telomere phenotype. Introduction of TERT and NBS1 rescues both the telomere shortening and proliferative life span phenotypes observed in NBS cells [183]. This conclusion suggests a role of NBS1 and the MRN complex in generation of the G-rich overhang, the required substrate for the extension of telomeres by telomerase. In accordance with this hypothesis, RNA interference of either MRE11 or NBS1 results in marked shortening of the G-rich overhang in human cells [23]. It is important to note, however, that even with stable knockdown of these proteins overhang length is eventually restored to wild type length, indicating that other factors can compensate for deficiencies of the MRN complex. Work in yeast and flies has also implicated MRN in telomere end-processing [220-223]. Furthermore, NBS1 associates with telomeric DNA specifically in S-phase when telomere end-processing is believed to occur [22].

An additional role for NBS1 at telomeres is indicated by virtue of its presence in APBs, which form when cells are maintaining telomeres via the ALT pathway [224]. NBS1 is required for recruitment of MRE11, RAD50 and BRCA1 to these bodies [91], and inhibiting the recruitment of NBS1 to APBs suppresses ALT [225]. This evidence supports the hypothesis that the MRN complex, and NBS1 in particular, is required for the ALT telomere length maintenance mechanism.

RATIONALE OF THIS STUDY

In 1996 several studies independently demonstrated the involvement of the DNA repair protein Ku in telomere length maintenance in yeast [226,227]. Work quickly ensued to determine the extent to which DNA repair proteins were involved in telomere metabolism, as well as whether these observations in yeast were conserved in mammalian systems. Today, it is well established that DNA repair proteins are involved in telomere length maintenance, end-capping, and replication from yeast to mouse to man, with over a dozen repair proteins from many repair pathways interacting with telomeres. However, the rapid identification of novel protein interactions with telomeres leads to the task of deciphering the function and temporal interplay between each of these protein interactions.

Through this study we sought to address the roles of two known DNA repair proteins, DNA-PKcs and NBS1, in telomere function. To do so, we utilized a variety of cells either mutated in or depleted of DNA-PKcs or NBS1 then analyzed the effects on telomere function via telomere FISH or CO-FISH. Through this approach we collected valuable information regarding the function of DNA-PKcs and NBS1 on telomeres, providing biological endpoints with which future *in vitro* studies must be reconciled.

During the course of this work, the telomere protein TRF2 was proposed to be involved in the DNA damage response pathway [135], presenting the possibility that the interactions between telomere proteins and DNA repair proteins may be bi-directional. We undertook a study to better characterize the interaction between TRF2 and DNA damage.

This work has, in large part, been published prior to the writing of this dissertation. Many of the studies reported here are the results of successful collaborations with groups located through the world, and I am indebted to many others for their expertise and assistance throughout the course of my graduate work.

II. MATERIALS & METHODS

CELL CULTURE

The human B-lymphoblast cell lines, TK6 and WTK1, were derived from the same progenitor, WIL2 [228,229] and kindly provided by Dr. Howard Liber. TK6 and WTK1 were maintained in RPMI 1640 (Gibco BRL, Invitrogen Corporation, Carlsbad, CA) supplemented with 10% horse serum, 100 units/mL penicillin, and 100 μg/mL streptomycin. Human HeLa and U2OS cells were cultured as monolayers in Dulbecco's Minimal Essential Medium (Gibco BRL) supplemented with 10% fetal bovine serum (FBS), 50 units/mL penicillin, and 50 μg/mL streptomycin. Primary Human Dermal Fibroblasts (HDF) were cultured as monolayers in MEM alpha medium (Gibco) supplemented with 10% fetal calf serum, 50 units/mL penicillin, and 50 μg/mL streptomycin. All human cells were incubated at 37°C in 5% CO_2 in air and subcultured (1:5 or 1:10) every five days.

The mouse DNA-PKcs auto-phosphorylation mutants were kindly provided by Dr. Kathryn Meek. These cells were cultured as monolayers in MEM alpha medium (Gibco) supplemented with 10% FBS, 50 units/mL penicillin, 50 μg/mL streptomycin, and 400 μg/mL G418 to maintain selection. Cells were incubated at 37°C in 5% CO_2 in air and subcultured (1:10) every four days. Balb/c and C57BL/6 mammary epithelial cells were cultured as monolayers in JRH Hams F-12 medium supplemented with 5 μg/mL insulin, 1 μg/mL hydrocortisone, 10 ng/mL epidermal growth factor, 0.5 μg/mL fungizone, 5 μg/mL gentamycin and 5% FBS. All other mouse cell lines (SCID, p53-/-/SCID) were cultured as monolayers in MEM alpha medium (Gibco) supplemented with 10% fetal bovine serum 50 units/mL penicillin, and 50 μg/mL streptomycin.

CYTOGENETIC TECHNIQUES

Cell Collection and Slide preparation

Colcemid (0.1 to 0.2 μg/mL) was added to cell cultures during the last 4 hours to accumulate mitotic figures that were collected as previously described [60]. Briefly, cells growing in monolayers were detached from the culture dish with 0.25% trypsin in Hank's balanced salt solution (Hyclone) and transferred to a 15 mL conical centrifuge tubes. Cells grown in suspension were transferred directly into centrifuge tubes. Cell pellets were then formed via centrifugation at 1000 RPM for 5 min. The media was aspirated and pellets were resuspended in 5 mL of 75mM KCl added dropwise to the tube. Cells were incubated in KCl at romm temperature (RT) for 15 min, then pre-fixed by the addition of 1 mL of Carnoy's fixative (3:1 methanol:acetic acid) and vortexed gently. Cells were again pelleted via centrifugation at 1000 RPM for 5 min, followed by the aspiration of the supernatant. Pellets were resuspended in 5mL Carnoy's fixative and left at RT for 10 min. Cells were then rinsed in Carnoy's fixative twice more by centrifuging the cells followed by resuspension in fixative. Cell suspensions were then dropped onto cold, wet microscope slides and dried at 37° for one hour or at RT for 2 to 3 days prior to telomere FISH.

Telomere Fluorescence in situ hybridization (FISH)

Peptide Nucleic Acid (PNA) Telomere probe

Microscope slides were rinsed in RT 1X PBS. Slides were then incubated in 37°C RNAse A (100 μg/mL H_20) for 10 min at 37°C, and rinsed in PBS. Next, slides were fixed in formaldehyde (4% in 1X PBS) for 10 min at room temperature, and rinsed in PBS. Slides

were then dehydrated in cold (−20°C) ethanol series (75%, 85%, 100%) for 2 min each and quickly dried in 37°C oven. Slides were denatured in 70% formamide in 2X SSC at 72°C for 2 min, and quickly moved to cold ethanol series as previously, and air dried. A hybridization mixture containing 70% formamide, 12mM Tris-HCl, 5mM KCl, 1mM $MgCl_2$ and 0.2 μg/ml Cy-3-conjugated $(TTAGGG)_3$ or fluorescein isothiocyanate (FITC)-conjugated $(CCCTAA)_3$ telomere PNA probe (Applied Biosystems) was denatured at 72°C for 5 min, and then vortexed well, spun down, and placed on ice for 5 min. 25μL of hybridization mixture was added to the dried slides, and the slides were coverslipped and allowed to hybridize in a moist chamber at RT for 3 hours. Following hybridization, the coverslips were removed and the slides were washed in 70% formamide for 15 min at 30°C, then in PN buffer for 5 min at room temperature. Antifade solution (Vectashield, Vector Laboratories) containing 1.5 μg/mL of 4'-6-diamidino-2-phenylindole (DAPI) was applied to the slide and coverslipped for analysis.

Oligonucleotide Telomere probe

Microscope slides were rinsed in 1X PBS. Slides were then incubated in 37°C RNAse A (100 μg/mL H_20) for 10 min at 37°C, and rinsed in PBS. Slides were then dehydrated in cold (−20°C) ethanol series (75%, 85%, 100%) for 2 min each and quickly dried in 37°C oven. Slides were denatured in 70% formamide in 2X SSC at 72°C for 2 min, and quickly moved to cold ethanol series as previously, and air dried. Probes to telomeric repeat DNA were prepared by synthesizing oligomers complementary to either the G-rich or C-rich strands; $(CCCTAA)_7$ or $(TTAGGG)_7$. Thirty-five pmol of oligomer was labeled by terminal deoxynucleotidyl transferase tailing (Boehringer Mannheim) with Cy3-dCTP according to the manufacturer's instructions. A hybridization mixture containing 0.4 μg/ml

probe DNA in 30% formamide and 2×SSC was denatured at 72°C for 5 min, and then vortexed well, spun down, and placed on ice for 5 min. 30μL of probe solution was added to the dried slides, and the slides were coverslipped and allowed to hybridize in a moist chamber at 37°C overnight (16 – 18 hours). Following hybridization, the coverslips were removed and the slides were washed in 2X SSC at 42°C for 15 min with shaking. The slides were washed 4 additional times under the same conditions, then in PN buffer for 5 min at room temperature. Antifade solution (Vectashield, Vector Laboratories) containing 1.5 μg/mL of 4'-6-diamidino-2-phenylindole (DAPI) was applied to the slide and coverslipped for analysis.

Chromosome-Orientation FISH (CO-FISH)

The CO-FISH procedure has been described in detail previously [175]. Cells were cultured for a single cell cycle of 5'-bromo-2'-deoxyuridine (BrdU; Sigma) at a final concentration of 10μM (50μM for TK6 and WTK1) was added. Cells were then collected as described above. Slides were then prepared according to appropriate telomere probe procedure above until the denaturation step. Prior to denaturation, slides were stained with Hoechst 33258 (0.5 μg/mL 2X SSC) at RT for 15 min in the dark, then air dried in dark. Slides were then flooded with approximately 50 μL 2X SSC and coverslipped. Slides were then exposed to 365 nm UVA light (Stratolinker) at RT for 30 min, followed by a rinse in dd. H_2O and drying. Enzymatic digestion of the BrdU-substituted DNA strands with 3 U/μl of Exonuclease III (Promega) in buffer supplied by the manufacturer (50mM Tris-HCl, 5mM $MgCl_2$, and 5 mM dithiothreitol, pH 8.0) was allowed to proceed at RT for 10 min, followed by a rinse in dd. H_2O. Slides were then denatured as described above, and continued through the appropriate telomere probe procedure.

Image Analysis

Preparations were observed using a Zeiss fluorescence microscope (Axioplan 2ie MOT). DAPI and Cy3 of FITC exicitor/dichroic/barrier filter sets (Zeiss) were used to detect counterstained chromosomes and telomere signals, respectively. Images of chromosomes were captured with a CCD camera (model CV-M4^{+}CL, JAI PULNiX Inc., San Jose, CA, USA), controlled by a Dell precision 360 workstation running Isis FISH imaging software (Metasystems, Altlussheim, Germany).

Scoring Criteria

Our scoring criteria require that to be scored as a telomeric fusion, the telomeres of adjoining chromosomes must fuse into a single FISH signal and the DAPI signal must be continuous through the point of fusion [60]. Telomere-DSB fusions were identified as single-sided (i.e. appearing on only one chromatid of a mitotic chromosome) interstitial blocks of CO-FISH telomere signal. Our scoring criteria requires that to be scored as a telomere association, telomeres of adjacent chromosomes must be touching or very close to one another (i.e., $\leq 1/4$ width of a chromatid) yet remain as separate and distinct signals. At least 25 metaphases were scored for each condition, for specific number of metaphases scored for each experiment see appropriate "Results" section.

IMMUNOFLUORESCENCE

Cells were fixed onto substrate (glass, mylar, or polypropylene) in formaldehyde (4% in 1X PBS) at RT for 6 min. Slides were then washed 3 times in PBST at RT for 5 min each wash. Cells were then permeabilized in triton X-100 solution (0.2% in 1X PBS), followed by blocking in blocking solution (5% dry milk in PBST) at RT for 30 min with shaking.

Primary antibody diluted in blocking solution (see below for antibodies and concentrations used) was applied to the cells at RT for one hour with shaking. Cells were then washed 3 times in PBST at RT for 5 minutes each wash. Secondary antibody diluted appropriately in blocking solution (see below) was then applied at RT for one to 1.5 hours with shaking in the dark. Cells are then washed 4 times in PBST at RT for 10 min each wash. Antifade solution (Vectashield, Vector Laboratories) containing 1.5 μg/mL of 4'-6-diamidino-2-phenylindole (DAPI) was applied to the slide and coverslipped for analysis.

1° antibodies and concentrations

Rabbit anti-γH2AX (Trevigen #4411 PC-100): [1:200]

Mouse anti-γH2AX, clone JBW301 (Upstate #05-636): [1:500]

Mouse anti-53BP1, clone BP18 (Upstate #05-725): [1:1000]

Rabbit anti-MDC1 (BL578) (Bethyl #A300-051A): [1:150]

Rabbit anti-TRF2 (H-300) (Santa Cruz #sc-9143): [1:200]

Rabbit anti-TRF2 (Abcam #ab4182): [1:500]

Mouse anti-TRF2 (Imgenex #IMG-124A): [1:100]

2° antibodies and concentrations

Goat anti-mouse CY3 (Jackson ImmunoResearch Laboratories #115-165-100): [1:200]

Goat anti-mouse Alexa488 (Invitrogen #A11029): [1:200]

Goat anti-rabbit FITC (Jackson, #111-095-144): [1:200]

Goat anti-rabbit Alexa594 (Invitrogen #A11012): [1:200]

COMBINED IMMUNOFLUORESCENCE AND FISH (IMMUNOFISH)

Steps for immunofluorescence were followed as described above until the washes after secondary antibody application. Following the last PBST wash, proteins were cross-linked in formaldehyde solution (4% in 1X PBS). Slides are then dehydrated in cold (−20°C) ethanol series (75%, 85%, and 100%) for 2 min each and quickly dried in 37°C oven. Slides were then denatured and the remainder of appropriate telomere FISH procedure was followed. The PNA telomere probe was the preferred probe to use in this procedure, although the oligonucleotide telomere probe produced scorable signals.

GAMMA IRRADIATION

All gamma irradiations were conducted by exposure of asynchronous cells in culture dishes to ^{137}Cs (Mark I, J.L. Shepherd) at a dose rate of 3.9 Gy/min at room temperature to the desired dose. Cells to be used as controls were kept at room temperature for similar lengths of time. Following irradiation, cells were incubated at 37°C unless otherwise noted.

HIGH-IONIZING HIGH ENERGY PARTICLE (HZE) IRRADIATION

Human lymphoblast cultures growing logarithmically were shipped in culture flasks to Brookhaven National Laboratory (BNL). Cells were exposed to 1GeV/nucleon (GeV/n) ^{56}Fe particles (LET of ≈150 keV/μm) to the desired dose. Cells were then returned to

Colorado State University for subsequent analysis. Cells to be used as controls were subjected to the same shipping treatment and storage as experimental cells.

GENERATION OF LOCALIZED DNA DAMAGE

Laser-induction of local DNA damage and live cell imaging

For induction of multiphoton damage, a Coherent Mira mode-locked Ti:Sapphire laser was used at 800 nm with a pulse length of 200 fs and repetition rate of 76 MHz. In parallel experiments, a 30 mW 405 nm diode laser supplied by Zeiss was used to induce local damage. Exposures were done with and without Hoechst 33258 (Sigma, bisbenzimidazole derivative, supravital minor groove-binding DNA stain with AT selectivity; final concentration 10 μg/ml added 30 minutes prior to treatment). All treated cells were analyzed at the same magnification and zoom factor using low laser power to minimize monitor bleaching during data collection. The region to be damaged was always the same size and shape, while laser treatment was done with calibrated lasers to exclude variations in dose. Confocal images of living HeLa cells expressing green fluorescent protein (GFP)-tagged TRF2 [230], Ku80 [231] and XPC (manuscript in preparation) were obtained using a Zeiss LSM 510 microscope equipped with a 25 mW Ar laser at 488 nm and 40X 1.3 N.A. oil immersion lens. Images of single nuclei were taken at a lateral sample interval of 100 nm. GFP fluorescence was detected using a dichroic beamsplitter (HFT488) with an additional 505-530 nm bandpass emission filter placed in front of the photomultiplier tube.

Ionizing Radiation-induced DNA damage

Longitudinal exposure to one or two α-particles (high LET, densely ionizing)

Our procedure is described elsewhere in detail [232]. In short, cells were cultured on ultra-thin Mylar film in custom-made culture dishes and irradiated with α-particles using an Americium (^{241}Am) source with an activity of 140 kBq. Cell cultures were irradiated so that α-particles entered at an average angle of 30° from the horizontal plane of the growth surface. Cells were fixed 90 seconds, 5 minutes, 10 minutes, 30 minutes and 60 minutes post-exposure. Preparations were observed using a Leica (Wetzlar, Germany) fluorescence microscope (DM RA HC). Micrographs were recorded using a cooled CCD camera (KX1400, Apogee Instruments, CA, USA). Stacks of 40 images were collected at intervals of 0.2 μm in the Z direction. The stacks of images were reconstructed and rendered using Huygens software (Scientific Volume Imaging, Hilversum, The Netherlands) and maximum intensity projections were made using Image Pro Plus software (Mediacybernetics, Carlsbad, CA, USA).

Perpendicular exposure to a high dose of localized α-particles

Cells were cultured on ultra-thin polypropylene foil in custom-made culture dishes and then irradiated with 6.0 MeV He ions (initial stopping power ~95 keV/μm). The charged particles are focused with a series of electrostatic lenses [233] to a beam diameter of less than 5μm. A detailed description of ion beam generation, cell-targeting techniques and beam positioning has been described elsewhere [234]. Cells were exposed to 0, 200, or 400 α-particles delivered perpendicularly (approximately 0, 30, and 60 Gy, respectively) and fixed immediately, 30 min, and 60 min after irradiation. Preparations were observed using a Zeiss (Thornwood, NY, USA) fluorescence microscope (Axioplan 2ie MOT). Images were

captured using a CCD camera (model CV-M4^{+}CL, JAI PULNiX Inc., San Jose, CA, USA). Stacks of 40 images were collected at intervals of 200nm in the Z direction. The stacks of images were reconstructed and rendered as above.

Scoring criteria

Maximal accumulation of TRF2 at damage sites was previously shown to occur approximately 2 minutes following exposure [135]; this was corroborated by our results from multiphoton laser experiments. Accordingly, we primarily investigated time points less than 10 minutes, although later time points were also examined as noted. Cells were scored qualitatively for the presence or absence of TRF2 recruitment to damage sites. Positive recruitment was scored when noticeable changes in the staining pattern of TRF2 were observed, or when there was an increase in the incidence of TRF2 foci at the damage site. A subset of these cells was also quantitatively analyzed as described in "Image Analysis."

Image analysis

The amount of TRF2 fluorescence co-localizing with DNA damage markers relative to the amount fluorescence in the background and on the telomeres was quantified by image analysis. Image analysis was performed using a custom-made macro created in Matlab (MathWorks, Natick, Massachusetts, USA), using DipImage (Quantitative Imaging Group, Delft University of Technology, Delft, The Netherlands), an image library for Matlab. 3D images of cells co-stained for TRF2, γ-H2AX (or MDC1) and DNA were used. For analysis of telomere-associated TRF2, the TRF2 channel was thresholded using the isodata algorithm

[235]. For the areas obtained by thresholding, the average TRF2 intensity was determined. For analysis of the TRF2 signal in the damage-containing areas, the γ-H2AX channel was thresholded using the isodata algorithm. Damage-containing areas that also contained telomere-associated TRF2 were excluded from analysis. The intensity of TRF2 was measured in the remaining areas. To measure intensity of TRF2 in the background, the damage-containing areas were expanded by dilation, the damage-containing and telomere-associated areas were subtracted and, in the remaining areas, the average TRF2 intensity was determined.

UVC-induction of local DNA damage and live cell imaging

HeLa cells expressing TRF2-GFP were transiently transfected with DDB2-mCherry [236] using Lipofectamine transfection reagent (Invitrogen, Breda, The Netherlands) according to manufacturer instructions. After transfection, cells were cultured for an additional 24 h to allow expression of the fusion proteins before experiments were performed. Cells were UVC-irradiated on an Axiovert 200M widefield fluorescence microscope using a UVC source containing four UV lamps (Philips TUV 9W PL-S) above the microscope stage. The UV dose rate was measured to be 3 W/m^2 at 254 nm. For induction of local UV-damage, cells were UV irradiated through a polycarbonate mask (Millipore Billerica, Massachusetts, USA) with pores of 5μ [237] and subsequently irradiated for 39s (100 J/m^2) or 390s (1000 J/m^2). The response of TRF2-GFP and DDB2-mCherry upon UV irradiation was measured on a Zeiss Axiovert 200M widefield fluorescence microscope, equipped with a 100x Plan-Apochromat (1.4 N.A.) oil immersion lens (Zeiss, Oberkochen, Germany) and a Cairn Xenon Arc lamp with monochromator (Cairn research,

Kent, U.K.). Images were recorded with a cooled CCD camera (Coolsnap HQ, Roper Scientific, USA). A 375-490 excitation filter, 490 dichroic mirror and 525-40 band-pass emission filter was used for EGFP imaging (monochromator: 470 nm ± 20 nm). A 375-580 excitation filter, 585 long-pass dichroic mirror and 620-60 band-pass emission filter was used for mCherry imaging (monochromator: 550 nm ± 20 nm).

Statistical Analysis

Results from two or more independent experiments were pooled and differences between control and experimental cell results were analyzed using the student's t-test. The resulting p-values (or pa-value ranges) are presented with the corresponding data set. In instances where a low number of data points were obtained (i.e. Figure 3.5), data points are presented as mean ± standard deviation.

III. TRF2

ABSTRACT

The human telomere binding factor TRF2 is rapidly recruited to sites of damage produced by high intensity laser microbeams, prompting the conclusion that it plays an early role in the repair of DNA DSBs. To characterize the types of damage initiating this recruitment, we generated well-defined, localized nuclear damage utilizing numerous sources of UV and IR, and then quantified accumulation of TRF2 at these sites. Whereas we could confirm earlier reports that TRF2 was recruited to sites damaged by a high intensity multiphoton laser beam, no evidence for such recruitment was observed following exposure to lower intensity sources of UV. Furthermore, and most significantly, whereas exposures to various types of IR—agents known for their ability to produce copious quantities of DSBs—generated easily recognizable damage foci, they failed to elicit a TRF2 response. Our results cast serious doubt on TRF2 playing a biologically relevant role in the early response to exogenous DNA damage, particularly DSBs. Moreover, they serve to illustrate meaningful differences in the cellular response to high-intensity laser systems versus other types of radiation damage.

INTRODUCTION

The human telomere protein TRF2 binds directly to duplex telomeric DNA and plays a crucial role in telomeric end-capping, as well as supporting roles in other telomere functions such as telomere length maintenance and replication [26]. TRF2 has been shown to interact with a large and varied complement of proteins, particularly those involved in DNA repair, replication, and recombination. The nature of these interactions remains somewhat undefined, particularly in timing and location, although dogma holds that these

interactions are necessary to facilitate t-loop formation and dampen improper telomere-induced damage responses [26,137]. Nevertheless, it is tempting to speculate a role for TRF2 in the DNA damage response, if solely due to the sheer numbers of TRF2 protein interactions.

TRF2 has been shown to interact with the DNA DSB repair proteins ATM [137], MRE11, RAD50, NBS1 [22], and Ku70 [152]. Additionally, DNA polymerase β (Polβ) and flap structure-specific nuclease (FEN1) [238], members of the base excision repair (BER) pathway, as well as nucleotide excision repair (NER) complex XPF/ERCC1 [138] all interact in some fashion with TRF2. Current information pertaining to the timing and nature of these interactions suggests that they occur in order to properly distinguish telomeres from DNA DSBs. For instance, NBS1, the regulatory component of the MRN complex, interacts with TRF2 only in S/G2 phase following replication, the time when end-capping is thought to occur [22]. The BER proteins Polβ and FEN1 also specifically associate with telomeres in late S/G2 phase, strengthening the hypothesis that repair proteins are necessary for end-cap formation [64].

TRF2 has also been shown to inhibit the DNA damage response. ATM activation is attenuated by TRF2, as is phosphorylation of downstream ATM targets such as p53 and NBS1 [137]. Furthermore, constitutive over-expression of TRF2 in a mouse model results in ultra sensitivity to UV light and an increased incidence of skin tumor development [239]. This phenotype is consistent with deficiencies in NER, thus supporting a role for TRF2 suppression of NER processes. These observations implicate TRF2 in dampening DNA damage responses which may be improperly activated by telomeres. Taken together, this evidence suggests that TRF2 interacts with DNA damage repair proteins to assist, in some

presently undefined manner, telomere end-capping, as well as dampening local ATM-mediated damage responses.

Thus, it was generally accepted that DNA repair proteins associate with telomeres. It was somewhat surprising, however, when a recent report provided evidence for a reciprocal kind of relationship. That is, TRF2 played a role in the early DNA damage response. Bradshaw et al. [135] showed that TRF2 rapidly and transiently migrates to sites of UV laser microbeam-induced DNA damage, a response that precedes the involvement of other DNA repair proteins, most notably ATM. This paper garnered much attention as the authors proposed that TRF2 plays an early role in the response to DNA DSBs and declared a role for the previously uncharacterized N-terminal basic domain of TRF2, as this domain is required for TRF2 recruitment to sites of damage. As is typical of papers describing novel phenomenon, many questions were generated: How is TRF2 localizing to the damage? What is the N-terminus doing? Could other shelterin components be involved in the DNA damage response? Questions pertaining to the paper's methodology also arose. Is TRF2 really being recruited to DNA DSBs, or could other laser microbeam-induced lesions be responsible? We found this question to be particularly relevant as high intensity UV laser systems are poorly characterized and current applications deviate greatly from the foundations on which they are based.

The use of UVA light (320 – 400 nm) to generate DNA DSBs was described in 1993 by Limoli and Ward [240] in their attempts to investigate the direct effects of radiation on DNA. They found that low fluence (0.2 – 8 kj/m^2) 365 nm light can generate DNA DSBs in cells sensitized with the thymidine analog BrdU if exposed in the presence of the photosensitizing dye Hoechst 33258, a minor groove binder. Importantly, UVA, BrdU and

Hoechst were all absolutely required to produce measurable quantities of DSBs in mammalian cells. DSBs can be formed from a single event when the bromine atom is cleaved from BrdU and abstracts an atom from the opposing strand, while the reactive uracilyl radical left following the cleavage abstracts an atom from the proximal strand producing two SSBs in close proximity, i.e. a DSB. Another possible mechanism is that DNA DSBs are formed when two SSBs are produced on opposing strands in close proximity as a result of the excitation of the bound Hoechst molecule. In either case, it is clear from these studies that the absence of any of these three key components, no DNA DSB is generated.

In 1999, Rogakou et al. [241] utilized a high intensity UVA (390 nm) laser microbeam to generate precise nuclear regions of DNA damage. Following the methodology of Limoli and Ward—first sensitizing the cells via growth in BrdU then exposure to Hoechst dye—the authors concluded that these sites of damage consisted primarily of DNA DSBs. While the overriding message of the paper was that the histone variant H2AX was phosphorylated specifically at sites of DNA DSBs (noteworthy in its own right), it also ushered in a novel way to produce DSBs in subcellular dimensions. It is important to note that the fluence (intensity) of the UVA laser microbeam was *significantly* higher than the UVA broad beam source used by Limoli and Ward. The authors estimated that at 1% of maximum power the laser generated 1000 kJ/m^2, fully two orders of magnitude more intense than conditions used to characterize the Limoli and Ward reaction. The authors later suggested that removing BrdU from the reaction would likely result in the formation of more precise DNA damage [106], although this assertion was not directly tested.

The approach proposed by Rogakou [241] was especially attractive in experimental settings, in that DNA damage could be generated in subnuclear volumes, a technique now known as laser microirradiation. The suggestion of removing BrdU from the reaction became, for some reason, widely accepted, and the vast majority of laser microirradiations are now done in the absence of this base analog (reviewed in [242]). As the altered methodology was applied experimentally, it is important to note that only indirect methods (i.e. methods other than those used to physically measure DSBs) have been utilized to characterize the types of DNA damage present, principally, recruitment of various DNA damage proteins. To us, the issue at hand is this: while DNA DSBs are undoubtedly present at these sites, the complete spectrum of damage present had yet to be defined.

We felt that while the recruitment of TRF2 to sites of laser microbeam-induced damage was a particularly interesting observation, the conclusion that TRF2 was recruited to these sites specifically as a result of the presence of DSBs was not solidly supported by the data. In other words, other lesions or unusual phenomenon present at the sites of laser microirradiation could be responsible for the recruitment of TRF2. Among other things, we were concerned about the biological relevance of these experiments, as the experimental protocol utilized the laser at 75% power (keeping in mind Rogakou's estimation [241]). To address these concerns, we undertook a study designed to more fully examine the effects of various DNA lesions on the recruitment of TRF2.

RESULTS

In an effort to confirm the original observation that TRF2 was recruited to sites damaged by high intensity laser beams (e.g. multiphoton lasers, pulsed laser microbeams)

[135], HeLa cells expressing GFP-tagged TRF2 were exposed to the highly focused beam of a pulsed 800 nm mulitphoton laser. With this source, coincident absorption of two photons results in energy deposition equivalent to that produced by a single 400 nm photon. TRF2 recruitment to exposed nuclear regions was measured by live-cell imaging and compared to the recruitment of Ku80-GFP, a NHEJ protein, or Xeroderma Pigmentosum C (XPC)-GFP, a critical NER protein. When cells were exposed in the presence of Hoechst 33258, a photo-sensitizing dye that promotes the photochemical reaction responsible for DSB production following UVA exposure [240,241], we observed immediate recruitment (within 10 seconds) of both Ku80 and XPC to sites of laser-induced damage following exposure at 15% of maximum laser output (**Figure 3.1**). Recruitment of TRF2 to these damaged sites occurred within 20 seconds of exposure and persisted for the duration of the experiment (3 minutes), but only after a 1.6-fold increase in laser power (24% of maximum laser output) (**Fig. 3.2a;** a summary of experimental results can be seen in **Table 3.1**). Fluorescent intensity of TRF2 at telomeres was not measurably affected. These results are largely in agreement with those of Bradshaw et al. [135] in that we confirmed TRF2 recruitment to damaged nuclear regions within seconds of exposure to a multiphoton laser beam.

We also found that when cells were exposed to a multiphoton laser beam in the *absence* of Hoechst 33258, TRF2, XPC and Ku80 were likewise recruited rapidly to damaged nuclear regions, but only after a significant increase in laser power (95% of maximum laser output for TRF2 recruitment, 60% of output for both Ku80 and XPC; **Figure 3.2b**). As in the presence of Hoechst, 1.6 times more laser power was needed to accumulate TRF2. In contrast to multiphoton treatment, TRF2 recruitment was not observed following exposure of cells in the presence of Hoechst 33258 to a more conventional, less intense, 405 nm laser

beam, whereas NER and NHEJ proteins were rapidly and abundantly recruited to such damaged sites (**Figure 3.3**). Taken together, these results imply that unusual features of the extremely concentrated energy deposition produced by multiphoton laser beams and other high intensity laser systems may be triggering TRF2 recruitment.

While IR produces a multitude of DNA lesions, it is specifically known for its ability to produce copious quantities of DSBs [243]. Unlike sparsely ionizing x- and γ-rays, α-particles deposit their energy along defined tracks, producing dense linear distributions of DSBs, which are readily recognizable following detection of γ-H2AX by immunofluorescence [232]. In one series of experiments, an average of 1-2 α-particles (^{241}Am) traversed HeLa cell nuclei in a longitudinal trajectory. We observed significant accumulation of γ-H2AX, as well as various DNA damage-response proteins (RAD51, NBS1, MRE11, MDC1 and 53BP1) as early as 90 seconds following α-particle exposure (**Figure 3.4** and data not shown). However, quantitative analysis of TRF2 fluorescence intensity at damage sites revealed *no* significant accumulation of TRF2 (**Figure 3.5**). Furthermore, TRF2 was not recruited to α-particle-induced damage sites in primary human dermal fibroblasts (HDF) or in the ALT-positive osteosarcoma cell line U2OS, indicating that failure of TRF2 to migrate to damage sites is independent of telomere maintenance mechanisms (**Figure 3.5**). Also, consistent with previous observations [137], TRF2 did not co-localize with IR-induced foci in response to 5 Gy of ^{137}Cs γ-rays (**Figure 3.6**).

Thus, although damage induced by high intensity (e.g., multi-photon) laser irradiation resulted in the positive recruitment of TRF2, α-particles and γ-rays—well known for their ability to produce DSBs—failed to elicit this response. In seeking an explanation for this

apparent discrepancy, we considered the possibility that damage from one or two α-particle tracks or intermediate doses of γ-rays might be insufficient to cause detectable TRF2 recruitment. To address this issue, we utilized the Columbia University charged-particle microbeam, which delivers defined numbers of charged particles (in this case α-particles) with high accuracy to specified locations [234]. Delivery of either 200 or 400 α-particles (roughly equivalent to 30 and 60 Gy) to a defined nuclear area of less than 5μm^2 resulted in well-defined damage clusters marked by γ-H2AX and MDC1 (**Figure 3.7**). However, even at these high fluences, TRF2 was never observed at the damage sites (**Figure 3.5**). Our results therefore demonstrate that TRF2 is *not* recruited to DNA damage created by ionizing radiations, regardless of dose or distribution.

We next considered the possibility that TRF2 was in fact recruited to the sites of high intensity laser-induced damage—*not* in response to DSBs, but instead in response to DNA damage more characteristic of UV exposure, e.g. cyclobutane pyrimidine dimers (CPDs) and 6-4 photoproducts. UVC light (254 nm) was used to expose HeLa cells expressing both TRF2-GFP and mCherry-tagged DDB2 (DNA damage binding protein 2), a heterodimeric protein involved in NER. UV damage was confined to discrete nuclear volumes by passing light though a polycarbonate filter (5μm pore size) as described previously [237]. Live cell imaging was performed to monitor recruitment of the fluorescently tagged proteins to damaged sites. Exposures of 100 J/m^2 resulted in rapid accumulation of DDB2. However, even following 1000 J/m^2 no aggregation of TRF2-GFP was present within 15 minutes of exposure (**Figure 3.8**). Thus, TRF2 is *not* recruited to damage sites created by UV exposure even when massive amounts of relatively concentrated UV-induced lesions are present.

DISCUSSION

The aforementioned experiments demonstrate that cellular damage required for TRF2 recruitment is not produced by IR, nor is it produced by (what most would consider) typical exposures to UVA or UVC light. Rather, TRF2 recruitment appears to be dependent on a type or spectrum of damage unique to high-intensity laser beams (e.g. multiphoton lasers or pulsed laser microbeams). The full spectrum of damage produced by the absorption of such a high local concentration of energy has yet to be adequately characterized, as discussed in the introduction. However, high intensity laser beams do produce (among other things) lesion moieties that are also typically found following exposure to IR or UV, including DNA single-strand breaks (SSBs), DSBs, and a variety of base damage products. Nevertheless, our results clearly show that none of these—outside the context of high-intensity laser exposure—are sufficient to elicit the TRF2 damage response.

The difference in damage spectra between laser microbeams and IR is somewhat disconcerting in light of the growing numbers of experiments relying solely on laser microbeams to generate DNA damage. A particularly worrisome point which arose in the course of the present study was the observation that Hoechst 33258 is dispensable for generation of DNA DSBs following UV exposure. Limoli and Ward [240] clearly demonstrated that following exposure to UVA, both Hoechst and BrdU were an absolute requirement for DSB formation. As mentioned in the introduction, most laser microirradiations are done in the absence of BrdU, and, by itself, this is not especially troublesome. It has been demonstrated that Hoechst dye alone can introduce SSBs

following excitation by UVA wavelength light [240]. The high intensity of laser exposure simply could cause a high degree of excitation in a discrete area generating many focused SSBs resulting in DSB formation. Indirect evidence confirms the existence of DSBs following laser microirradiation as known DNA DSB repair proteins are recruited to damage sites with kinetics similar to recruitment to IR-induced foci [244]. However, the crux of the matter returns to the proven assumption that DNA DSB formation under soft UV-irradiation is based on the presence of Hoechst and BrdU. That is, eliminating these factors immediately changes conclusions regarding the nature of damage induction. Experiments directly testing the types of damage present after laser microirradiation, as well as examining the effects of high fluences of 800nm light on cells, are essential in establishing and transitioning laser microbeam-based experiments into reliable analytical tools to study DSB damage response.

Our data clearly demonstrate that DNA DSBs alone are insufficient for TRF2 recruitment, and therefore TRF2 is not involved in the early cellular response to DSBs. We believe this conclusion to be congruous with a number of previously published reports. For example, TRF2, and telomeres in general, have been shown to hinder proper repair by locally dampening the ATM-mediated damage response [137] and impairing cell cycle arrest [245]. Also, the TRF2/Rap1 complex inhibits local NHEJ [246], strengthening the view that TRF2, as well as other shelterin components, do not participate in the cellular response to DNA damage, but rather hamper repair of DSBs. Counter to this notion is the demonstration that TRF2, like many DNA repair proteins, is phosphorylated in an ATM-dependent fashion following IR [141]. However, as the specificity of the phospho-specific

TRF2 antibody has been questioned [T. de Lange, personal communication], it may be prudent to view the presence of phosho-TRF2 following IR with a degree of caution.

A primary argument that has been raised in opposition to our conclusions regarding TRF2 recruitment is that absence of evidence is not evidence of absence. This idiom has been applied to our study for two primary reasons; one because the sensitivity of indirect immunofluorescence may not detect low numbers of TRF2 at damage sites, and two, because essential DNA repair proteins, namely DNA-PKcs, do not readily show visible foci at damage sites. However, we believe that we have suitably addressed these issues in our experimental design by utilizing the Columbia charged particle microbeam. The sensitivity for indirect immunofluorescence is not strictly known, although estimates put the detection limit at around 1000 molecules, provided these molecules are localized [247]. Since these estimates were first made nearly twenty years ago, microscopes and cameras have significantly improved and increased the sensitivity of immunofluorescent detection. Our utilization of the charged particle microbeam was principally to address the issue of sensitivity by generating dense regions of DNA damage. We delivered 200 and 400 α-particles to a 5μm area roughly correlating to 40 and 60 Gy and producing 1500 to 2500 DSBs. If only one TRF2 molecule were present at each DSB end— which is highly unlikely given that TRF2 acts en masse at telomeres and forms homodimers *in vivo* [27]—this would be within our detection limit, given the highly focused damage pattern of the charged particle microbeam. Therefore, if TRF2 were present at DNA DSBs even at very low concentrations we would have been able to detect it following the charged particle microbeam experiments, and never was a TRF2-positive damage foci observed.

Repair proteins not normally considered to form foci, such as DNA-PKcs, should be visible following charged particle microbeam exposure for the same reason. It is known that at least one molecule of DNA-PKcs binds to each DNA end [248], thus thousands of localized breaks should bring the number of DNA-PKcs molecules up to a detectable level. Furthermore, it has been demonstrated that under optimized conditions DNA-PKcs foci can be visualized following exposure to γ-rays (J. Nickoloff, personal communication) suggesting that the vast majority of DNA repair proteins do indeed form measurable foci.

An interesting sidebar that resulted from this study was our observation that TRF2 localized to the nucleolus, particularly following exposure to high doses of alpha particles (**Figure 3.9**). This observation was especially striking given the juxtaposition of nucleoli with damage foci in some cells, emphasizing the total lack of co-localization between TRF2 and DNA damage. Several studies have reported TRF2 localization to the nucleolus, though the significance of this remains unclear. Zhang et al. [249] attempted a more careful examination of this localization and found TRF2 existed in the nucleolus throughout the majority of the cell cycle with a significant diffusion from the nucleolus in G2/M phase. They also showed that exposure to actinomycin D sequestered TRF2 in the nucleolus, resulting in telomere fusions and prompting the authors to postulate a regulatory pathway for the nucleolar localization of TRF2. However, Verdun et al. [58] later showed that TRF2 was present at the telomeres throughout the cell cycle, raising doubt to the significance of TRF2 localizing to the nucleolus, particularly as a regulation mechanism, as Zhang et al. [249] proposed. Our studies were unable to discern any predictable pattern of TRF2 nucleolar localization in regards to dose or radiation type, timing, or cell line dependency; although the staining was most prominent in HeLa cells following high doses of alpha

particles. We cannot exclude the possibility that this phenomenon was artifactual, as some treatments, particularly localized UV exposure, caused numerous proteins to localize within the nucleolus. However, even with robust nucleolus staining, the TRF2 staining at the telomeres was not affected, suggesting a large fraction of unbound or non-telomeric TRF2 protein in the cell.

Presently, we can say only that TRF2 is responding to uncharacterized features of the high-intensity laser systems that are not reproducible with other radiation sources. One possibility is that unusual DNA configurations may arise after exposure to such highly concentrated energy deposition. TRF2 has recently been shown to bind DNA in a sequence-independent, yet structure-dependent manner, interacting with replication-related intermediates such as four-way strand-junctions [136]. These interactions require the basic N-terminal domain of TRF2, which has also been implicated in TRF2 recruitment to laser-damaged sites [135]. It may be possible that DNA structures resembling replication intermediates are formed in response to high-intensity laser exposure, although without direct experimental evidence, this is merely conjecture. In any case, while the initiating lesion(s) responsible for TRF2 recruitment remain elusive, our results cast serious doubt on TRF2 playing a biologically relevant role in response to exogenous DNA damage, particularly DSBs. Moreover, they serve to illustrate meaningful differences in the cellular response to high-intensity laser systems versus other types of radiation damage.

TABLE 3.1. Summary of protein responses following exposure to various DNA damaging sources

Exposure			*Detection*	*Protein Recruitment*			
				TRF2	NHEJ	NER	General DSB Marker
Laser-induced damage	Multiphoton	800 nm multiphoton laser +Hoechst 33258	Live cell imaging	Present (24% laser power)	Ku80 (15%)	XPC (15%)	N.D.
		800 nm multiphoton laser –Hoechst 33258	Live cell imaging	Present (95% laser power)	Ku80 (60%)	XPC (60%)	N.D.
	UVA	405 nm laser + Hoechst 33258	Live cell imaging and immunofluorescence	Absent	N.D.	XPC present (live cell)	γ-H2AX present (IF)
Ionizing Radiation	High LET	Single α-particle (Longitudinal)	Immunofluorescence	Absent	Data not shown	N.D.	γ-H2AX, MDC1, and 53BP1 present
		High Localized α-particle (Perpendicular)	Immunofluorescence	Absent (200 and 400 α-particles; ~30 and 60 Gy)	N.D.	N.D.	γ-H2AX and MDC1 present (200 and 400 α-particles)
	Low LET	γ-Ray Exposure	Immunofluorescence	Absent (5 Gy)	N.D.	N.D.	γ-H2AX present
UVC		Localized UVC (254 nm)	Live cell imaging	Absent (100 and 1000 J/m^2)	N.D.	DDB2 present (100 and 1000 J/m^2)	N.D.

N.D. not determined

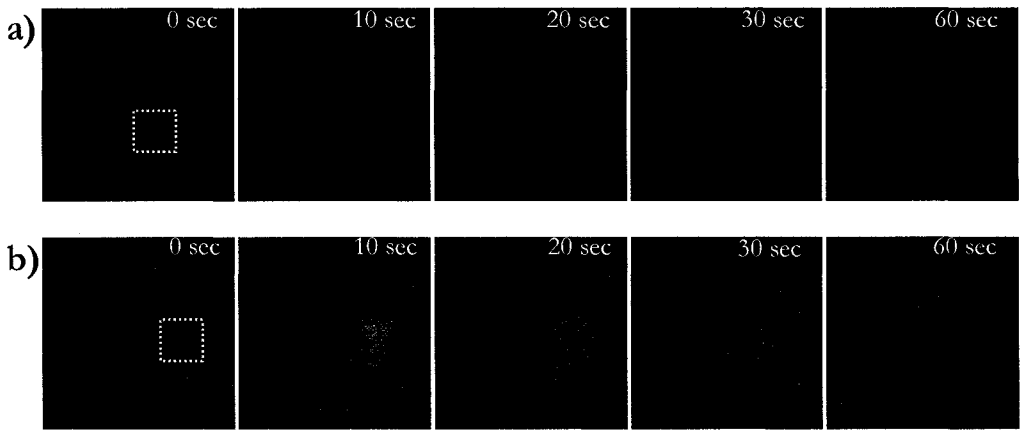

Figure 3.1. Recruitment of repair proteins in response to laser microirradiation. Exposure of cells to multiphoton laser beams at 15% of maximum laser output in the presence of Hoechst 33258 recruits the repair proteins (a) XPC and (b) Ku80 within 10 seconds of exposure.

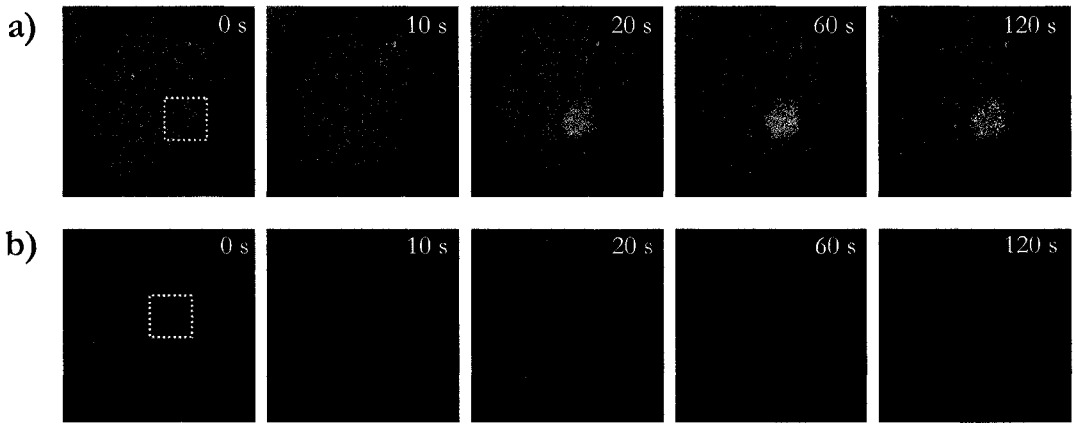

Figure 3.2. TRF2 recruitment to laser microirradiation. HeLa cells expressing TRF-GFP were exposed to a multiphoton laser beam (a) in the presence of Hoechst 33258 (10μg/mL) or (b) in the absence of Hoechst 33258. TRF2 recruitment in the presence of Hoechst was significantly more robust and required lower laser output (24% versus 90%) than in the absence of Hoechst.

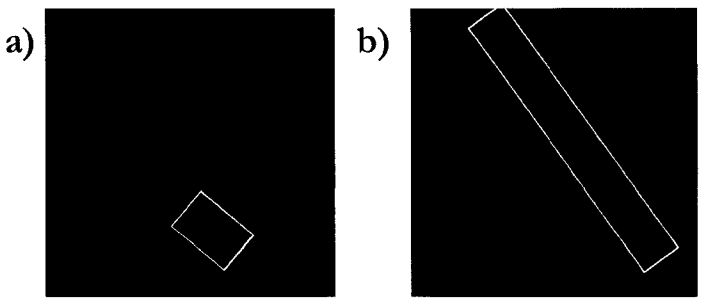

Figure 3.3. TRF2 response to 405nm UVA exposure in the presence of Hoechst 33258. A 405nm UVA laser was exposed to a confined area in (a) a single HeLa nucleus or (b) across two HeLa nuclei (damaged area marked by rectangles) in the presence of Hoechst 33258. Dual staining for γ-H2AX (green) and TRF2 (red) shows no evidence of co-localization 10 minutes following exposure.

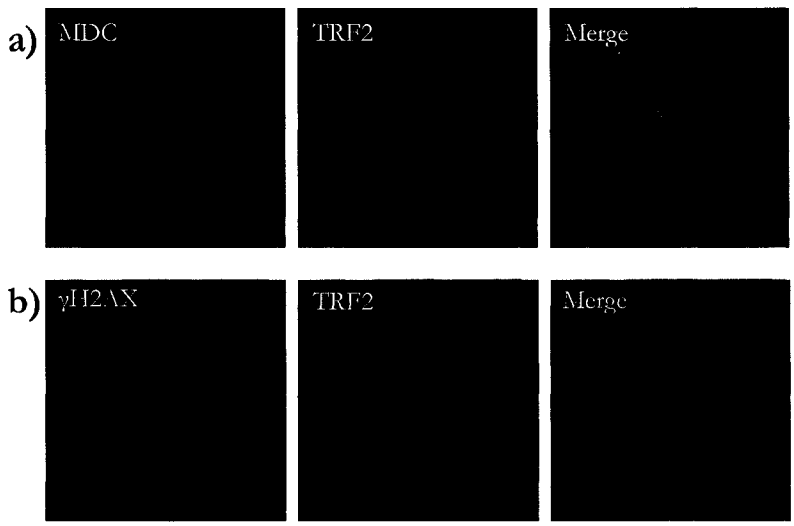

Figure 3.4. TRF2 fails to co-localize with DNA damage generated by α-particle irradiation. (a) Maximum intensity projection from a reconstructed stack of images of a U2OS nucleus 90 sec after *longitudinal* transversal by two α-particles shows well-defined damage tracks (MDC1− green) with no change in TRF2 staining pattern (red). (b) Maximum intensity projection from a reconstructed stack of images of HeLa nuclei 90 sec after *longitudinal* transversal by a single particle shows well-defined damage tracks (γ-H2AX− red) with no change in TRF2 staining pattern (green).

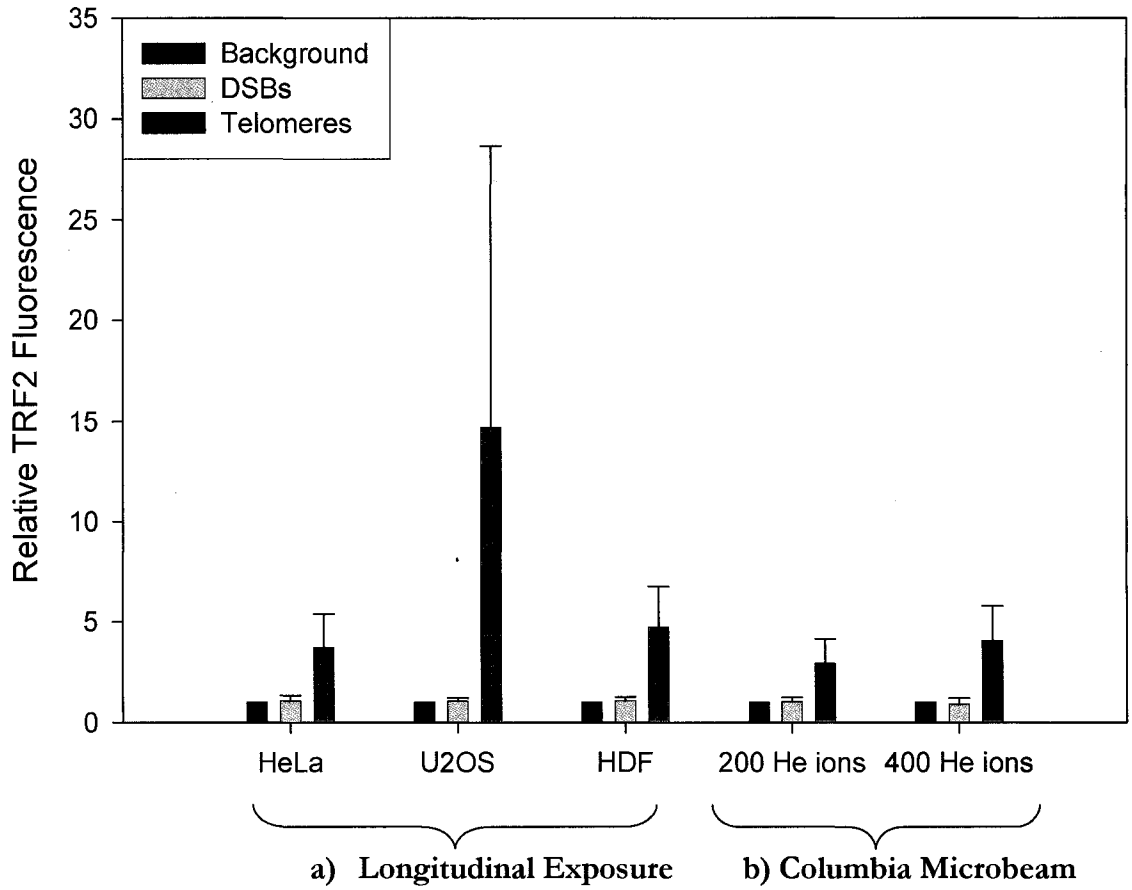

Figure 3.5. Quantitation of TRF2 fluorecence intensity following various exposures to high LET ionizing radiation. TRF2 fluorescence intensity (mean ± s.d.; n=10) was measured after (a) exposure of three cell types of varying telomerase status to longitudinal exposure to one or two α-particles or (b) exposure of HeLa cells to varying numbers of He ions. TRF2 fluorescence intensity is measured 10 minutes after exposure.

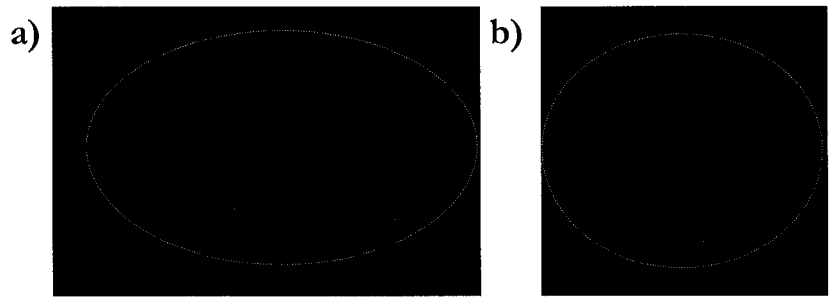

Figure 3.6. TRF2 recruitment to γ-ray induced DNA damage. HeLa cells exposed to 2 Gy low LET γ-rays shows no recruitment of TRF2 (green) to sites of damage marked by γ–H2AX (green) at (a) 2 minutes or (b) 5 minutes after exposure. Cell nuclei are outlined in white for clarity.

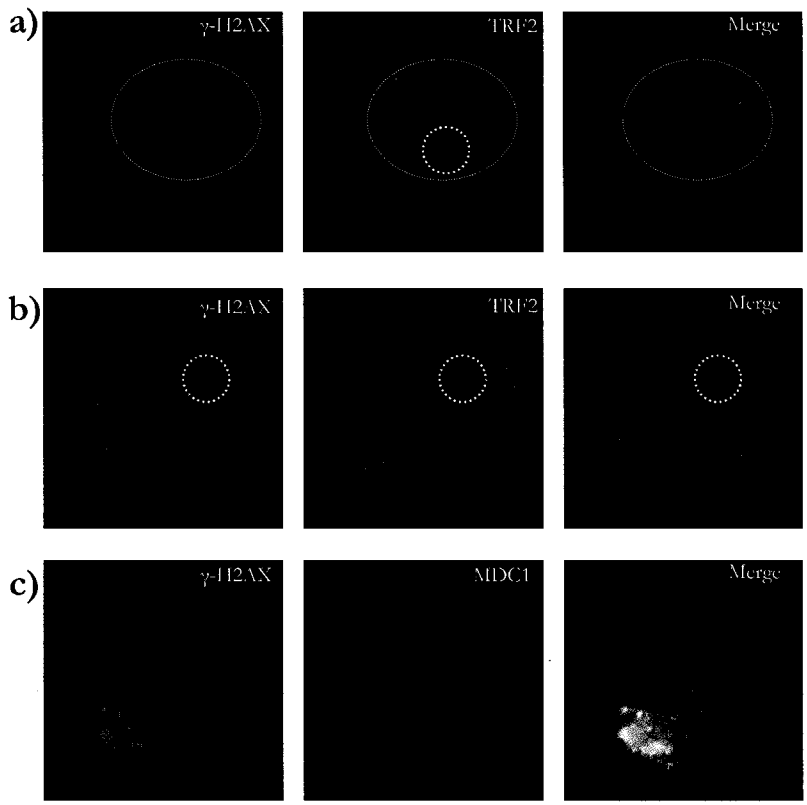

Figure 3.7. Protein response to high LET He ions delivered by the Columbia charged particle microbeam. Perpendicular exposure of either (a) 200 He ions or (b) 400 He ions to a 5μm diameter area of HeLa cell nuclei shows robust γH2AX recruitment but no recruitment of TRF2 10 minutes following exposure. (c) DNA damage markers γ-H2AX and MDC1 are rapidly recruited and co-localize at damage sites 30 minutes following exposure.

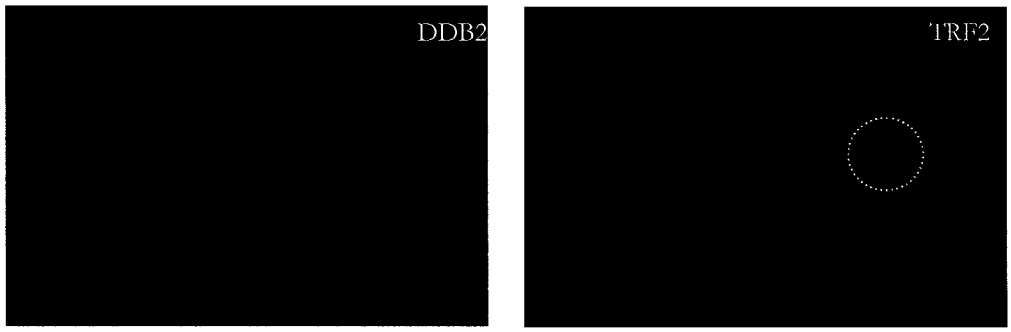

Figure 3.8. TRF2 recruitment to localized UVC damage. Cell nuclei show no recruitment of TRF2-GFP (green) to damage sites as marked by DDB2-mCherry (red) after exposure to localized UVC irradiation in this representative image ($1000J/m^2$, t=5 minutes after illumination).

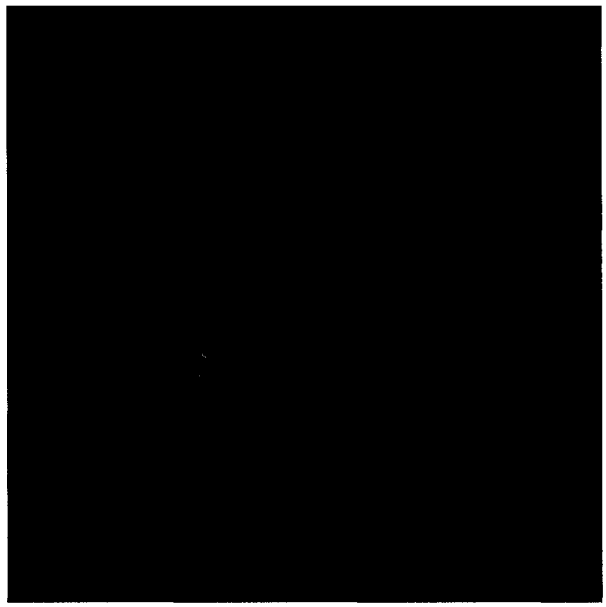

Figure 3.9. TRF2 accumulates in the nucleolus following IR exposure. In some instances, TRF2 showed strong nucleolar staining following exposure to localized damage. Even when this large pool of nucleolar TRF2 (red) was juxtaposed with localized DNA damage (γH2AX-green) induced by high numbers of He ions, no significant co-localization is seen.

IV. DNA-PKcs

ABSTRACT

The essential DNA repair protein, DNA-PKcs, has been shown to play a critical role in capping of mammalian telomeres. However, the precise manner of interaction remains unclear, and the contribution of telomere dysfunction to genomic instability and organism survival remains controversial. Recent work examining the role of DNA-PKcs in NHEJ has demonstrated that auto-phosphorylation of DNA-PKcs is critical for proper end-joining. In the current study, we investigate the effects of mutations in DNA-PKcs auto-phosphorylation sites on telomere end-capping and find that these sites are *in vivo* targets in telomere capping. The telomere phenotype of the Balb/c mouse is also characterized, and we demonstrate that, like other DNA-PKcs deficient cells, cells from the Balb/c mouse show telomere dysfunction. Utilization of the Balb/c mouse will be useful in determining the impact of telomere dysfunction on the delayed genomic instability observed in the Balb/c mouse, addressing the issue of the contribution of telomere dysfunction in carcinogenesis. Finally, we show that RNA interference (RNAi) knockdown of DNA-PK subunits induces telomere dysfunction in human cells, which is significant given that all previous studies of DNA-PKcs and telomeres have used mouse models.

INTRODUCTION

DNA-PKcs plays an important, yet undefined, role at the telomeres of vertebrate cells. Cells deficient in DNA-PKcs, such as cells derived from severe combined immunodeficiency (SCID) mice, display end-to-end chromosome fusions which maintain telomere sequence at the point of fusion (telomere fusions) [60]. Telomere fusions arise as a result of improper capping of the telomere following replication, not from the stochastic

telomere loss reported in cells deficient in the RecQ helicase WRN [66]. Instead, significant telomere length remains at the point of fusion implicating a disruption in the cap structure as the causative event.

The frequency of telomere fusions has been shown to vary somewhat depending on cell line and other experimental conditions, with an approximate occurrence of 0.1 fusions per cell [60,62,178,250]. In contrast, depletion of the telomere specific end-capping protein, TRF2, results in a much higher frequency of telomere fusions, approximately three per cell [175]. The relatively mild telomere fusion phenotype in DNA-PKcs deficient cells suggests that DNA-PKcs may not be strictly necessary for telomeric end-capping or may be required only at a subset of telomeres. A mechanistic explanation may also account for this discrepancy as NHEJ is suggested to misjoin the majority of telomere fusions. DNA-PKcs is an essential element of NHEJ, thus dysfunctional telomeres in DNA-PKcs deficient cells may not be fused together as readily as TRF2 deficient cells. We show that absence of ligase IV, the essential end-joining protein of NHEJ, is required for telomere fusion formation following chemical inhibiton of DNA-PKcs kinase activity. This observation clearly points to a required role for NHEJ in fusing dysfunctional telomeres.

Recent investigations into the role of DNA-PKcs in NHEJ have provided clues as to the manner in which DNA-PKcs interacts with DNA ends that may be relevant to its role at telomeres. Two auto-phosphorylation clusters are present on the DNA-PKcs protein which are phosphorylated in response to DNA damage *in vivo* [167,168,170]. It is becoming clear that phosphorylation of these sites promotes a conformational change in the DNA-PKcs protein allowing processing of DNA ends for rejoining [170,171,174]. Cells expressing an unphosphorylatable form of DNA-PKcs shows more severe radiosensitivity then cells

simply lacking DNA-PKcs [171]. Furthermore, the inability to phosphorylate DNA-PKcs inhibits Artemis nuclease acitivity at the DNA end [174]. Together these data support the hypothesis that once bound to the DNA end, DNA-PKcs is auto-phosphorylated to relieve the steric hindrance caused by its binding, thereby promoting end processing and rejoining. Interestingly, it was demonstrated that a catalytically inactive DNA-PKcs more severely impedes telomere end-capping than absence of DNA-PKcs alone, perhaps through a similar dominant negative effect [59]. This evidence leads one to hypothesize, as Bailey et al. [59] propose, that kinase inhibition results in the inability of DNA-PKcs to auto-phosphorylate, resulting in a conformational change promoting telomere end processing. We directly test this hypothesis in the current study by performing CO-FISH analysis of DNA-PKcs auto-phosphorylation mutants. We find that auto-phosphorylation of DNA-PKcs is indeed an important *in vivo* target for proper telomere function [manuscript in preparation].

The role of DNA-PKcs in telomere end-capping has been demonstrated independently by several laboratories in a variety of experimental systems. However, the impact of this interaction on organism survival and carcinogenesis remains controversial. Work from the Blasco lab [177] has pointed to accelerated aging and tissue atrophy in mice doubly deficient for DNA-PKcs and Terc compared to those deficient in Terc alone, however no evidence for increased tumorigenesis was observed. Bailey et al. [178] has demonstrated the ability of dysfunctional telomeres to fuse with DNA DSBs to produce chromosomal translocations, an aberration known to promote carcinogenesis in some situations. The frequency of telomere-DSBs was shown to increase in a dose dependent manner, however, the contribution of this event in generating genomic instability, particularly in unirradiated cells or cells many generations after irradiation is unknown.

The Balb/c mouse has been used extensively as a model for genomic instability and thus provides a model for investigating the effects of telomeres on instability. Previous work with the Balb/c mouse has demonstrated an increased incidence of radiation-induced mammary cancer compared to other mouse strains [251]. It has been established that this difference in strain susceptibility results from differences in the sensitivity of mammary epithelial target cells to radiation-induced transformation [252]. Work from our laboratory has demonstrated that Balb/c mammary epithelial cells display increased radiation-induced chromosomal instability [253] strengthening the hypothesis that genomic instability is linked to the mechanism of radiation carcinogenesis. In seeking an explanation for these phenotypes, the efficiency of DNA DSB rejoining in Balb/c mouse cells was investigated and it was discovered that the Balb/c mouse possessed significantly reduced levels and activity of DNA-PKcs [254]. This observation naturally leads to the investigation of telomere status in the Balb/c mouse. We show that, in fact, telomeres in Balb/c cells show an increased dysfunction compared to telomeres in the C57BL/6 mouse. This observation supports the view that Balb/c is a good experimental model for investigating the role of telomere dysfunction in promoting genomic instability, a topic of active investigation in our laboratory.

The majority of experimental models used to examine the role of DNA-PKcs in telomere function have utilized mouse models [175,250,255], as do the studies already discussed in this introduction. In many regards, mouse telomeres serve as good models for human telomeres, however differences do exist. Recently it was demonstrated that mouse cells have two distinct POT1 proteins, POT1a and POT1b, whereas human cells only have one [256,257] raising concerns over the homology of telomere metabolism in the two

organisms. Furthermore, it has been demonstrated that telomeres of inbred mouse strains are an order of magnitude longer than human telomeres and telomerase is constitutively active in mouse cells [258]. In order to determine the contribution of DNA-PKcs and Ku80 in human telomere end-capping, we depleted cells of each protein individually, or in tandem, via RNAi. A significant induction of telomere fusions was observed in cells knocked down for either protein demonstrating a conservation of function between mouse and human.

RESULTS

Cells expressing mutations in the threonine 2609 auto-phosphorylation cluster show increased telomere dysfunction

Cells used in this study included those expressing either (a) wild type DNA-PKcs, (b) kinase dead DNA-PKcs, (c) DNA-PKcs in which six of the previously identified threonine 2609 cluster auto-phosphorylation sites (threonines 2609, 2638, and 2647, and serines 2612, 2620, 2624) have been mutated to alanine (named ABCDE mutant), or (d) DNA-PKcs in which five of the previously identified serine 2056 cluster of auto-phosphorylation sites (serines 2023, 2029, 2041, 2053, 2056) have been mutated to alanine (named PQR mutant) [170]. To determine the extent of telomere dysfunction in these cells, telomere FISH was performed. Cells expressing the ABCDE mutation show an increased induction of telomere signals occurring interstitially compared to WT (**Figures 4.1, 4.2, 4.3 and Table 4.1**). The frequency of internal telomere sequences (ITS) in the ABCDE mutant was nearly as abundant as internal telomere signals seen in cells expressing a kinase dead form of DNA-PKcs, which is known to be essential in DNA-PKcs' function at telomeres. Cells expressing

the PQR mutant surprisingly showed a decrease of internal telomere signals compared to WT. While this supports the proposed reciprocal action of the two auto-phosphorylation sites [170], the relatively high background observed in cells expressing WT DNA-PKcs may skew this data. The significance of internal telomere signals in cells expressing WT DNA-PKcs is unknown, but may arise from the clonal expansion of a single event. While clonal events are excluded in the scoring of these cells, the inability to identify individual mouse chromosomes may allow the inclusion of a small number of these events. Exposure of cells to ionizing radiation did not significantly increase the frequency of internal telomere signals, indicating that these signals are a result of telomere-telomere fusions, not telomere-DSB fusions (**Figure 4.3 and Table 4.2**).

To further confirm the presence of dysfunctional telomeres in these cells, we employed a novel method called immunoFISH. With this technique, telomere FISH is performed followed by staining for the DNA damage marker γ-H2AX, thereby allowing the identification of telomeres triggering the DNA damage response, i.e. dysfunctional telomeres. Cells expressing the ABCDE mutation showed a significant increase in the number of telomere/γ-H2AX co-localizations supporting the notion that the threonine 2609 auto-phosphorylation cluster is an important *in vivo* target for proper telomere capping (**Figures 4.4, 4.5 and Table 4.3**). As in the telomere FISH analysis, the frequency of telomere dysfunction in the ABCDE mutant was similar to that of cells expressing a kinase dead DNA-PKcs, indicating that this site is a critical *in vivo* targe for proper telomere function. The frequency of telomere dysfunction in cells expressing the PQR mutant showed no change compared to WT, suggesting that auto-phosphorylation of the Serine 2056 is not needed for proper telomere function.

Ligase IV is essential for telomere fusion formation in DNA-PKcs inhibited cells

Mouse embryonic fibroblasts (MEFs) deficient in p53 ($p53^{-/-}$) or MEFs doubly deficient for p53 and ligase IV ($p53^{-/-}$, $ligIV^{-/-}$) were exposed to a chemical inhibitor of the kinase activity of DNA-PKcs. This drug, NU7026 (2-(morpholin-4-yl)-benzo[h]chomen-4-one) is a selective and highly competitive inhibitor of the kinase activity of DNA-PKcs, and inactive to ATM and ATR [259]. Following exposure for one cell cycle in NU7026, cells were collected and analyzed via telomere FISH. A dramatic induction of telomere fusions was observed in $p53^{-/-}$ MEFs grown in the presence of the inhibitor compared to control $p53^{-/-}$ MEFs (**Figure 4.6 and Table 4.4**). These results are consistent with previous work showing that the inhibition of the kinase activity of the DNA-PKcs is a potent inducer of telomere dysfunction [59]. In contrast, $p53^{-/-}$, $ligIV^{-/-}$ MEFs showed no significant increase in telomere fusions when grown in the presence of NU7026, rather an increase in telomere associations, the unusually close proximity of two telomeres of the same or different metaphase chromosomes. This clearly demonstrates that ligase IV (and therefore NHEJ) is the primary pathway in generating fusions in DNA-PKcs deficient cells.

Characterizing the telomeres in the Balb/c mouse

The incidence of telomere-DSB fusions in mammary fibroblasts derived from the Balb/c and C57BL/6 mice is shown in figure 4.7. The frequency of telomere-DSB fusions in Balb/c increases as a function of dose, indicating that dysfunctional telomeres, rather than

breaks, limit the formation of telomere-DSB fusions. Furthermore, the prevalence of telomere-DSB fusions was higher at all dose points than that of dicentric chromosome formation suggesting that telomere-DSB formation is an abundant event following IR in DNA-PKcs deficient backgrounds. Telomere-DSB fusions were never observed in C57BL/6 cells.

We examined whether Balb/c had an increased level of DNA DSBs compared to C57BL/6 immediately following IR, as measured by the γ-H2AX assay. While Balb/c appears to have a slight, but statistically insignificant, increase in the number of foci present in unirradiated mammary fibroblasts (MFs) compared to C57BL/6, the number of foci following exposure to 1 Gy γ-rays was the same (**Figure 4.8** and **Table 4.5)**. This is not surprising, since it has been shown that ATM is primarily responsible for phosphorylating H2AX following IR [260]. Next, we were interested to determine if the slight increase seen in unirradiated Balb/c MFs could be due to dysfunctional telomeres signaling a DNA damage response. To address this we utilized immunoFISH to determine the co-localization of γ-H2AX with telomeric DNA. ImmunoFISH analysis shows an increased incidence of telomere dysfunction in Balb/c MFs compared to C57, and this dysfunction is further exacerbated by the induction of DSBs via exposure to IR (**Figures 4.9, 4.10** and **Table 4.6**). These data further support the hypothesis that DNA-PKcs is necessary for proper telomere capping, and that deficiencies in DNA-PKcs result in telomeres signaling DNA damage responses, becoming fused to other dysfunctional telomeres or DNA DSBs.

To determine the effect of Balb/c telomere dysfunction in promoting the genomic instability seen following IR, we exposed Balb/c, $p53^{-/-}$ mammary epithelial cells to IR and monitored the induction of telomere dysfunction via telomere CO-FISH. An unanticipated

spike in the level of telomere-DSB fusions was observed at P2 (day 10) following exposure to 0.25 Gy, but not at higher doses (**Figure 4.11**). The significance of this observation is unknown. It may indicate that, in the presence of few DNA DSBs, dysfunctional telomeres are more abundant substrate for joining. The contribution of telomere dysfunction to genomic instability was not able to be determined in this study, as cells could not be kept in culture for times corresponding to the reported increase in genomic instability in the Balb/c mouse [253]. Other than the noted "spike" in telomere-DSBs, no evidence of increased or delayed telomere dysfunction was observed. Further experiments to determine the role of telomere dysfunction in driving genomic instability in the Balb/c mouse are on-going. Evidence for telomere dysfunction driving genomic instability has come from studies in SCID/p53$^{-/-}$ MFs. Utilizing a combined Spectral Karyotyping (SKY) and CO-FISH technique allows us to identify clonal chromosome rearrangements, as well as telomere localization (**Figure 4.12**). Indeed, one of three clonal populations identified via this method identified a telomere at the point of chromosome fusion, thus providing direct evidence of telomere-DSB fusions promoting chromosomal rearrangements.

Suppression of DNA-PK by RNAi in human lymphoblastoid cell lines results in increased telomere-telomere fusions

Human TK6 (TP53 wild-type) and WTK1 (TP53 mutant) were transfected with siRNA for DNA-PKcs, Ku80, or the two combined. Western blotting confirmed that protein levels were significantly decreased, with maximal depletion of protein levels 72 hours

after transfection [261]. Following transfection of siRNA, we performed cytogenetic analysis via telomere FISH and CO-FISH.

Knockdown of DNA-PKcs and Ku80 in TK6 cells showed similar levels of spontaneous telomere-telomere fusions (**Figure 4.13** and **Table 4.7**). Telomere-telomere fusions in TK6 cells transfected with a non-specific siRNA occurred in approximately 2% of metaphases, whereas knockdown of DNA-PKcs and Ku resulted in 17 % and 19% of metaphases showing telomere-telomere fusions, respectively. The combined knockdown of both proteins resulted in a further increase in the frequency of telomere-telomere fusions with 32% of metaphases containing a telomere-telomere fusion. It is extremely unlikely that Ku80 and DNA-PKcs act in different pathways at telomeres, given that they are subunits of the same protein, so we surmise that this apparent additive effect is a result of residual protein activity in the single knockdowns.

We next conducted experiments to compare the effects of different qualities of radiation on telomere function in cells compromised for NHEJ. WTK1 cells were transfected with siRNA specific for DNA-PKcs and then exposed to 1.5 Gy ^{56}Fe ions. In parallel, TK6 cells underwent the same siRNA treatment followed by exposure to 1.5 Gy γ-rays. For both irradiations, cells were collected and prepared for telomere CO-FISH and analyzed for telomere-telomere and telomere-DSB fusions. A significant increase in telomere-DSB fusions was observed following exposure to ^{56}Fe ions in cells depleted of DNA-PKcs, but not in cells transfected with a nonspecific siRNA (**Figure 4.14** and **Table 4.8**). Both unirradiated cells and cells transfected with nonspecific siRNA caused 10% of metaphases to be positive for telomere-DSB fusions, while exposure following DNA-PKcs knockdown reached levels near 80% of fusion positive metaphases. In comparison, cells

exposed to γ-rays following RNAi depletion of DNA-PKcs showed only a modest increase in telomere-DSB fusions. No significant effect on the frequency of telomere-telomere fusions was observed following exposure to either type of radiation.

DISCUSSION

The results presented here provide the first evidence that auto-phosphorylation of DNA-PKcs at threonine-2609 is an important *in vivo* target for telomere end-capping. It is reasonable to assume that the effects of auto-phosphorylation of DNA-PKcs at telomeres mimic those at sites of DNA DSBs, which is to cause a conformational change allowing protein access to the DNA end [170,171,174]. However, some key differences exist between DNA-PKcs binding to telomeres compared to DNA DSBs. A primary difference is that only one telomeric end exists, whereas at DNA DSBs there will presumably be two ends in close proximity. It was recently demonstrated that the auto-phosphorylation of DNA-PKcs occurs in *trans-* [173] which is facilitated by the juxtaposition of two DNA-PKcs molecules at each synapse. Unless two or more DNA-PKcs molecules are recruited to telomeres, the ability to auto-phosphorylate in *trans-* is lost.

Interestingly, ATM was recently shown to phosphorylate the threonine-2609 cluster in response to IR, but not the serine-2056 cluster [172]. This observation fits well with our data that the threonine-2609 cluster, but not the serine-2056 cluster, is important for telomere function, and suggests that ATM, not DNA-PKcs, may be the kinase responsible for phosphorylation of this cluster at telomeres. However, the kinase activity of ATM has been shown to be attenuated at telomeres through interactions with TRF2 [137]. While the responsible kinase for DNA-PKcs phosphorylation at telomeres remains to be determined,

our data supports a model in which DNA-PKcs rapidly binds to telomeres produced by leading strand DNA synthesis. The specificity of DNA-PKcs for leading-strand telomeres also remains to be determined, but our working hypothesis is that the blunt-ended leading-strand telomere acts to trigger a DNA damage response, whereas the single-strand overhang of the lagging strand telomere does not. Once DNA-PKcs binds to leading strand telomeres, it sterically blocks the telomere from further processing. Phosphorylation of the threonine-2609 cluster of DNA-PKcs induces a conformational change allowing as yet unidentified factors access to properly cap the telomere, thereby distinguishing it from a DNA DSB.

Our work in the Balb/c mouse has demonstrated this mouse model to be an excellent system for determining the contribution of telomere dysfunction in driving genomic instability. The similarity in frequency of γ-H2AX foci in Balb/c and C57BL/6 cells indicates that telomere dysfunction does not induce an overt DNA damage response. Rather, when presented with a suitable substrate for ligation, such as an IR-induced DNA DSB, cells can (and will) improperly fuse telomeres to DSBs at levels consistent with, or even higher than, common chromosome rearrangements like dicentrics. We have shown that telomere-DSB fusions can promote a cellular growth advantage as this type of event was observed clonally. The DNA-PKcs deficiency in Balb/c results in telomere uncapping consistent with other DNA-PKcs deficient cells. Tracking the levels of telomere dysfunction through the known genomic instability of Balb/c will provide clear evidence to determine the relationship between telomeres and genomic instability.

Our results demonstrate that RNAi depletion of DNA-PK protein levels in human lymphoblastoid cells leads to increased telomere-telomere and telomere-DSB, and this

induction of telomere dysfunction in human cells mimics that seen in DNA-PKcs deficient mouse cells. This is an important observation given the wide use of mouse models for telomere structure and function studies, and the recent reports of subtle, but significant, differences in telomere proteins between mice and humans [256,257]. Additionally, we demonstrate that different qualities of radiation have different quantitative effects on telomere dysfunction, with high-energy heavy ion exposure being especially effective at generating the telomere-DSB endpoint, while γ-ray exposure showed only a modest increase in telomere-DSB fusions. The use of IR in studying telomeres has proven to be an especially valuable, as it increases the sensitivity of telomere FISH in detecting dysfunctional telomeres. Our study shows that following IR the frequency of telomere dysfunction is increased, indicating that telomeres are the limiting factor in the formation of these cytogenetically measurable end points. This is logical as two dysfunctional telomeres, in close proximity, are required to produce a measurable event in unirradiated cells; the induction of DNA DSBs via IR provides multiple substrates suitable (i.e. DSBs) for a single dysfunctional telomere to fuse.

Table 4.1. Telomere dysfunction in cells expressing DNA-PKcs mutants (0 Gy)					
DNA-PKcs status	Cells scored	Telomere Fusions (TF)	TF per Cell	Internal Telomere Signal (ITS)	ITS per Cell
Wild-type	75	0	0	18	0.24
Kinase Dead	75	5	0.067	37	0.49*
ABCDE Mutant	75	5	0.067	36	0.48*
PQR Mutant	50	0	0	2	0.04*

* indicates significant deviation from WT ($p < 0.05$)

Table 4.2. Telomere dysfunction in cells expressing DNA-PKcs mutants (1 Gy)					
DNA-PKcs status	Cells scored	Telomere Fusions (TF)	TF per Cell	Internal Telomere Signal (ITS)	ITS per Cell
Wild-type	25	6	0.24	6	0.24
Kinase Dead	25	5	0.20	16	0.64*
ABCDE Mutant	25	1	0.04	14	0.56*
PQR Mutant	25	4	0.16	4	0.16

* indicates significant deviation from WT ($p < 0.05$)

Table 4.3. ImmunoFISH analysis of cells expressing DNA-PKcs mutants (0 Gy)			
DNA-PKcs status	Cells scored	Telomere and γH2AX co-localizations	Co-localizations per cell
Wild-type	100	88	0.88
Kinase Dead	100	220	2.2*
ABCDE Mutant	100	216	2.16*
PQR Mutant	100	75	0.75

* indicates significant deviation from WT ($p < 0.01$)

Table 4.4. DNA-PKcs kinase inhibition leads to an increase in telomere fuisions only in the presence of Ligase IV

Cell Line	NU7026 Concentration	Cells Scored	Telomere Fusions	Telomere Fusions per cell
p53-/- MEFs	0 μM	10	0	0.0
	55 μM	10	16	1.6*
p53-/-, LigIV-/- MEFs	0 μM	10	0	0.0
	55 μM	10	2	0.2*

*indicates a significant difference compared to control ($p < 0.05$)

Table 4.5. Frequency of γ-H2AX foci in C57BL/6 and Balb/c mammary fibroblasts								
Cell Line	Dose	Cells Scored	γH2AX Foci per Cell					
			0	1 – 5	6 – 15	16 – 25	26 – 50	51+
C57BL/6	0 Gy	506	286	105	77	25	7	6
		100%	56.5%	20.8%	15.2%	4.9%	1.4%	1.2%
	1 Gy	505	0	20	270	159	55	1
		100%	0.0%	4.0%	53.5%	31.5%	10.9%	0.2%
Balb/c	0 Gy	501	287	124	76	12	1	1
		100%	57.3%	24.8%	15.2%	2.4%	0.2%	0.2%
	1 Gy	530	2	39	284	142	60	3
		100%	0.4%	7.4%	53.6%	26.8%	11.3%	0.6%

Table 4.6. ImmunoFISH analysis of C57 BL/6 and Balb/c mice				
Cell Line	Dose	Cells Scored	Telomere and γH2AX co-localizations	Co-localizations per cell
C57BL/6	0 Gy	238	0	0.0
	1 Gy	208	12	0.058
Balb/c	0 Gy	222	4	0.018*
	1 Gy	220	30	0.136*

*indicates significant deviation from control

Table 4.7. Spontaneous telomere fusions in TK6 cells following RNAi knockdown of DNA-PK subunits

siRNA Target	Cells scored	Telomere Fusions	Telomere Fusions per cell
Non-specific	105	2	0.02
Ku80	21	4	0.19
DNA-PKcs	46	8	0.17
Both Ku80 and PKcs	25	8	0.32

Table 4.8. Telomere dysfunction following knockdown of DNA-PKcs and exposure to γ-rays and HZE particles in human lymphoblasts

Cell line	Dose	Condition	Cells scored	Telomere-Telomere Fusions	T-T Fusions per cell	Telomere-DSB Fusions	T-DSB Fusions per cell
TK6	0 Gy (γ-rays)	Mock	105	2	0.019	20	0.19
		siRNA	46	8	0.17	8	0.17
	1.5 Gy (γ rays)	Mock	21	1	0.04	3	0.14
		siRNA	37	7	0.19	11	0.30
WTK1	0 Gy (HZE)	Mock	30	0	0.0	3	0.10
		siRNA	35	6	0.17	2	0.05
	1.5 Gy (HZE)	Mock	30	0	0.0	3	0.10
		siRNA	19	4	0.21	15	0.79

Figure 4.1. Cells mutated at the Thr-2609 cluster of autophosphorylation site of DNA-PKcs (ABCDE mutants) show large internal blocks of telomere signal.

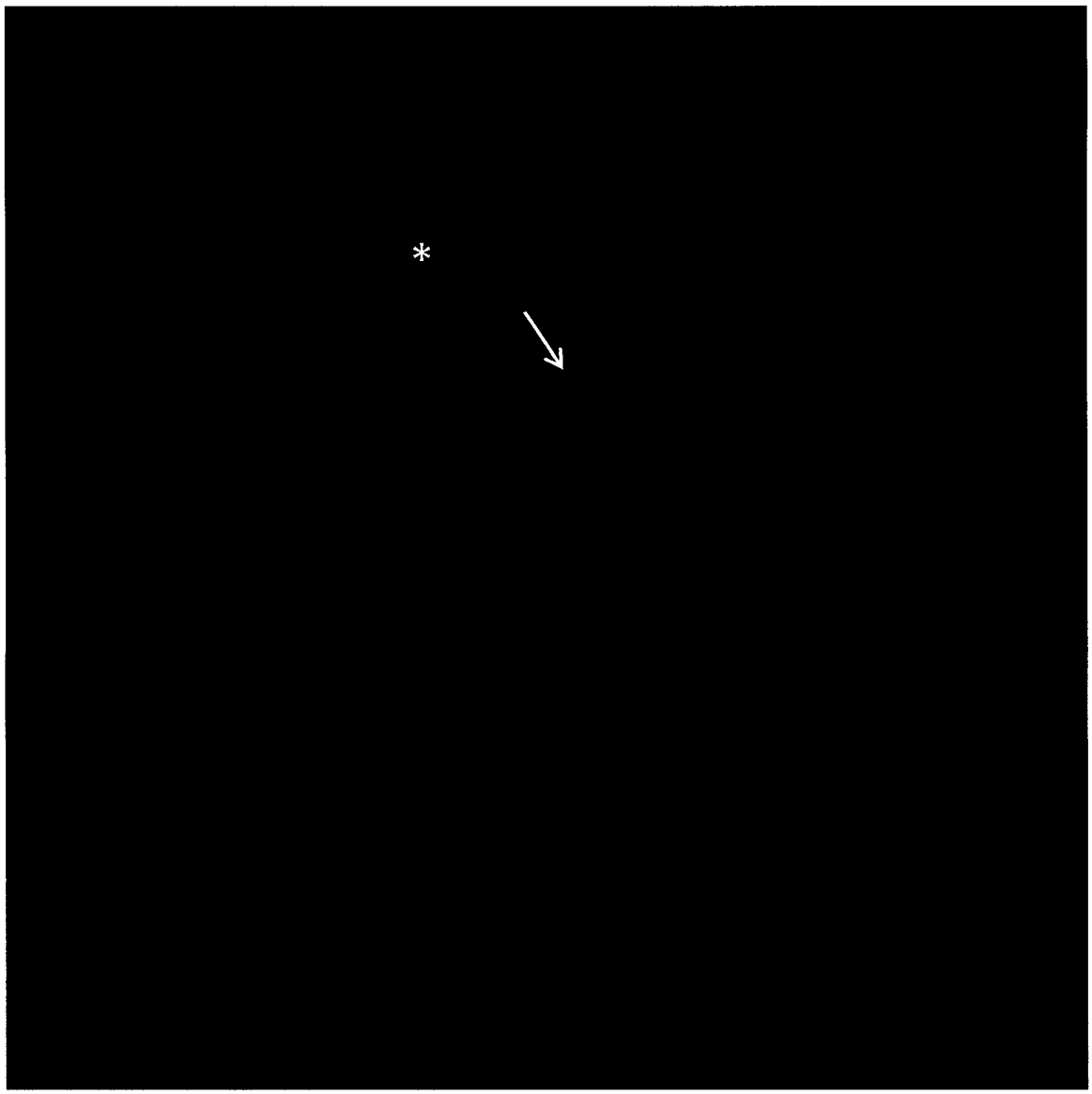

Figure 4.2. Internal telomere signals (ITS) in ABCDE mutant. This typical metaphase spread shows a chromosome displaying an ITS on both chromatid arms (marked by arrow) demonstrating telomere dysfunction in this cell line. Also, note the long "train" of chromosomes (marked by star) devoid of telomere sequence at the point of fusion, indicating the presence of telomere-independent genomic instability.

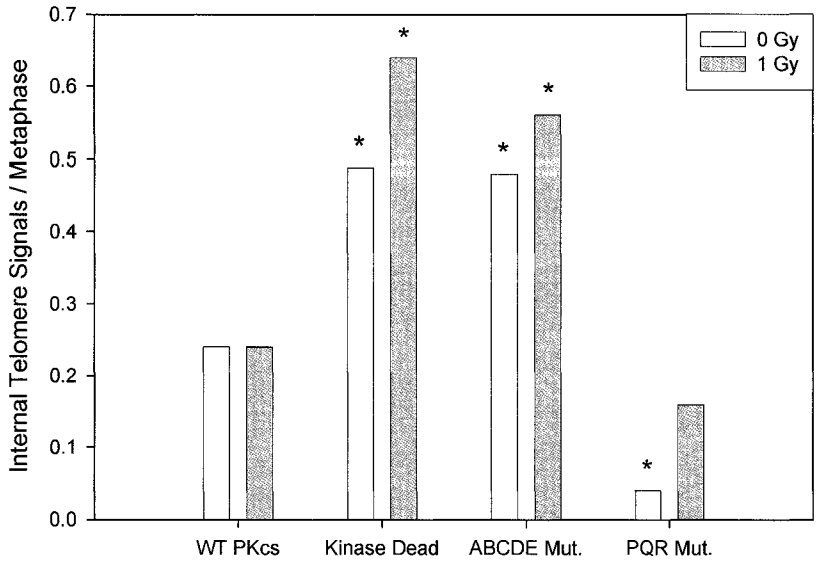

Figure 4.3. Frequency of ITS in DNA-PKcs auto-phosphorylation mutants. Significant increases (*$p < 0.05$) are seen in ITS frequency in cells expressing a kinase dead DNA-PKcs and ABCDE mutant compared to WT control, both in unirradiated and irradiated cells. The increase in ITS between irradiated samples and unirradiated samples is likely due to the formation of telomere-DSB fusions, although this increase is insignificant.

Figure 4.4. ImmunoFISH analysis of the ABCDE mutant reveals the co-localization of telomere DNA and the DNA damage marker γ-H2AX, indicating that telomeres are triggering a DNA damage response.

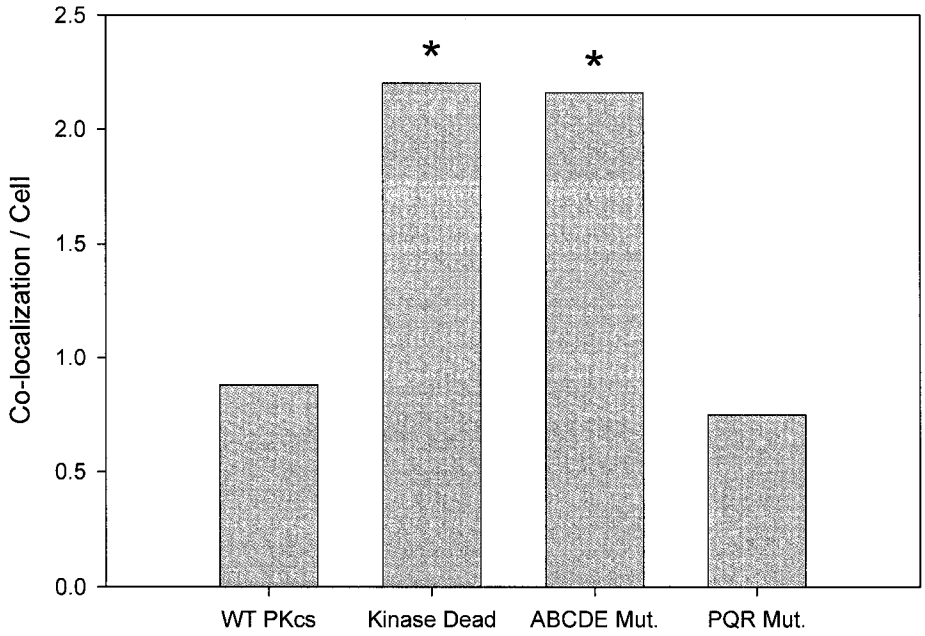

Figure 4.5. ImmunoFISH analysis of DNA-PKcs auto-phosphorylation mutants. A significant increase in the frequency of co-localizations between telomeric DNA and γ-H2AX foci is observed in kinase-dead and ABCDE mutant cells compared to WT. (*$p < 0.05$).

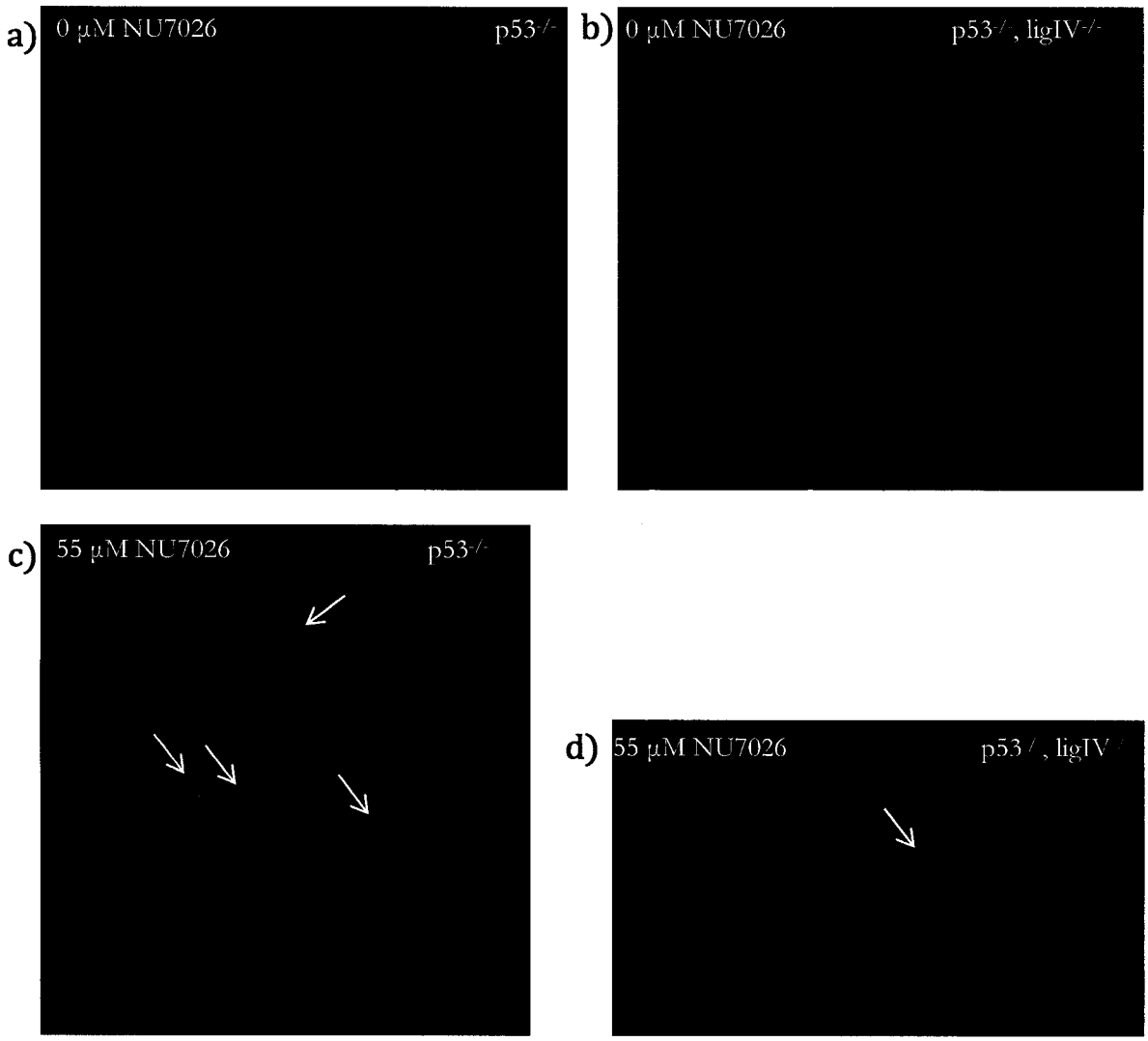

Figure 4.6. LigIV is essential for telomere fusions following inhibition of DNA-PKcs kinase activity. In the presence of the inhibitor NU2076 a significant induction of telomere fusions is seen in $p53^{-/-}$ cells, whereas only telomere associations are induced in the presence of inhibitor in $p53^{-/-}$, $ligIV^{-/-}$ cells.

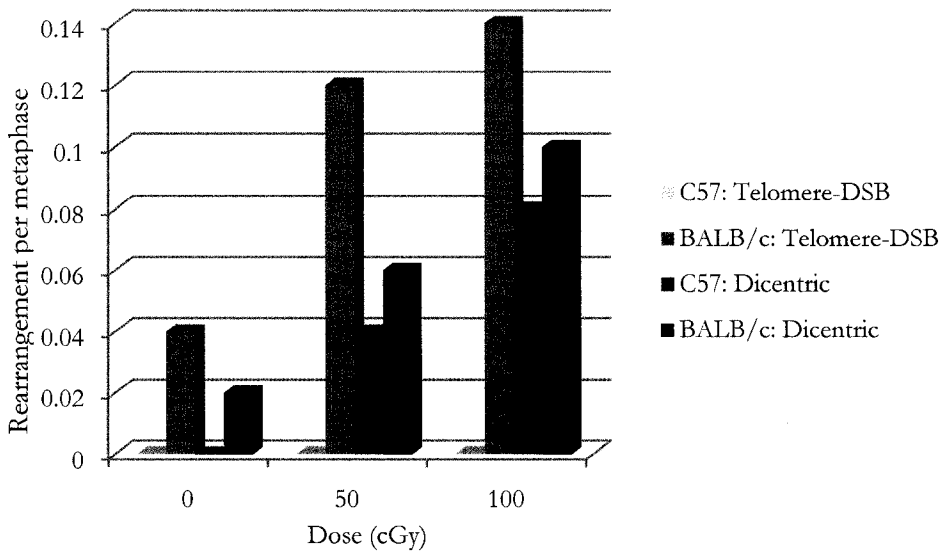

Figure 4.7. Frequency of chromosome rearrangements in Balb/c and C57BL/6 mice. Telomere-DSB fusions are observed only in Balb/c cells and increase in a dose-dependent manner. The frequency of telomere-DSB is greater than that of dicentrics indicating these are significant events within the cell.

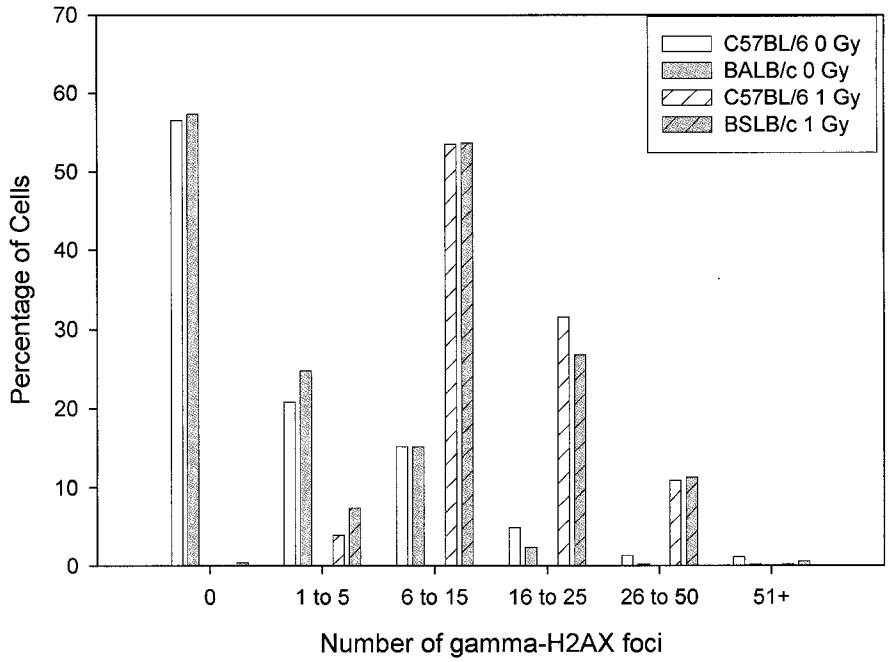

Figure 4.8. γ-H2AX foci formation in Balb/c and C57BL/6 mammary fibroblasts. Quantification of γ-H2AX foci in unirradiated (0 Gy) and irradiated (1Gy) cells shows similar levels of foci formation in Balb/c and C57BL/6 cells 15 minutes after exposure.

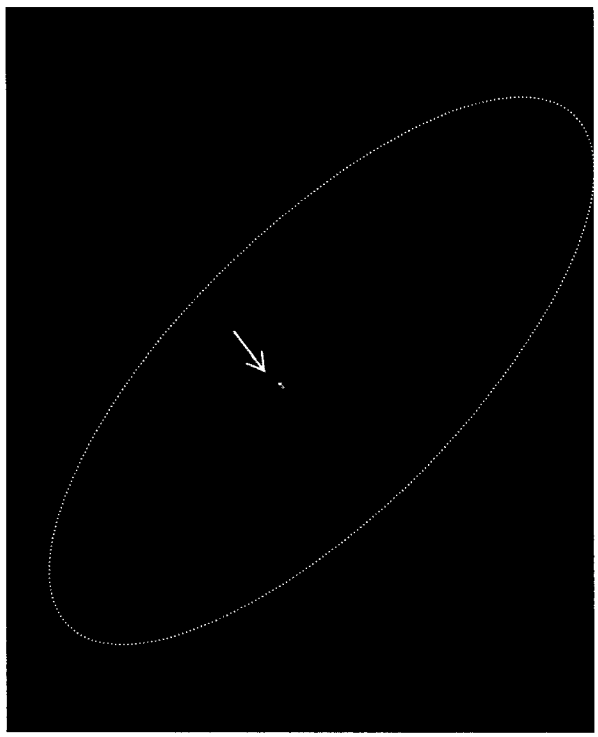

Figure 4.9. Representative image of Balb/c fibroblast showing a positive co-localization of telomeric DNA (red) with γ-H2AX (green) via immunoFISH assay. Cells derived from the Balb/c mouse show an increase incidence of co-localizations compared to cells from C57BL/6.

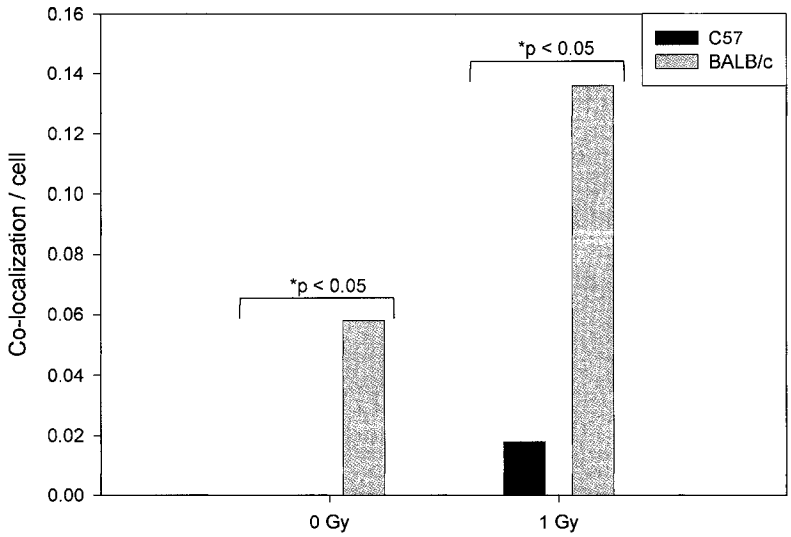

Figure 4.10. ImmunoFISH analysis of Balb/c and C57 mammary fibroblasts reveals a statistically significant increase in co-localization in Balb/c, regardless of exposure to IR. ($p < 0.05$).

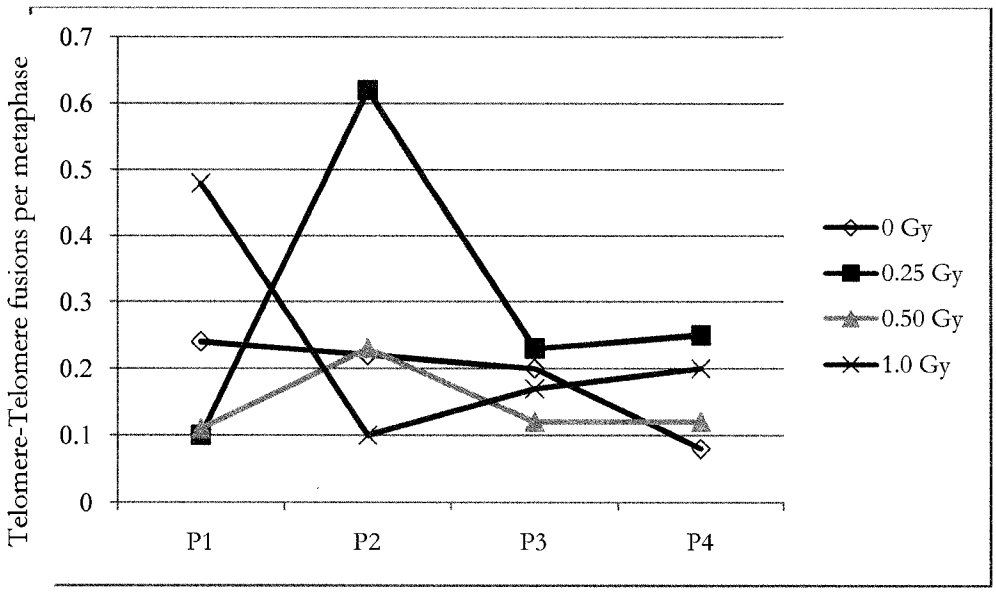

Figure 4.11. Telomere FISH analysis of Balb/c, $p53^{-/-}$ mammary epithelial cells indicates a spike in telomere fusions after exposure to 0.25 Gy only. This may indicate that, in the presence of only a few DSBs, telomeres serve as the more abundant substrate for end-joining events.

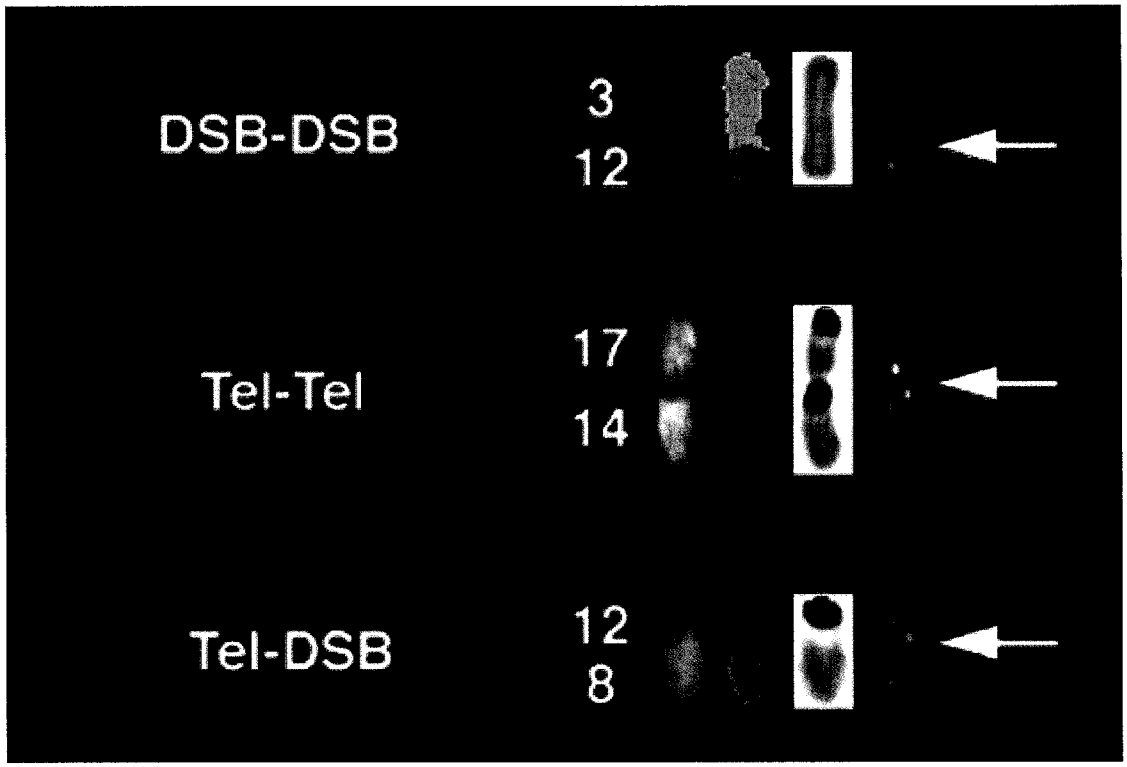

Figure 4.12. SKY-CO-FISH analysis of SCID, $p53^{-/-}$ cells demonstrates the presence of a telomere at the point of fusion. This telomere-DSB rearrangement was clonal, indicating that these events result from covalent linkages and, therefore, are transmissible.

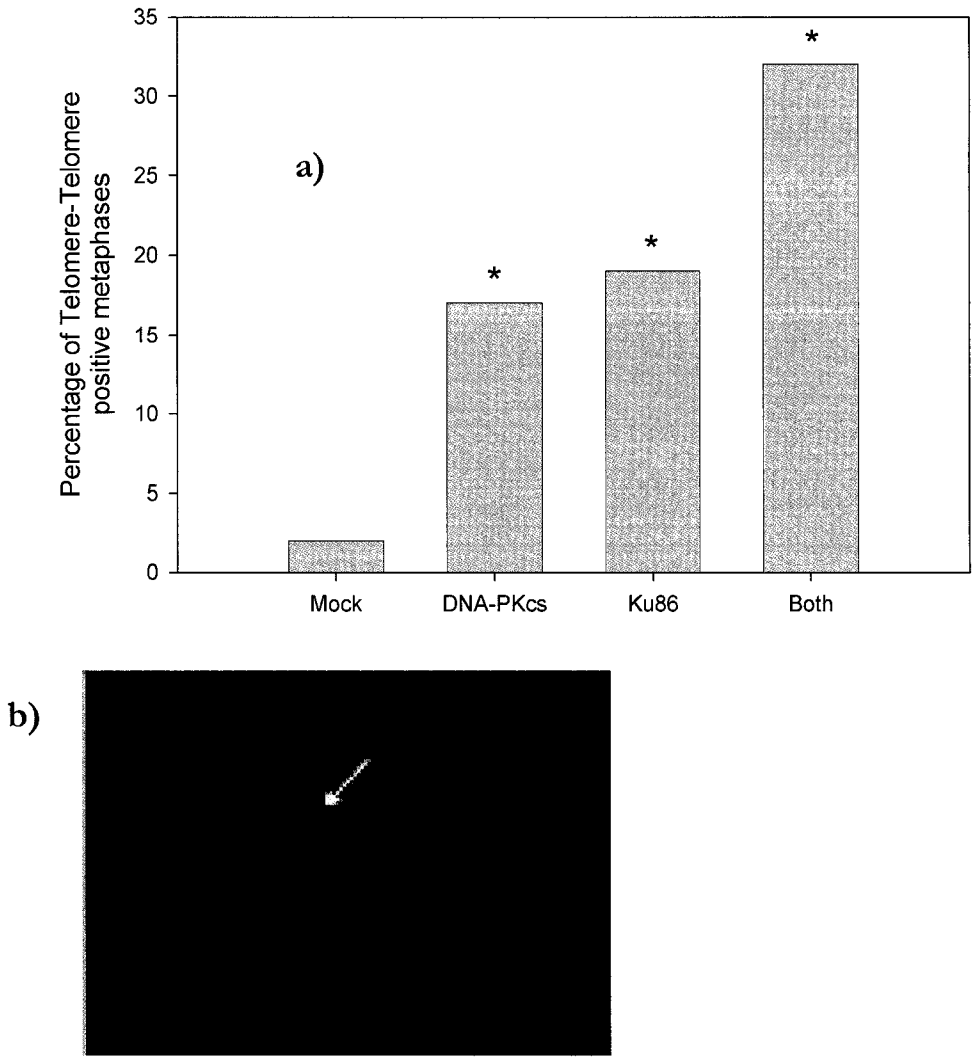

Figure 4.13. Telomere-Telomere fusions in cells human cells knocked down for DNA-PK. a) siRNA knockdown of DNA-PK components reveals a significant increase in the frequency of telomere fusions compared to mock-transfected cells. (*$p < 0.05$) (b) A chromtaid type telomere-telomere fusion of the leading strand telomere is depicted.

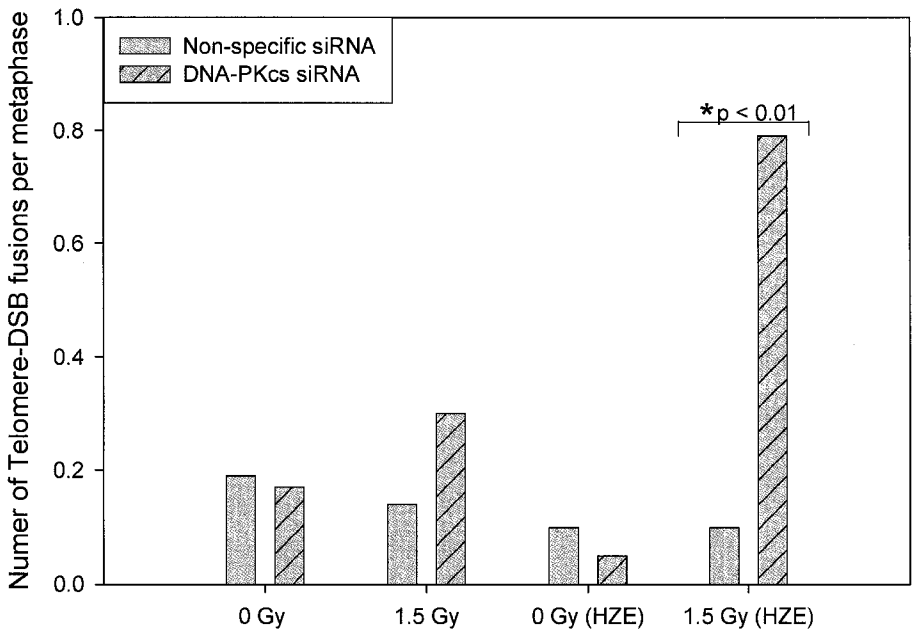

Figure 4.14. Differential quantitative effects on telomere dysfunction of γ-rays and HZE particles in cells knocked down for DNA-PKcs. Two closely related cell lines, TK6 and WTK1, were exposed to γ-rays and 1 GeV/n ^{56}Fe ions, respectively. Exposure to 1.5 Gy γ-rays caused only a slight increase in telomere-DSB fusions, whereas exposure to 1.5 Gy HZE particles produced a significant increase in this phenotype.

V. NBS1

ABSTRACT

Hypomorphic mutation of the NBS1 gene results in Nijmegen Breakage Syndrome, a disease characterized by chromosomal instability and cancer predisposition. NBS1 forms a complex with MRE11 and RAD50, called the MRN complex that plays a multifaceted role in the processing of double-stranded DNA ends. Cells from NBS patients exhibit hypersensitivity to IR, as well as decreased HR and accelerated telomere shortening. Further evidence of a role for NBS1 at telomeres is the report of an S-phase-specific interaction with the telomere repeat binding factor TRF2 at mammalian telomeres. Here, we examine the effects of siRNA knockdown of NBS1 protein levels in two lymphoblastoid cell lines. Utilizing CO-FISH, we find a significant induction of telomere associations (TA)— a phenomenon in which telomeres of the same or different chromosomes are observed in unusually close proximity in metaphase spreads—following treatment. These TAs are equally distributed among telomeres produced via leading and lagging strand DNA synthesis. Our results support the hypothesis that NBS1 plays a role in the suppression of telomere-telomere interactions, while arguing against an essential role for NBS1 and the MRN complex in telomere end-capping.

INTRODUCTION

Nijmegen Breakage Syndrome is a rare autosomal recessive disorder whose patients suffer from a predisposition to immunological disease, lymphatic cancers and leukemia [179,180]. Cells from these patients demonstrate sensitivity to IR and RDS pointing to a defect in the intra S-phase checkpoint [181,182,215]. In 1998 two groups independently distinguished NBS1 (also called Nibrin/p95) as the culprit of NBS, and work quickly began

identifying roles for NBS1 in DNA damage and cell cycle checkpoint control [186,188]. As was predicted [188], NBS1 plays essential roles in the cell's ability to respond to and repair DNA damage, as well as central functions in the S-phase (and possibly other) cell cycle checkpoints.

Cloning of the gene expressing NBS1 has helped to identify three functional domains of the protein. These domains are comprised of the N-terminal FHA/BRCT domain, which directly binds to γ-H2AX [101,102], a central activation domain encompassing two PIKK phosphorylation sites [191-193], and the highly conserved MRE11 binding site at the C-terminus [194,195]. MRE11 is typically found complexed with RAD50 [189], and interaction of MRE11 with NBS1 forms a functional trimeric complex known as the MRN complex. NBS1 has been shown to regulate the activities of the MRN complex through its phosphorylation by ATM in response to DNA damage [191-193]. NBS1 can then localize MRN directly to sites of damage through its contacts with γ-H2AX [262]. Once localized to the break, RAD50 is believed to tether DNA ends together by virtue of its long coiled-coiled domain [205,206]. The model maintains that two RAD50 molecules on either side of the break can form a homodimer through interaction of the coiled-coiled domain, thereby physically linking DNA break ends. MRE11 possesses a host of nuclease activities and, along with RAD50, enables the MRN complex to effectively bridge and process a DNA DSB (reviewed in [263]).

The MRN complex has also been shown to be important in the activation of cell cycle checkpoints, particularly S-phase as indicated by the RDS phenotype [181,182,215]. The signaling cascade following IR consists of numerous branches and levels of signaling, but exactly where MRN falls on this map is unclear (reviewed in [264]). The MRN complex

interacts intimately with ATM, and is known to be required for activation of a number of downstream targets of ATM, including p53 and Chk2 [99,100,219]. However, the MRN complex has also been implicated upstream of ATM as *in vitro* tests indicated the presence of the MRN complex, particularly NBS1, greatly increases phosphorylation and activation of ATM [265]. However, the decreased severity of RDS compared to cells deficient in ATM suggests that NBS1 exerts its function primarily downstream of ATM [181]. NBS1 has also been suggested to play a role in the G1 and G2 checkpoints as well, but conflicting evidence from different experimental models has hindered a clear assessment of NBS1 contribution in this regard (reviewed in [266]).

There is increasing evidence that telomeres must be recognized as DNA damage to be properly processed. The first indication that MRN may be important in this regard was the observation that NBS patients had shorter telomeres than unaffected individuals [183]. The result of Chromatin immunoprecipitation (ChIP) studies place MRE11 and RAD50 at telomeres throughout the cell cycle, while NBS1 is associated with telomeric DNA in S-phase only [22]. This S-phase interaction suggests a role for MRN in replication, and the 3' to 5' exonuclease activity of MRE11 makes it an attractive candidate for generating the G-rich overhang necessary for proper telomere end-capping. Stronger evidence now exists for this claim, as RNAi of either MRE11 or NBS1 results in a shortening of the G-rich overhang [23]. This evidence comes with a caveat, however: cells expressing a stable knock-down of MRE11 soon see a return of G-rich overhang length to wild type, thereby implying as-of-yet unidentified protein(s) in overhang generation that are independent of the MRN complex.

Our study seeks to define a role for NBS1 in telomere function, by utilizing telomere FISH to identify telomere dysfunction cytogenetically. We chose to use human TK6 and

WTK1 cells in the current study, as these cells showed a consistent, robust response to RNAi and allowed us the ability to perform mutation analysis, in addition to telomeric analysis, following knockdown of NBS1. TK6 and WTK1 cells that are transiently knocked down for NBS1 demonstrate an increase in TAs. These associations occur with equal frequencies at telomeres formed by leading strand DNA synthesis and lagging strand synthesis, suggesting that NBS1 (and therefore the MRN complex) acts on all telomeres. Furthermore, induction of telomere associations is unaffected by exposure to IR and cellular p53 status, indicating that NBS1 functions at telomeres independent of its role in DNA damage and cell cycle functions.

RESULTS

siRNA transfection led to a marked silencing effect of NBS1 protein expression on days 4 and 5 after transfection [267]. The relative NBS1 protein level on these days was roughly 10% of that in the mock-transfected control. These observations were true for both the TK6 and WTK1 cells. Accordingly, cytogenetic analysis using telomere FISH and CO-FISH was performed at day 5 after transfection.

Telomere FISH analysis was used to determined the extent of telomere dysfunction following depletion of NBS1 in both WTK1 and TK6 cell lines. Both TK6 and WTK1 cells are derived from the same progenitor and differ only in their p53 status [228,229]; TK6 expresses a wild type p53 and WTK1 expresses a mutated form that results in decreased protein levels resulting in slower (but not abolished) p53-mediated pathways [229]. A significant induction of telomere instability—displayed as TAs (**Figure 5.1** and **5.2**), the unusually close proximity of two telomeres of the same or different metaphase

chromosomes—can be seen in both cell lines following knock down of NBS1 (**Table 5.1**). The roughly 3 to 4-fold increase in TAs was independent of p53 status, as both cell lines showed comparable induction of this phenotype. Furthermore, exposure to IR did not affect the induction of TAs, indicating that the role of NBS1 at telomeres is independent of its role in the activation of DNA repair pathways or cell cycle checkpoints. It is important to note that there was not a significant induction of telomere fusions following knockdown of NBS1 in these cells (**Table 5.1**).

There is strong evidence that telomeres are processed differently depending on whether they are formed via leading-strand DNA synthesis or lagging-strand synthesis [175]. We performed telomere CO-FISH to determine if the increased telomere associations observed following knockdown of NBS1 were strand-specific. Again, there was an increase in the number of telomere associations observed in the cells knocked down for NBS1, regardless of p53 status or exposure to IR (**Table 5.2**). Significantly, however, there was no difference in the induction of telomere associations in leading versus lagging strand telomeres, indicating that NBS1 is involved in the processing of telomeres synthesized by the two modes of replication.

DISCUSSION

In this study, we have examined the effects of transient knockdown of NBS1 on telomere stability. Our data demonstrates that depletion of NBS1 induces the formation of TAs, but not telomere-telomere fusions. These associations form in equal numbers on both leading and lagging stand telomeres. Telomere associations are independent of p53 status and are not altered following exposure to IR, supporting the notion that the function of

NBS1 at telomeres is distinct from its other cellular functions, such as DNA repair and cell cycle regulation. TAs have also been reported in ataxia telangiectasia cell lines and ATM-deficient tissues [268,269]. This is significant because of the intimacy with which ATM and NBS1 interact in the early cellular response to DNA damage. This shared phenotype may indicate that ATM and NBS1 act in the same pathway in regard to telomere function, resembling their interactions as an early response to DNA DSBs.

The mechanism by which TAs are formed remains obscure. One hypothesis is that TAs result from G-rich overhang invasion in *trans* [47]. This would suggest that TAs are the result of increased telomere recombination, implicating a role for NBS1 in suppressing inter-chromosomal recombination. Several lines of evidence support this hypothesis, as NBS1-mutant mice show increased inter-chromosomal recombination in V(D)J assays [195,270] and NBS1 deficient cells show a significant increase in inter-chromosome recombination via HR [196]. It is possible, then, that NBS1 is serving to repress improper recombination events at telomeres. On the other hand, evidence exists which demonstrates a role for NBS1 and the MRN complex in promoting recombination at DNA ends, as the recombination-based ALT mechanism requires the presence of MRN at telomeres [91,225]. Thus, cells depleted of NBS1 would be predicted to have decreased telomere recombination and TAs when, in fact, levels of recombination are actually increased.

The hypothesis for TA formation as described above also predicts the necessity of the G-rich overhang [47]. The effect of siRNA knockdown of NBS1 on G-rich overhang length was not measured in this study, although Chai et al. [23] previously showed that NBS1 knockdown results in significantly shorter G-rich overhangs. While G-rich overhangs were not completely abolished, the fraction of short overhangs (<50 nucleotides) was greatly

increased. However, the function of the MRN complex in generating the G-rich overhang appears dispensable as the short overhang observed after knockdown of MRN components is restored in stably transfected cell lines [23]. In general, the lack of knowledge about formation of telomere associations complicates the task of assigning a role for NBS1 at telomeres.

The absence of a significant induction of telomere fusions following siRNA knockdown of NBS1 argues against an essential role for the MRN complex in telomere end-capping. Cells deficient in the proteins TRF2 and DNA-PKcs show a significant increase in telomere fusions providing obvious evidence of a role in end-capping [175]. While a slight increase in telomere fusions is observed in cells depleted of NBS1, the number of telomere fusion events did not reach significance in the current study. The inability of siRNA techniques to fully abolish protein levels in the cell makes interpretation of these data more difficult, as some functional NBS1 remains in the cell, and its contribution in preventing abnormal telomere phenotypes is unknown.

Telomere shortening has been reported in cells from NBS patients, as well as in cell lines with a mutant NBS1 protein [183]. Furthermore, cells expressing NBS1 protein containing mutations in the ATM phosphorylation sites (serines 278 and 343) demonstrate stochastic loss of telomeres, but no overall effect on telomere length [271]. While telomere length was not directly measured in this study, the transient nature of the knockdown as well as active telomerase in these cell lines makes measurable telomere shortening unlikely. Indeed, there was no noticeable decrease in telomeric signal fluorescence in cells knocked down for NBS1 versus control cells, nor was there an increase in signal free ends. Pandita et

al. [268] showed that while shortened telomeres promote telomere association formation, long telomeres did not preclude telomere association formation.

This study further characterizes the nature of the interaction of NBS1 and telomeres by showing that NBS1 functions at telomeres independently of its role in DNA damage repair and cell cycle checkpoints, and serves to prevent telomere associations. Furthermore, the failure to increase the incidence of telomere fusions in NBS1 knockdown cells argues against an essential role of the MRN complex in telomere end-capping. An understanding of TA formation would facilitate the interpretation of these data. Continuing investigation into the interactions of NBS1 with telomeric DNA and telomeric proteins may help to fully elucidate the function of NBS1 and the MRN complex at the telomere.

Table 5.1. Telomere phenotype after NBS1 knockdown							
Cell Line	**Condition**	**Dose (Gy)**	**# cells scored**	**TF**	**TF per cell**	**TA**	**TA per cell**
TK6	mock	0	50	1	0.02	40	0.80
	siRNA		25	1	0.04	80	3.20*
	mock	0.75	25	0	0.00	19	0.76
	siRNA		56	7	0.13	167	2.98*
WTK1	mock	0	25	0	0.00	12	0.48
	siRNA		30	4	0.13	58	1.93*
	mock	0.75	25	0	0.00	15	0.60
	siRNA		36	2	0.06	80	2.22*

*indicates significant deviation from control ($p < 0.05$)

Table 5.2. Strand-specificity of telomere phenotype after NBS1 knockdown							
Telomeric DNA Strand	**Condition**	**Dose (Gy)**	**# cells scored**	**TF**	**TF per cell**	**TA**	**TA per cell**
Leading	mock	0	25	0	0.00	9	0.36
	siRNA		25	0	0.00	15	0.60
	mock	0.75	25	0	0.00	8	0.32
	siRNA		25	0	0.00	17	0.68
Lagging	mock	0	25	1	0.04	7	0.28
	siRNA		25	0	0.00	10	0.40
	mock	0.75	25	0	0.00	5	0.20
	siRNA		25	0	0.00	14	0.56

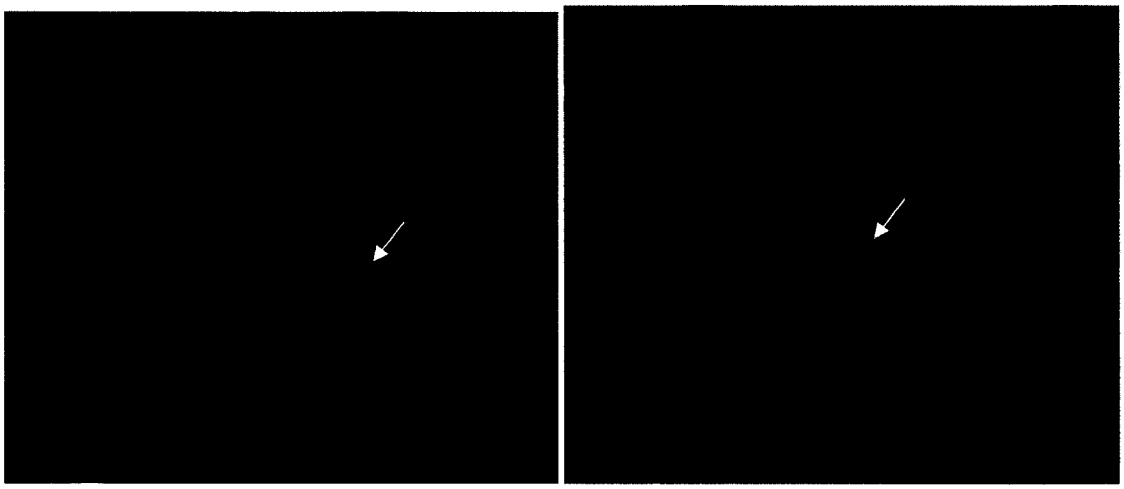

Figure 5.1. Telomere association versus telomere fusion. An example of a telomere association (left) and a telomere fusion (right) can be seen here. Notice that telomere associations, despite the proximity of the two telomere signals, maintain distinct signals. Telomere fusions show a single telomere signal at the point of fusion, with no break in DAPI signal between the two chromosomes.

Figure 5.2. Telomere associations. Representative examples of the telomere association phenotype show an unusually close proximity of telomere signals while maintaining two distinct signals.

VI. THE END PIECE

It is well established that telomeres must be protected from improper repair, so the involvement of DNA repair proteins in this process seems paradoxical. However, the work presented in this study, along with current literature, indicates that this is indeed the case. To date, over a dozen DNA repair and recombination proteins have been shown to localize to telomeres (reviewed in [272]) and determining the manner in which these proteins interact to form a functional, capped telomere remains a priority. Our work investigating the role of DNA-PKcs at telomeres demonstrates a strong parallel with its role in the NHEJ. We also demonstrate that NBS1 functions to suppress the recombination-mediated telomere association phenotype, consistent with several reports showing that NBS1 suppresses inter-chromosomal recombination in both V(D)J recombination [195,270] and HR [196]. Certainly the presence of the shelterin complex at telomeres shapes the interactions of DNA repair proteins, but our results indicate that it is reasonable to assume that the initial response to DNA DSBs and the initial processing of telomeres shares a high degree of homology.

We believe the DNA repair proteins investigated in this study, DNA-PKcs and NBS1, are involved in the early processing of the telomeres, that is to say, from the time telomeres are initially replicated to the time when the long G-rich overhang is generated. While NBS1 and the MRN complex may be involved in later stages of telomere capping, such as suppression of improper telomere recombination and recruitment of ATM; the early involvement of the MRN complex in the response to DNA DSBs suggests an early involvement of the MRN complex at telomeres. Thus, in considering how a telomere is processed, we will focus on the early steps following replication up to G-rich overhang

generation, and avoid the troublesome topic of T-loop versus G-quadruplex formation, a debate in which neither side has much direct, *in vivo* experimental evidence.

The passage of the replication fork is required for telomere processing [273] suggesting that proteins are removed and higher order structures resolved for efficient telomere replication. While there is some debate as to whether telomere-bound TRF2 hinders or facilitates replication fork passage [274,275], there is little doubt that the t-loop (or G-quadruplex) must be resolved for complete telomere replication. Expression of a dominant negative form of the RecQ helicase WRN, a protein shown to resolve *in vitro* displacement loops (and by extension t-loops) [67], results in the stochastic loss of telomere sequence, presumably a result of replication fork stalling and collapse in the telomeric sequence [66]. Telomeres pose additional problems for cell replication machinery, including the sensitivity of G-rich sequences to oxidative stress resulting in bulky adducts [276], the highly repetitive nature of telomeres [7], and the "end-replication problem" [13,14]. Despite these obstacles, cells are able to effectively replicate telomeres except for the most terminal five to fifteen nucleotides [277], resulting in a blunt-ended leading strand telomere and a short, 3' single strand overhang on the lagging strand telomere.

The structure of these newly replicated telomere ends following replication is indistinguishable from the structure of a DNA DSB, leading to the hypothesis that telomeres trigger a DNA damage response immediately following replication. Chromatin immunoprecipitation assays demonstrate an increase of PIKK family members ATM and ATR at telomeres in late S/G2, along with the HR proteins RAD51 and RAD52, providing support for this hypothesis [64]. Furthermore, the activated form of ATM (S1981-ATM) and NBS1 (S343-NBS1) were found to co-localize with telomeres at these times [58],

indicating the activation of DNA damage response pathways. Surprisingly, despite this activation cell cycle arrest is not observed, nor is p53 phosphorylated [58] suggesting that this damage response is locally confined to the telomeres. The inhibition of a global DNA response seems advantageous to the cell in this scenario, as it localizes activated DNA repair proteins to the telomere, proteins which are required for further processing of the telomeric DNA, as well as preventing a cell cycle arrest following every round of replication. It has been shown that TRF2 can inhibit the kinase activity of ATM and decrease phosphorylation of downstream targets, such as p53 [137], thus providing a logical explanation for the lack of p53 phosphorylation, despite ATM activation.

The DNA-damage response proteins recruited to the telomere are likely the same as those recruited to DNA DSBs, thereby placing such proteins as the Ku^{70}/Ku^{86} heterodimer, the MRN complex, the RAD9-Hus1-RAD1 complex (of which RAD9 was recently shown to promote telomere stability [278]), and likely others, at the telomere. The mechanism that determines which of these proteins bind the telomeres is unknown, but competition for the binding site is likely a primary factor, just as it is at DNA repair. This competition for the binding of telomeres may help to explain why deficiencies in DNA repair proteins, such as DNA-PKcs, do not result in the robust telomere fusion phenotype seen in TRF2, which is present at every telomere. The Ku^{70}/Ku^{86} heterodimer likely binds a significant number of telomeric ends given the moderately abundant protein (approximately 500,000 molecules per cell [279]) and the presence of Ku at telomeres throughout the cell cycle [152,280]. Furthermore, the Ku heterodimer has been proposed to compete with RAD52 for DNA DSBs thus triggering either the NHEJ or HR pathways [281]. The fact that the majority of

DNA DSBs are repaired by NHEJ in mammalian cells, indicates that Ku is an especially efficient end-binding protein.

The binding of Ku to the telomere results in the recruitment of DNA-PKcs and subsequent localization of DNA-PKcs to the telomere. Once associated with Ku-bound telomeric DNA, the kinase activity of DNA-PKcs becomes active, and while the target of this kinase activity remains unknown, it is tempting to speculate that it is required for recruitment of processing factors similar to the recruitment and activation of Artemis in NHEJ [119,282]. The recently identified Apollo nuclease, a member of the same protein family as Artmeis, is a likely candidate for this phosphorylation. Two groups independently demonstrated that Apollo is localized at telomeres and plays in telomere processing, as siRNA depletion of Apollo results in telomere-induced foci (TIFs) and telomere-induced senescence [283,284]. The nuclease of Apollo was shown to be 5' to 3', the correct orientation for 3' single strand overhang generation. While siRNA knockdown of Apollo generated an aberrant telomere phenotype, no telomere fusion events were reported, indicating it is probably not the primary nuclease in telomere end-processing [284].

It is likely that the binding of DNA-PKcs to telomeric DNA sterically blocks access to the DNA end, thus preventing unchecked nucleolytic processing. Relief of this steric hindrance comes in the form of *trans*- auto-phosphorylation in the NHEJ pathway [121,170,171,173], a mechanism not possible at telomeres as there is only one DNA end. The observation that ATM can phosphorylate the Thr-2609 cluster of sites [172] offers an excellent alternative to this dilemma, especially given our data demonstrating that only Thr-2609 is involved in telomere end-processing. Therefore, we propose that ATM phosphorylates telomeric bound DNA-PKcs at the Thr-2609 cluster, causing a

conformational change that promotes nucleolytic activity, perhaps via the Apollo nuclease, and the generation of the 3' single strand overhang.

DNA-PKcs has been shown to act only on telomeres formed by leading strand DNA synthesis [175]; the reason for this remains unclear. One possibility is that Ku binds differently to leading verus lagging strand telomeres, although this explanation seems unlikely. Ku has been shown to bind DNA ends even with long (~200nt) overhangs [285], thus the short overhang of lagging strand telomeres would not impede Ku binding. It is more likely that leading and lagging strand telomeres are processed slightly differently following replication, a hypothesis supported by the strand specificity of WRN and DNA-PKcs telomere interactions [66,175]. However, it is known that both strands are subjected to nucleolytic processing following replication [21], which would lead one to hypothesize that this function is the same on both telomeres. Perhaps, however, differences exist in the proteins that are recruited to leading versus lagging strand telomeres, or in the manner in which the two are processed. Also, the contribution of end structure to the processing of telomeres (short overhang versus blunt-ended) remains to be determined.

The model presented here provides several avenues of future direction worthy of further investigation. Examining the relationship (if any) between the Apollo nuclease and DNA-PKcs may provide important clues to nucleolytic processing of leading versus lagging strand telomeres. Taking this further, it would be informative to examine protein localization to telomeres in the presence and absence of DNA-PKcs, as DNA-PKcs may be required to recruit critical proteins (e.g. shelterin components or DNA repair proteins) to the telomere. The effects of DNA-PKcs on G-rich overhang length should also be examined. Previous work has shown that DNA-PKcs does not affect G-rich overhang length [62],

however no distinction was made between leading and lagging strand telomeres. Recent work out of the Wright and Shay lab [21,23] has produced a method by which you can separate leading versus lagging strand telomeres and then measure overhang length. The application of this technique to DNA-PKcs studies could provide evidence for changes in overhang length thereby directly implicating DNA-PKcs in this process.

The processing and capping of telomeres *in vivo* remains an enigma. Clearly, telomeres are dynamic structures that require the presence of a multitude of proteins whose precise functions and interactions remain unknown. The role of a properly functioning telomere to long-term cellular survival is paramount. As such, the cell has developed redundancy in this key pathway, further complicating our already confusing picture of the telomere. However, strong parallels can be drawn between early events in telomere processing and early events in DNA DSB repair. Indeed, recent discoveries in the DNA repair field have provided important clues to the way telomeres are recognized and processed. The elucidation of the role of DNA-PKcs auto-phosphorylation is but one example. Continued clarification of the early events in the DNA damage response and telomere processing is a daunting, yet vital task. These two closely related processes serve to safe-guard the genome, preventing genomic instability and progression to tumorigenesis, thus a clear picture of their function will provide a greater understanding of cancer and aging.

VII. BIBLIOGRAPHY

[1] H.J. Muller Studies in genetics: The selected papers of H.J. Muller, in, Indiana University Press, Bloomington, 1962, pp. 384-408.

[2] P. Baumann Taking control of G-quadruplexes, Nat Struct Mol Biol 12 (2005) 832-833.

[3] B. McClintock The stability of broken ends of chromosomes in Zea mays, Genetics 26 (1941) 234-282.

[4] J.D. Griffith, L. Comeau, S. Rosenfield, R.M. Stansel, A. Bianchi, H. Moss and T. de Lange Mammalian telomeres end in a large duplex loop, Cell 97 (1999) 503-514.

[5] D. Hanahan and R.A. Weinberg The hallmarks of cancer, Cell 100 (2000) 57-70.

[6] H. Biessmann and J.M. Mason Genetics and molecular biology of telomeres, Adv Genet 30 (1992) 185-249.

[7] E.H. Blackburn Structure and function of telomeres, Nature 350 (1991) 569-573.

[8] V.L. Makarov, Y. Hirose and J.P. Langmore Long G tails at both ends of human chromosomes suggest a C strand degradation mechanism for telomere shortening, Cell 88 (1997) 657-666.

[9] R.J. Wellinger and D. Sen The DNA structures at the ends of eukaryotic chromosomes, Eur J Cancer 33 (1997) 735-749.

[10] E.R. Henderson and E.H. Blackburn An overhanging 3' terminus is a conserved feature of telomeres, Mol Cell Biol 9 (1989) 345-348.

[11] A. Sugino, S. Hirose and R. Okazaki RNA-linked nascent DNA fragments in Escherichia coli, Proc Natl Acad Sci U S A 69 (1972) 1863-1867.

[12] A. Sugino and R. Okazaki RNA-linked DNA fragments in vitro, Proc Natl Acad Sci U S A 70 (1973) 88-92.

[13] A.M. Olovnikov A theory of marginotomy. The incomplete copying of template margin in enzymic synthesis of polynucleotides and biological significance of the phenomenon, J Theor Biol 41 (1973) 181-190.

[14] J.D. Watson Origin of concatemeric T7 DNA, Nat New Biol 239 (1972) 197-201.

[15] C.B. Harley Telomere loss: mitotic clock or genetic time bomb?, Mutat Res 256 (1991) 271-282.

[16] R. McElligott and R.J. Wellinger The terminal DNA structure of mammalian chromosomes, Embo J 16 (1997) 3705-3714.

[17] S.A. Stewart, I. Ben-Porath, V.J. Carey, B.F. O'Connor, W.C. Hahn and R.A. Weinberg Erosion of the telomeric single-strand overhang at replicative senescence, Nat Genet 33 (2003) 492-496.

[18] J. Lingner, J.P. Cooper and T.R. Cech Telomerase and DNA end replication: no longer a lagging strand problem?, Science 269 (1995) 1533-1534.

[19] R. Ohki, T. Tsurimoto and F. Ishikawa In vitro reconstitution of the end replication problem, Mol Cell Biol 21 (2001) 5753-5766.

[20] W.E. Wright, V.M. Tesmer, K.E. Huffman, S.D. Levene and J.W. Shay Normal human chromosomes have long G-rich telomeric overhangs at one end, Genes Dev 11 (1997) 2801-2809.

[21] W. Chai, Q. Du, J.W. Shay and W.E. Wright Human telomeres have different overhang sizes at leading versus lagging strands, Mol Cell 21 (2006) 427-435.

[22] X.D. Zhu, B. Kuster, M. Mann, J.H. Petrini and T. de Lange Cell-cycle-regulated association of RAD50/MRE11/NBS1 with TRF2 and human telomeres, Nat Genet 25 (2000) 347-352.

[23] W. Chai, A.J. Sfeir, H. Hoshiyama, J.W. Shay and W.E. Wright The involvement of the Mre11/Rad50/Nbs1 complex in the generation of G-overhangs at human telomeres, EMBO Rep 7 (2006) 225-230.

[24] W.I. Sundquist and A. Klug Telomeric DNA dimerizes by formation of guanine tetrads between hairpin loops, Nature 342 (1989) 825-829.

[25] D. Liu, M.S. O'Connor, J. Qin and Z. Songyang Telosome, a mammalian telomere-associated complex formed by multiple telomeric proteins, J Biol Chem 279 (2004) 51338-51342.

[26] T. de Lange Shelterin: the protein complex that shapes and safeguards human telomeres, Genes Dev 19 (2005) 2100-2110.

[27] D. Broccoli, A. Smogorzewska, L. Chong and T. de Lange Human telomeres contain two distinct Myb-related proteins, TRF1 and TRF2, Nat Genet 17 (1997) 231-235.

[28] Z. Zhong, L. Shiue, S. Kaplan and T. de Lange A mammalian factor that binds telomeric TTAGGG repeats in vitro, Mol Cell Biol 12 (1992) 4834-4843.

[29] P. Baumann and T.R. Cech Pot1, the putative telomere end-binding protein in fission yeast and humans, Science 292 (2001) 1171-1175.

[30] M. Lei, E.R. Podell and T.R. Cech Structure of human POT1 bound to telomeric single-stranded DNA provides a model for chromosome end-protection, Nat Struct Mol Biol 11 (2004) 1223-1229.

[31] D. Loayza and T. De Lange POT1 as a terminal transducer of TRF1 telomere length control, Nature 423 (2003) 1013-1018.

[32] S.H. Kim, P. Kaminker and J. Campisi TIN2, a new regulator of telomere length in human cells, Nat Genet 23 (1999) 405-412.

[33] B.R. Houghtaling, L. Cuttonaro, W. Chang and S. Smith A dynamic molecular link between the telomere length regulator TRF1 and the chromosome end protector TRF2, Curr Biol 14 (2004) 1621-1631.

[34] D. Liu, A. Safari, M.S. O'Connor, D.W. Chan, A. Laegeler, J. Qin and Z. Songyang PTOP interacts with POT1 and regulates its localization to telomeres, Nat Cell Biol 6 (2004) 673-680.

[35] J.Z. Ye, D. Hockemeyer, A.N. Krutchinsky, D. Loayza, S.M. Hooper, B.T. Chait and T. de Lange POT1-interacting protein PIP1: a telomere length regulator that recruits POT1 to the TIN2/TRF1 complex, Genes Dev 18 (2004) 1649-1654.

[36] B. Li, S. Oestreich and T. de Lange Identification of human Rap1: implications for telomere evolution, Cell 101 (2000) 471-483.

[37] T. Bilaud, C. Brun, K. Ancelin, C.E. Koering, T. Laroche and E. Gilson Telomeric localization of TRF2, a novel human telobox protein, Nat Genet 17 (1997) 236-239.

[38] R. Court, L. Chapman, L. Fairall and D. Rhodes How the human telomeric proteins TRF1 and TRF2 recognize telomeric DNA: a view from high-resolution crystal structures, EMBO Rep 6 (2005) 39-45.

[39] L. Fairall, L. Chapman, H. Moss, T. de Lange and D. Rhodes Structure of the TRFH dimerization domain of the human telomeric proteins TRF1 and TRF2, Mol Cell 8 (2001) 351-361.

[40] A. Bianchi, R.M. Stansel, L. Fairall, J.D. Griffith, D. Rhodes and T. de Lange TRF1 binds a bipartite telomeric site with extreme spatial flexibility, Embo J 18 (1999) 5735-5744.

[41] A. Bianchi, S. Smith, L. Chong, P. Elias and T. de Lange TRF1 is a dimer and bends telomeric DNA, Embo J 16 (1997) 1785-1794.

[42] D. Broccoli, L. Chong, S. Oelmann, A.A. Fernald, N. Marziliano, B. van Steensel, D. Kipling, M.M. Le Beau and T. de Lange Comparison of the human and mouse genes encoding the telomeric protein, TRF1: chromosomal localization, expression and conserved protein domains, Hum Mol Genet 6 (1997) 69-76.

[43] C.W. Greider and E.H. Blackburn Identification of a specific telomere terminal transferase activity in Tetrahymena extracts, Cell 43 (1985) 405-413.

[44] B. van Steensel and T. de Lange Control of telomere length by the human telomeric protein TRF1, Nature 385 (1997) 740-743.

[45] K. Ancelin, M. Brunori, S. Bauwens, C.E. Koering, C. Brun, M. Ricoul, J.P. Pommier, L. Sabatier and E. Gilson Targeting assay to study the cis functions of human telomeric proteins: evidence for inhibition of telomerase by TRF1 and for activation of telomere degradation by TRF2, Mol Cell Biol 22 (2002) 3474-3487.

[46] B. van Steensel, A. Smogorzewska and T. de Lange TRF2 protects human telomeres from end-to-end fusions, Cell 92 (1998) 401-413.

[47] S. Amiard, M. Doudeau, S. Pinte, A. Poulet, C. Lenain, C. Faivre-Moskalenko, D. Angelov, N. Hug, A. Vindigni, P. Bouvet, J. Paoletti, E. Gilson and M.J. Giraud-Panis A topological mechanism for TRF2-enhanced strand invasion, Nat Struct Mol Biol 14 (2007) 147-154.

[48] A. Smogorzewska, B. van Steensel, A. Bianchi, S. Oelmann, M.R. Schaefer, G. Schnapp and T. de Lange Control of human telomere length by TRF1 and TRF2, Mol Cell Biol 20 (2000) 1659-1668.

[49] D. Loayza, H. Parsons, J. Donigian, K. Hoke and T. de Lange DNA binding features of human POT1: a nonamer 5'-TAGGGTTAG-3' minimal binding site, sequence specificity, and internal binding to multimeric sites, J Biol Chem 279 (2004) 13241-13248.

[50] Q. Yang, Y.L. Zheng and C.C. Harris POT1 and TRF2 Cooperate To Maintain Telomeric Integrity, Mol Cell Biol 25 (2005) 1070-1080.

[51] F. Wang, E.R. Podell, A.J. Zaug, Y. Yang, P. Baciu, T.R. Cech and M. Lei The POT1-TPP1 telomere complex is a telomerase processivity factor, Nature 445 (2007) 506-510.

[52] H. Xin, D. Liu, M. Wan, A. Safari, H. Kim, W. Sun, M.S. O'Connor and Z. Songyang TPP1 is a homologue of ciliate TEBP-beta and interacts with POT1 to recruit telomerase, Nature 445 (2007) 559-562.

[53] J.Z. Ye, J.R. Donigian, M. van Overbeek, D. Loayza, Y. Luo, A.N. Krutchinsky, B.T. Chait and T. de Lange TIN2 binds TRF1 and TRF2 simultaneously and stabilizes the TRF2 complex on telomeres, J Biol Chem 279 (2004) 47264-47271.

[54] S.H. Kim, S. Han, Y.H. You, D.J. Chen and J. Campisi The human telomere-associated protein TIN2 stimulates interactions between telomeric DNA tracts in vitro, EMBO Rep 4 (2003) 685-691.

[55] S.H. Kim, C. Beausejour, A.R. Davalos, P. Kaminker, S.J. Heo and J. Campisi TIN2 mediates functions of TRF2 at human telomeres, J Biol Chem 279 (2004) 43799-43804.

[56] M.S. O'Connor, A. Safari, D. Liu, J. Qin and Z. Songyang The human Rap1 protein complex and modulation of telomere length, J Biol Chem 279 (2004) 28585-28591.

[57] G.B. Celli and T. de Lange DNA processing is not required for ATM-mediated telomere damage response after TRF2 deletion, Nat Cell Biol 7 (2005) 712-718.

[58] R.E. Verdun, L. Crabbe, C. Haggblom and J. Karlseder Functional human telomeres are recognized as DNA damage in G2 of the cell cycle, Mol Cell 20 (2005) 551-561.

[59] S.M. Bailey, M.A. Brenneman, J. Halbrook, J.A. Nickoloff, R.L. Ullrich and E.H. Goodwin The kinase activity of DNA-PK is required to protect mammalian telomeres, DNA Repair (Amst) 3 (2004) 225-233.

[60] S.M. Bailey, J. Meyne, D.J. Chen, A. Kurimasa, G.C. Li, B.E. Lehnert and E.H. Goodwin DNA double-strand break repair proteins are required to cap the ends of mammalian chromosomes, Proc Natl Acad Sci U S A 96 (1999) 14899-14904.

[61] E. Samper, F.A. Goytisolo, P. Slijepcevic, P.P. van Buul and M.A. Blasco Mammalian Ku86 protein prevents telomeric fusions independently of the length of TTAGGG repeats and the G-strand overhang, EMBO Rep 1 (2000) 244-252.

[62] F.A. Goytisolo, E. Samper, S. Edmonson, G.E. Taccioli and M.A. Blasco The absence of the dna-dependent protein kinase catalytic subunit in mice results in anaphase bridges and in increased telomeric fusions with normal telomere length and G-strand overhang, Mol Cell Biol 21 (2001) 3642-3651.

[63] M. Tarsounas, P. Munoz, A. Claas, P.G. Smiraldo, D.L. Pittman, M.A. Blasco and S.C. West Telomere maintenance requires the RAD51D recombination/repair protein, Cell 117 (2004) 337-347.

[64] R.E. Verdun and J. Karlseder The DNA damage machinery and homologous recombination pathway act consecutively to protect human telomeres, Cell 127 (2006) 709-720.

[65] A. Machwe, L. Xiao and D.K. Orren TRF2 recruits the Werner syndrome (WRN) exonuclease for processing of telomeric DNA, Oncogene 23 (2004) 149-156.

[66] L. Crabbe, R.E. Verdun, C.I. Haggblom and J. Karlseder Defective telomere lagging strand synthesis in cells lacking WRN helicase activity, Science 306 (2004) 1951-1953.

[67] P.L. Opresko, M. Otterlei, J. Graakjaer, P. Bruheim, L. Dawut, S. Kolvraa, A. May, M.M. Seidman and V.A. Bohr The Werner syndrome helicase and exonuclease cooperate to resolve telomeric D loops in a manner regulated by TRF1 and TRF2, Mol Cell 14 (2004) 763-774.

[68] J.R. Williamson, M.K. Raghuraman and T.R. Cech Monovalent cation-induced structure of telomeric DNA: the G-quartet model, Cell 59 (1989) 871-880.

[69] D.E. Gottschling and V.A. Zakian Telomere proteins: specific recognition and protection of the natural termini of Oxytricha macronuclear DNA, Cell 47 (1986) 195-205.

[70] S. Burge, G.N. Parkinson, P. Hazel, A.K. Todd and S. Neidle Quadruplex DNA: sequence, topology and structure, Nucleic Acids Res 34 (2006) 5402-5415.

[71] C. Schaffitzel, I. Berger, J. Postberg, J. Hanes, H.J. Lipps and A. Pluckthun In vitro generated antibodies specific for telomeric guanine-quadruplex DNA react with Stylonychia lemnae macronuclei, Proc Natl Acad Sci U S A 98 (2001) 8572-8577.

[72] A.G. Bodnar, M. Ouellette, M. Frolkis, S.E. Holt, C.P. Chiu, G.B. Morin, C.B. Harley, J.W. Shay, S. Lichtsteiner and W.E. Wright Extension of life-span by introduction of telomerase into normal human cells, Science 279 (1998) 349-352.

[73] J.W. Shay and S. Bacchetti A survey of telomerase activity in human cancer, Eur J Cancer 33 (1997) 787-791.

[74] E.H. Blackburn, C.W. Greider, E. Henderson, M.S. Lee, J. Shampay and D. Shippen-Lentz Recognition and elongation of telomeres by telomerase, Genome 31 (1989) 553-560.

[75] J. Feng, W.D. Funk, S.S. Wang, S.L. Weinrich, A.A. Avilion, C.P. Chiu, R.R. Adams, E. Chang, R.C. Allsopp, J. Yu and et al. The RNA component of human telomerase, Science 269 (1995) 1236-1241.

[76] J. Lingner, T.R. Hughes, A. Shevchenko, M. Mann, V. Lundblad and T.R. Cech Reverse transcriptase motifs in the catalytic subunit of telomerase, Science 276 (1997) 561-567.

[77] A.A. Avilion, M.A. Piatyszek, J. Gupta, J.W. Shay, S. Bacchetti and C.W. Greider Human telomerase RNA and telomerase activity in immortal cell lines and tumor tissues, Cancer Res 56 (1996) 645-650.

[78] X. Yi, V.M. Tesmer, I. Savre-Train, J.W. Shay and W.E. Wright Both transcriptional and posttranscriptional mechanisms regulate human telomerase template RNA levels, Mol Cell Biol 19 (1999) 3989-3997.

[79] N.W. Kim, M.A. Piatyszek, K.R. Prowse, C.B. Harley, M.D. West, P.L. Ho, G.M. Coviello, W.E. Wright, S.L. Weinrich and J.W. Shay Specific association of human telomerase activity with immortal cells and cancer, Science 266 (1994) 2011-2015.

[80] W.E. Wright, M.A. Piatyszek, W.E. Rainey, W. Byrd and J.W. Shay Telomerase activity in human germline and embryonic tissues and cells, Dev Genet 18 (1996) 173-179.

[81] A.L. Ducrest, H. Szutorisz, J. Lingner and M. Nabholz Regulation of the human telomerase reverse transcriptase gene, Oncogene 21 (2002) 541-552.

[82] G. Cristofari, K. Sikora and J. Lingner Telomerase unplugged, ACS Chem Biol 2 (2007) 155-158.

[83] T.M. Bryan, A. Englezou, L. Dalla-Pozza, M.A. Dunham and R.R. Reddel Evidence for an alternative mechanism for maintaining telomere length in human tumors and tumor-derived cell lines, Nat Med 3 (1997) 1271-1274.

[84] T.M. Bryan, A. Englezou, J. Gupta, S. Bacchetti and R.R. Reddel Telomere elongation in immortal human cells without detectable telomerase activity, Embo J 14 (1995) 4240-4248.

[85] M.P. Hande, E. Samper, P. Lansdorp and M.A. Blasco Telomere length dynamics and chromosomal instability in cells derived from telomerase null mice, J Cell Biol 144 (1999) 589-601.

[86] R.P. Sanders, R. Drissi, C.A. Billups, N.C. Daw, M.B. Valentine and J.S. Dome Telomerase expression predicts unfavorable outcome in osteosarcoma, J Clin Oncol 22 (2004) 3790-3797.

[87] G.A. Ulaner, A.R. Hoffman, J. Otero, H.Y. Huang, Z. Zhao, M. Mazumdar, R. Gorlick, P. Meyers, J.H. Healey and M. Ladanyi Divergent patterns of telomere maintenance mechanisms among human sarcomas: sharply contrasting prevalence of the alternative lengthening of telomeres mechanism in Ewing's sarcomas and osteosarcomas, Genes Chromosomes Cancer 41 (2004) 155-162.

[88] J.P. Murnane, L. Sabatier, B.A. Marder and W.F. Morgan Telomere dynamics in an immortal human cell line, Embo J 13 (1994) 4953-4962.

[89] T.R. Yeager, A.A. Neumann, A. Englezou, L.I. Huschtscha, J.R. Noble and R.R. Reddel Telomerase-negative immortalized human cells contain a novel type of promyelocytic leukemia (PML) body, Cancer Res 59 (1999) 4175-4179.

[90] F.B. Johnson, R.A. Marciniak, M. McVey, S.A. Stewart, W.C. Hahn and L. Guarente The Saccharomyces cerevisiae WRN homolog Sgs1p participates in telomere maintenance in cells lacking telomerase, Embo J 20 (2001) 905-913.

[91] G. Wu, X. Jiang, W.H. Lee and P.L. Chen Assembly of functional ALT-associated promyelocytic leukemia bodies requires Nijmegen Breakage Syndrome 1, Cancer Res 63 (2003) 2589-2595.

[92] K. Rothkamm, I. Kruger, L.H. Thompson and M. Lobrich Pathways of DNA double-strand break repair during the mammalian cell cycle, Mol Cell Biol 23 (2003) 5706-5715.

[93] M. Honma, M. Izumi, M. Sakuraba, S. Tadokoro, H. Sakamoto, W. Wang, F. Yatagai and M. Hayashi Deletion, rearrangement, and gene conversion; genetic consequences of chromosomal double-strand breaks in human cells, Environ Mol Mutagen 42 (2003) 288-298.

[94] S.J. DiBiase, Z.C. Zeng, R. Chen, T. Hyslop, W.J. Curran, Jr. and G. Iliakis DNA-dependent protein kinase stimulates an independently active, nonhomologous, end-joining apparatus, Cancer Res 60 (2000) 1245-1253.

[95] J.H. Hoeijmakers Genome maintenance mechanisms for preventing cancer, Nature 411 (2001) 366-374.

[96] C.E. Canman, D.S. Lim, K.A. Cimprich, Y. Taya, K. Tamai, K. Sakaguchi, E. Appella, M.B. Kastan and J.D. Siliciano Activation of the ATM kinase by ionizing radiation and phosphorylation of p53, Science 281 (1998) 1677-1679.

[97] J.Y. Ahn, J.K. Schwarz, H. Piwnica-Worms and C.E. Canman Threonine 68 phosphorylation by ataxia telangiectasia mutated is required for efficient activation of Chk2 in response to ionizing radiation, Cancer Res 60 (2000) 5934-5936.

[98] S. Matsuoka, G. Rotman, A. Ogawa, Y. Shiloh, K. Tamai and S.J. Elledge Ataxia telangiectasia-mutated phosphorylates Chk2 in vivo and in vitro, Proc Natl Acad Sci U S A 97 (2000) 10389-10394.

[99] J.H. Lee and T.T. Paull Direct activation of the ATM protein kinase by the Mre11/Rad50/Nbs1 complex, Science 304 (2004) 93-96.

[100] J.H. Lee and T.T. Paull ATM activation by DNA double-strand breaks through the Mre11-Rad50-Nbs1 complex, Science 308 (2005) 551-554.

[101] J. Kobayashi, H. Tauchi, S. Sakamoto, A. Nakamura, K. Morishima, S. Matsuura, T. Kobayashi, K. Tamai, K. Tanimoto and K. Komatsu NBS1 localizes to gamma-H2AX foci through interaction with the FHA/BRCT domain, Curr Biol 12 (2002) 1846-1851.

[102] D. Durocher, I.A. Taylor, D. Sarbassova, L.F. Haire, S.L. Westcott, S.P. Jackson, S.J. Smerdon and M.B. Yaffe The molecular basis of FHA domain:phosphopeptide binding specificity and implications for phospho-dependent signaling mechanisms, Mol Cell 6 (2000) 1169-1182.

[103] G.S. Stewart, B. Wang, C.R. Bignell, A.M. Taylor and S.J. Elledge MDC1 is a mediator of the mammalian DNA damage checkpoint, Nature 421 (2003) 961-966.

[104] A. Celeste, S. Petersen, P.J. Romanienko, O. Fernandez-Capetillo, H.T. Chen, O.A. Sedelnikova, B. Reina-San-Martin, V. Coppola, E. Meffre, M.J. Difilippantonio, C. Redon, D.R. Pilch, A. Olaru, M. Eckhaus, R.D. Camerini-Otero, L. Tessarollo, F. Livak, K. Manova, W.M. Bonner, M.C. Nussenzweig and A. Nussenzweig Genomic instability in mice lacking histone H2AX, Science 296 (2002) 922-927.

[105] I.M. Ward, K. Minn, K.G. Jorda and J. Chen Accumulation of checkpoint protein 53BP1 at DNA breaks involves its binding to phosphorylated histone H2AX, J Biol Chem 278 (2003) 19579-19582.

[106] A. Celeste, O. Fernandez-Capetillo, M.J. Kruhlak, D.R. Pilch, D.W. Staudt, A. Lee, R.F. Bonner, W.M. Bonner and A. Nussenzweig Histone H2AX phosphorylation is dispensable for the initial recognition of DNA breaks, Nat Cell Biol 5 (2003) 675-679.

[107] E.P. Rogakou, D.R. Pilch, A.H. Orr, V.S. Ivanova and W.M. Bonner DNA double-stranded breaks induce histone H2AX phosphorylation on serine 139, J Biol Chem 273 (1998) 5858-5868.

[108] A. Meier, H. Fiegler, P. Munoz, P. Ellis, D. Rigler, C. Langford, M.A. Blasco, N. Carter and S.P. Jackson Spreading of mammalian DNA-damage response factors studied by ChIP-chip at damaged telomeres, Embo J 26 (2007) 2707-2718.

[109] S.V. Costes, A. Boissiere, S. Ravani, R. Romano, B. Parvin and M.H. Barcellos-Hoff Imaging features that discriminate between foci induced by high- and low-LET radiation in human fibroblasts, Radiat Res 165 (2006) 505-515.

[110] T.M. Marti, E. Hefner, L. Feeney, V. Natale and J.E. Cleaver H2AX phosphorylation within the G1 phase after UV irradiation depends on nucleotide excision repair and not DNA double-strand breaks, Proc Natl Acad Sci U S A 103 (2006) 9891-9896.

[111] I.M. Ward and J. Chen Histone H2AX is phosphorylated in an ATR-dependent manner in response to replicational stress, J Biol Chem 276 (2001) 47759-47762.

[112] T. Yu, S.H. Macphail, J.P. Banath, D. Klokov and P.L. Olive Endogenous expression of phosphorylated histone H2AX in tumors in relation to DNA double-strand breaks and genomic instability, DNA Repair (Amst) (2006).

[113] L.H. Thompson and D. Schild Recombinational DNA repair and human disease, Mutat Res 509 (2002) 49-78.

[114] T.M. Gottlieb and S.P. Jackson The DNA-dependent protein kinase: requirement for DNA ends and association with Ku antigen, Cell 72 (1993) 131-142.

[115] A. Suwa, M. Hirakata, Y. Takeda, S.A. Jesch, T. Mimori and J.A. Hardin DNA-dependent protein kinase (Ku protein-p350 complex) assembles on double-stranded DNA, Proc Natl Acad Sci U S A 91 (1994) 6904-6908.

[116] A. Kurimasa, S. Kumano, N.V. Boubnov, M.D. Story, C.S. Tung, S.R. Peterson and D.J. Chen Requirement for the kinase activity of human DNA-dependent protein kinase catalytic subunit in DNA strand break rejoining, Mol Cell Biol 19 (1999) 3877-3884.

[117] D.W. Chan, R. Ye, C.J. Veillette and S.P. Lees-Miller DNA-dependent protein kinase phosphorylation sites in Ku 70/80 heterodimer, Biochemistry 38 (1999) 1819-1828.

[118] R. Leber, T.W. Wise, R. Mizuta and K. Meek The XRCC4 gene product is a target for and interacts with the DNA-dependent protein kinase, J Biol Chem 273 (1998) 1794-1801.

[119] Y. Ma, U. Pannicke, H. Lu, D. Niewolik, K. Schwarz and M.R. Lieber The DNA-dependent protein kinase catalytic subunit phosphorylation sites in human Artemis, J Biol Chem 280 (2005) 33839-33846.

[120] D.W. Chan, B.P. Chen, S. Prithivirajsingh, A. Kurimasa, M.D. Story, J. Qin and D.J. Chen Autophosphorylation of the DNA-dependent protein kinase catalytic subunit is required for rejoining of DNA double-strand breaks, Genes Dev 16 (2002) 2333-2338.

[121] Q. Ding, Y.V. Reddy, W. Wang, T. Woods, P. Douglas, D.A. Ramsden, S.P. Lees-Miller and K. Meek Autophosphorylation of the catalytic subunit of the DNA-dependent protein kinase is required for efficient end processing during DNA double-strand break repair, Mol Cell Biol 23 (2003) 5836-5848.

[122] S. Soubeyrand, L. Pope, B. Pakuts and R.J. Hache Threonines 2638/2647 in DNA-PK are essential for cellular resistance to ionizing radiation, Cancer Res 63 (2003) 1198-1201.

[123] J. Drouet, C. Delteil, J. Lefrancois, P. Concannon, B. Salles and P. Calsou DNA-PK and XRCC4/DNA ligase IV mobilization in the cell in response to DNA double-strand breaks, J Biol Chem (2004).

[124] P. Ahnesorg, P. Smith and S.P. Jackson XLF interacts with the XRCC4-DNA ligase IV complex to promote DNA nonhomologous end-joining, Cell 124 (2006) 301-313.

[125] D. Buck, L. Malivert, R. de Chasseval, A. Barraud, M.C. Fondaneche, O. Sanal, A. Plebani, J.L. Stephan, M. Hufnagel, F. le Deist, A. Fischer, A. Durandy, J.P. de Villartay and P. Revy Cernunnos, a novel nonhomologous end-joining factor, is mutated in human immunodeficiency with microcephaly, Cell 124 (2006) 287-299.

[126] C.J. Tsai, S.A. Kim and G. Chu Cernunnos/XLF promotes the ligation of mismatched and noncohesive DNA ends, Proc Natl Acad Sci U S A 104 (2007) 7851-7856.

[127] Y. Ma, U. Pannicke, K. Schwarz and M.R. Lieber Hairpin opening and overhang processing by an Artemis/DNA-dependent protein kinase complex in nonhomologous end joining and V(D)J recombination, Cell 108 (2002) 781-794.

[128] Y. Ma, K. Schwarz and M.R. Lieber The Artemis:DNA-PKcs endonuclease cleaves DNA loops, flaps, and gaps, DNA Repair (Amst) 4 (2005) 845-851.

[129] Y. Yamaguchi-Iwai, E. Sonoda, M.S. Sasaki, C. Morrison, T. Haraguchi, Y. Hiraoka, Y.M. Yamashita, T. Yagi, M. Takata, C. Price, N. Kakazu and S. Takeda Mre11 is essential for the maintenance of chromosomal DNA in vertebrate cells, Embo J 18 (1999) 6619-6629.

[130] T.E. Wilson, U. Grawunder and M.R. Lieber Yeast DNA ligase IV mediates non-homologous DNA end joining, Nature 388 (1997) 495-498.

[131] L. Chong, B. van Steensel, D. Broccoli, H. Erdjument-Bromage, J. Hanish, P. Tempst and T. de Lange A human telomeric protein, Science 270 (1995) 1663-1667.

[132] A.Y. Sakaguchi, S.S. Padalecki, V. Mattern, A. Rodriguez, R.J. Leach, J.R. McGill, M. Chavez and T.A. Giambernardi Chromosomal sublocalization of the transcribed human telomere repeat binding factor 2 gene and comparative mapping in the mouse, Somat Cell Mol Genet 24 (1998) 157-163.

[133] R.L. Strausberg, E.A. Feingold, L.H. Grouse, J.G. Derge, R.D. Klausner, F.S. Collins, L. Wagner, C.M. Shenmen, G.D. Schuler, S.F. Altschul, B. Zeeberg, K.H. Buetow, C.F. Schaefer, N.K. Bhat, R.F. Hopkins, H. Jordan, T. Moore, S.I. Max, J. Wang, F. Hsieh, L. Diatchenko, K. Marusina, A.A. Farmer, G.M. Rubin, L. Hong, M. Stapleton, M.B. Soares, M.F. Bonaldo, T.L. Casavant, T.E. Scheetz, M.J. Brownstein, T.B. Usdin, S. Toshiyuki, P. Carninci, C. Prange, S.S. Raha, N.A. Loquellano, G.J. Peters, R.D. Abramson, S.J. Mullahy, S.A. Bosak, P.J. McEwan, K.J. McKernan, J.A. Malek, P.H. Gunaratne, S. Richards, K.C. Worley, S. Hale, A.M. Garcia, L.J. Gay, S.W. Hulyk, D.K. Villalon, D.M. Muzny, E.J. Sodergren, X. Lu, R.A. Gibbs, J. Fahey, E. Helton, M. Ketteman, A. Madan, S. Rodrigues, A. Sanchez, M. Whiting, A. Madan, A.C. Young, Y. Shevchenko, G.G. Bouffard, R.W. Blakesley, J.W. Touchman, E.D. Green, M.C. Dickson, A.C. Rodriguez, J. Grimwood, J. Schmutz, R.M. Myers, Y.S. Butterfield, M.I. Krzywinski, U. Skalska, D.E. Smailus, A. Schnerch, J.E. Schein, S.J. Jones and M.A. Marra Generation and initial analysis of more than 15,000 full-length human and mouse cDNA sequences, Proc Natl Acad Sci U S A 99 (2002) 16899-16903.

[134] R.C. Wang, A. Smogorzewska and T. de Lange Homologous recombination generates T-loop-sized deletions at human telomeres, Cell 119 (2004) 355-368.

[135] P.S. Bradshaw, D.J. Stavropoulos and M.S. Meyn Human telomeric protein TRF2 associates with genomic double-strand breaks as an early response to DNA damage, Nat Genet 37 (2005) 193-197.

[136] N. Fouche, A.J. Cesare, S. Willcox, S. Ozgur, S.A. Compton and J.D. Griffith The Basic Domain of TRF2 Directs Binding to DNA Junctions Irrespective of the Presence of TTAGGG Repeats, J Biol Chem 281 (2006) 37486-37495.

[137] J. Karlseder, K. Hoke, O.K. Mirzoeva, C. Bakkenist, M.B. Kastan, J.H. Petrini and T. de Lange The telomeric protein TRF2 binds the ATM kinase and can inhibit the ATM-dependent DNA damage response, PLoS Biol 2 (2004) E240.

[138] X.D. Zhu, L. Niedernhofer, B. Kuster, M. Mann, J.H. Hoeijmakers and T. de Lange ERCC1/XPF removes the 3' overhang from uncapped telomeres and represses formation of telomeric DNA-containing double minute chromosomes, Mol Cell 12 (2003) 1489-1498.

[139] K. Lillard-Wetherell, A. Machwe, G.T. Langland, K.A. Combs, G.K. Behbehani, S.A. Schonberg, J. German, J.J. Turchi, D.K. Orren and J. Groden Association and regulation of the BLM helicase by the telomere proteins TRF1 and TRF2, Hum Mol Genet 13 (2004) 1919-1932.

[140] P.L. Opresko, C. von Kobbe, J.P. Laine, J. Harrigan, I.D. Hickson and V.A. Bohr Telomere-binding protein TRF2 binds to and stimulates the Werner and Bloom syndrome helicases, J Biol Chem 277 (2002) 41110-41119.

[141] H. Tanaka, M.S. Mendonca, P.S. Bradshaw, D.J. Hoelz, L.H. Malkas, M.S. Meyn and D. Gilley DNA damage-induced phosphorylation of the human telomere-associated protein TRF2, Proc Natl Acad Sci U S A 102 (2005) 15539-15544.

[142] J.Y. Chan, M.I. Lerman, B.S. Prabhakar, O. Isozaki, P. Santisteban, R.C. Kuppers, E.L. Oates, A.L. Notkins and L.D. Kohn Cloning and characterization of a cDNA that encodes a 70-kDa novel human thyroid autoantigen, J Biol Chem 264 (1989) 3651-3654.

[143] G.E. Taccioli, T.M. Gottlieb, T. Blunt, A. Priestley, J. Demengeot, R. Mizuta, A.R. Lehmann, F.W. Alt, S.P. Jackson and P.A. Jeggo Ku80: product of the XRCC5 gene and its role in DNA repair and V(D)J recombination, Science 265 (1994) 1442-1445.

[144] J.R. Walker, R.A. Corpina and J. Goldberg Structure of the Ku heterodimer bound to DNA and its implications for double-strand break repair, Nature 412 (2001) 607-614.

[145] D. Gell and S.P. Jackson Mapping of protein-protein interactions within the DNA-dependent protein kinase complex, Nucleic Acids Res 27 (1999) 3494-3502.

[146] P. Calsou, P. Frit, O. Humbert, C. Muller, D.J. Chen and B. Salles The DNA-dependent protein kinase catalytic activity regulates DNA end processing by means of Ku entry into DNA, J Biol Chem 274 (1999) 7848-7856.

[147] P. Calsou, C. Delteil, P. Frit, J. Drouet and B. Salles Coordinated assembly of Ku and p460 subunits of the DNA-dependent protein kinase on DNA ends is necessary for XRCC4-ligase IV recruitment, J Mol Biol 326 (2003) 93-103.

[148] D. Merkle, P. Douglas, G.B. Moorhead, Z. Leonenko, Y. Yu, D. Cramb, D.P. Bazett-Jones and S.P. Lees-Miller The DNA-dependent protein kinase interacts with DNA to form a protein-DNA complex that is disrupted by phosphorylation, Biochemistry 41 (2002) 12706-12714.

[149] S. Yoo and W.S. Dynan Geometry of a complex formed by double strand break repair proteins at a single DNA end: recruitment of DNA-PKcs induces inward translocation of Ku protein, Nucleic Acids Res 27 (1999) 4679-4686.

[150] B. Kysela, A.J. Doherty, M. Chovanec, T. Stiff, S.M. Ameer-Beg, B. Vojnovic, P.M. Girard and P.A. Jeggo Ku stimulation of DNA ligase IV-dependent ligation requires inward movement along the DNA molecule, J Biol Chem 278 (2003) 22466-22474.

[151] S.Y. Roth, J.M. Denu and C.D. Allis Histone acetyltransferases, Annu Rev Biochem 70 (2001) 81-120.

[152] K. Song, D. Jung, Y. Jung, S.G. Lee and I. Lee Interaction of human Ku70 with TRF2, FEBS Lett 481 (2000) 81-85.

[153] H.L. Hsu, D. Gilley, S.A. Galande, M.P. Hande, B. Allen, S.H. Kim, G.C. Li, J. Campisi, T. Kohwi-Shigematsu and D.J. Chen Ku acts in a unique way at the mammalian telomere to prevent end joining, Genes Dev 14 (2000) 2807-2812.

[154] P. Karmakar, C.M. Snowden, D.A. Ramsden and V.A. Bohr Ku heterodimer binds to both ends of the Werner protein and functional interaction occurs at the Werner N-terminus, Nucleic Acids Res 30 (2002) 3583-3591.

[155] B. Li and L. Comai Functional interaction between Ku and the werner syndrome protein in DNA end processing, J Biol Chem 275 (2000) 39800.

[156] M.P. Cooper, A. Machwe, D.K. Orren, R.M. Brosh, D. Ramsden and V.A. Bohr Ku complex interacts with and stimulates the Werner protein, Genes Dev 14 (2000) 907-912.

[157] S.M. Yannone, S. Roy, D.W. Chan, M.B. Murphy, S. Huang, J. Campisi and D.J. Chen Werner syndrome protein is regulated and phosphorylated by DNA-dependent protein kinase, J Biol Chem 276 (2001) 38242-38248.

[158] P. Karmakar, J. Piotrowski, R.M. Brosh, Jr., J.A. Sommers, S.P. Miller, W.H. Cheng, C.M. Snowden, D.A. Ramsden and V.A. Bohr Werner protein is a target of DNA-dependent protein kinase in vivo and in vitro, and its catalytic activities are regulated by phosphorylation, J Biol Chem 277 (2002) 18291-18302.

[159] K.O. Hartley, D. Gell, G.C. Smith, H. Zhang, N. Divecha, M.A. Connelly, A. Admon, S.P. Lees-Miller, C.W. Anderson and S.P. Jackson DNA-dependent protein kinase catalytic subunit: a relative of phosphatidylinositol 3-kinase and the ataxia telangiectasia gene product, Cell 82 (1995) 849-856.

[160] J.D. Sipley, J.C. Menninger, K.O. Hartley, D.C. Ward, S.P. Jackson and C.W. Anderson Gene for the catalytic subunit of the human DNA-activated protein kinase maps to the site of the XRCC7 gene on chromosome 8, Proc Natl Acad Sci U S A 92 (1995) 7515-7519.

[161] P. Baumann and S.C. West DNA end-joining catalyzed by human cell-free extracts, Proc Natl Acad Sci U S A 95 (1998) 14066-14070.

[162] S.P. Lees-Miller, K. Sakaguchi, S.J. Ullrich, E. Appella and C.W. Anderson Human DNA-activated protein kinase phosphorylates serines 15 and 37 in the amino-terminal transactivation domain of human p53, Mol Cell Biol 12 (1992) 5041-5049.

[163] L.D. Mayo, J.J. Turchi and S.J. Berberich Mdm-2 phosphorylation by DNA-dependent protein kinase prevents interaction with p53, Cancer Res 57 (1997) 5013-5016.

[164] R.G. Shao, C.X. Cao, H. Zhang, K.W. Kohn, M.S. Wold and Y. Pommier Replication-mediated DNA damage by camptothecin induces phosphorylation of RPA by DNA-dependent protein kinase and dissociates RPA:DNA-PK complexes, Embo J 18 (1999) 1397-1406.

[165] A.Y. Karpova, M. Trost, J.M. Murray, L.C. Cantley and P.M. Howley Interferon regulatory factor-3 is an in vivo target of DNA-PK, Proc Natl Acad Sci U S A 99 (2002) 2818-2823.

[166] S.P. Lees-Miller, Y.R. Chen and C.W. Anderson Human cells contain a DNA-activated protein kinase that phosphorylates simian virus 40 T antigen, mouse p53, and the human Ku autoantigen, Mol Cell Biol 10 (1990) 6472-6481.

[167] B.P. Chen, D.W. Chan, J. Kobayashi, S. Burma, A. Asaithamby, K. Morotomi-Yano, E. Botvinick, J. Qin and D.J. Chen Cell cycle dependence of DNA-dependent protein kinase phosphorylation in response to DNA double strand breaks, J Biol Chem 280 (2005) 14709-14715.

[168] P. Douglas, G.P. Sapkota, N. Morrice, Y. Yu, A.A. Goodarzi, D. Merkle, K. Meek, D.R. Alessi and S.P. Lees-Miller Identification of in vitro and in vivo phosphorylation sites in the catalytic subunit of the DNA-dependent protein kinase, Biochem J 368 (2002) 243-251.

[169] D.W. Chan and S.P. Lees-Miller The DNA-dependent protein kinase is inactivated by autophosphorylation of the catalytic subunit, J Biol Chem 271 (1996) 8936-8941.

[170] X. Cui, Y. Yu, S. Gupta, Y.M. Cho, S.P. Lees-Miller and K. Meek Autophosphorylation of DNA-dependent protein kinase regulates DNA end processing and may also alter double-strand break repair pathway choice, Mol Cell Biol 25 (2005) 10842-10852.

[171] W.D. Block, Y. Yu, D. Merkle, J.L. Gifford, Q. Ding, K. Meek and S.P. Lees-Miller Autophosphorylation-dependent remodeling of the DNA-dependent protein kinase catalytic subunit regulates ligation of DNA ends, Nucleic Acids Res 32 (2004) 4351-4357.

[172] B.P. Chen, N. Uematsu, J. Kobayashi, Y. Lerenthal, A. Krempler, H. Yajima, M. Lobrich, Y. Shiloh and D.J. Chen Ataxia telangiectasia mutated (ATM) is essential for DNA-PKcs phosphorylations at the Thr-2609 cluster upon DNA double strand break, J Biol Chem 282 (2007) 6582-6587.

[173] K. Meek, P. Douglas, X. Cui, Q. Ding and S.P. Lees-Miller trans Autophosphorylation at DNA-dependent protein kinase's two major autophosphorylation site clusters facilitates end processing but not end joining, Mol Cell Biol 27 (2007) 3881-3890.

[174] A.A. Goodarzi, Y. Yu, E. Riballo, P. Douglas, S.A. Walker, R. Ye, C. Harer, C. Marchetti, N. Morrice, P.A. Jeggo and S.P. Lees-Miller DNA-PK

autophosphorylation facilitates Artemis endonuclease activity, Embo J 25 (2006) 3880-3889.

[175] S.M. Bailey, M.N. Cornforth, A. Kurimasa, D.J. Chen and E.H. Goodwin Strand-specific postreplicative processing of mammalian telomeres, Science 293 (2001) 2462-2465.

[176] S. Espejel, S. Franco, A. Sgura, D. Gae, S.M. Bailey, G.E. Taccioli and M.A. Blasco Functional interaction between DNA-PKcs and telomerase in telomere length maintenance, Embo J 21 (2002) 6275-6287.

[177] S. Espejel, P. Klatt, J. Menissier-de Murcia, J. Martin-Caballero, J.M. Flores, G. Taccioli, G. de Murcia and M.A. Blasco Impact of telomerase ablation on organismal viability, aging, and tumorigenesis in mice lacking the DNA repair proteins PARP-1, Ku86, or DNA-PKcs, J Cell Biol 167 (2004) 627-638.

[178] S.M. Bailey, M.N. Cornforth, R.L. Ullrich and E.H. Goodwin Dysfunctional mammalian telomeres join with DNA double-strand breaks, DNA Repair (Amst) 3 (2004) 349-357.

[179] A.M. Taylor Chromosome instability syndromes, Best Pract Res Clin Haematol 14 (2001) 631-644.

[180] C.M. Weemaes, D.F. Smeets and C.J. van der Burgt Nijmegen Breakage syndrome: a progress report, Int J Radiat Biol 66 (1994) S185-188.

[181] J. Falck, J.H. Petrini, B.R. Williams, J. Lukas and J. Bartek The DNA damage-dependent intra-S phase checkpoint is regulated by parallel pathways, Nat Genet 30 (2002) 290-294.

[182] W. Jongmans, M. Vuillaume, K. Chrzanowska, D. Smeets, K. Sperling and J. Hall Nijmegen breakage syndrome cells fail to induce the p53-mediated DNA damage response following exposure to ionizing radiation, Mol Cell Biol 17 (1997) 5016-5022.

[183] V. Ranganathan, W.F. Heine, D.N. Ciccone, K.L. Rudolph, X. Wu, S. Chang, H. Hai, I.M. Ahearn, D.M. Livingston, I. Resnick, F. Rosen, E. Seemanova, P. Jarolim, R.A. DePinho and D.T. Weaver Rescue of a telomere length defect of Nijmegen breakage syndrome cells requires NBS and telomerase catalytic subunit, Curr Biol 11 (2001) 962-966.

[184] K.E. Sullivan, E. Veksler, H. Lederman and S.P. Lees-Miller Cell cycle checkpoints and DNA repair in Nijmegen breakage syndrome, Clin Immunol Immunopathol 82 (1997) 43-48.

[185] V. Dumon-Jones, P.O. Frappart, W.M. Tong, G. Sajithlal, W. Hulla, G. Schmid, Z. Herceg, M. Digweed and Z.Q. Wang Nbn heterozygosity renders mice susceptible to tumor formation and ionizing radiation-induced tumorigenesis, Cancer Res 63 (2003) 7263-7269.

[186] J.P. Carney, R.S. Maser, H. Olivares, E.M. Davis, M. Le Beau, J.R. Yates, 3rd, L. Hays, W.F. Morgan and J.H. Petrini The hMre11/hRad50 protein complex and Nijmegen breakage syndrome: linkage of double-strand break repair to the cellular DNA damage response, Cell 93 (1998) 477-486.

[187] S. Matsuura, H. Tauchi, A. Nakamura, N. Kondo, S. Sakamoto, S. Endo, D. Smeets, B. Solder, B.H. Belohradsky, V.M. Der Kaloustian, M. Oshimura, M. Isomura, Y. Nakamura and K. Komatsu Positional cloning of the gene for Nijmegen breakage syndrome, Nat Genet 19 (1998) 179-181.

[188] R. Varon, C. Vissinga, M. Platzer, K.M. Cerosaletti, K.H. Chrzanowska, K. Saar, G. Beckmann, E. Seemanova, P.R. Cooper, N.J. Nowak, M. Stumm, C.M. Weemaes, R.A. Gatti, R.K. Wilson, M. Digweed, A. Rosenthal, K. Sperling, P. Concannon and A. Reis Nibrin, a novel DNA double-strand break repair protein, is mutated in Nijmegen breakage syndrome, Cell 93 (1998) 467-476.

[189] G.M. Dolganov, R.S. Maser, A. Novikov, L. Tosto, S. Chong, D.A. Bressan and J.H. Petrini Human Rad50 is physically associated with human Mre11: identification of a conserved multiprotein complex implicated in recombinational DNA repair, Mol Cell Biol 16 (1996) 4832-4841.

[190] H. Tauchi, J. Kobayashi, K. Morishima, S. Matsuura, A. Nakamura, T. Shiraishi, E. Ito, D. Masnada, D. Delia and K. Komatsu The forkhead-associated domain of NBS1 is essential for nuclear foci formation after irradiation but not essential for hRAD50[middle dot]hMRE11[middle dot]NBS1 complex DNA repair activity, J Biol Chem 276 (2001) 12-15.

[191] M. Gatei, D. Young, K.M. Cerosaletti, A. Desai-Mehta, K. Spring, S. Kozlov, M.F. Lavin, R.A. Gatti, P. Concannon and K. Khanna ATM-dependent phosphorylation of nibrin in response to radiation exposure, Nat Genet 25 (2000) 115-119.

[192] D.S. Lim, S.T. Kim, B. Xu, R.S. Maser, J. Lin, J.H. Petrini and M.B. Kastan ATM phosphorylates p95/nbs1 in an S-phase checkpoint pathway, Nature 404 (2000) 613-617.

[193] X. Wu, V. Ranganathan, D.S. Weisman, W.F. Heine, D.N. Ciccone, T.B. O'Neill, K.E. Crick, K.A. Pierce, W.S. Lane, G. Rathbun, D.M. Livingston and D.T. Weaver ATM phosphorylation of Nijmegen breakage syndrome protein is required in a DNA damage response, Nature 405 (2000) 477-482.

[194] A. Desai-Mehta, K.M. Cerosaletti and P. Concannon Distinct functional domains of nibrin mediate Mre11 binding, focus formation, and nuclear localization, Mol Cell Biol 21 (2001) 2184-2191.

[195] J. Kang, R.T. Bronson and Y. Xu Targeted disruption of NBS1 reveals its roles in mouse development and DNA repair, Embo J 21 (2002) 1447-1455.

[196] H. Tauchi, J. Kobayashi, K. Morishima, D.C. van Gent, T. Shiraishi, N.S. Verkaik, D. vanHeems, E. Ito, A. Nakamura, E. Sonoda, M. Takata, S. Takeda, S. Matsuura and K. Komatsu Nbs1 is essential for DNA repair by homologous recombination in higher vertebrate cells, Nature 420 (2002) 93-98.

[197] T.T. Paull and M. Gellert The 3' to 5' exonuclease activity of Mre 11 facilitates repair of DNA double-strand breaks, Mol Cell 1 (1998) 969-979.

[198] K.M. Trujillo, S.S. Yuan, E.Y. Lee and P. Sung Nuclease activities in a complex of human recombination and DNA repair factors Rad50, Mre11, and p95, J Biol Chem 273 (1998) 21447-21450.

[199] J.S. Bleuit, H. Xu, Y. Ma, T. Wang, J. Liu and S.W. Morrical Mediator proteins orchestrate enzyme-ssDNA assembly during T4 recombination-dependent DNA replication and repair, Proc Natl Acad Sci U S A 98 (2001) 8298-8305.

[200] K.M. Trujillo and P. Sung DNA structure-specific nuclease activities in the Saccharomyces cerevisiae Rad50*Mre11 complex, J Biol Chem 276 (2001) 35458-35464.

[201] T.T. Paull and M. Gellert Nbs1 potentiates ATP-driven DNA unwinding and endonuclease cleavage by the Mre11/Rad50 complex, Genes Dev 13 (1999) 1276-1288.

[202] K.P. Hopfner, A. Karcher, D. Shin, C. Fairley, J.A. Tainer and J.P. Carney Mre11 and Rad50 from Pyrococcus furiosus: cloning and biochemical characterization reveal an evolutionarily conserved multiprotein machine, J Bacteriol 182 (2000) 6036-6041.

[203] K.P. Hopfner, A. Karcher, D.S. Shin, L. Craig, L.M. Arthur, J.P. Carney and J.A. Tainer Structural biology of Rad50 ATPase: ATP-driven conformational control in

DNA double-strand break repair and the ABC-ATPase superfamily, Cell 101 (2000) 789-800.

[204] C.H. Haering, J. Lowe, A. Hochwagen and K. Nasmyth Molecular architecture of SMC proteins and the yeast cohesin complex, Mol Cell 9 (2002) 773-788.

[205] K.P. Hopfner, L. Craig, G. Moncalian, R.A. Zinkel, T. Usui, B.A. Owen, A. Karcher, B. Henderson, J.L. Bodmer, C.T. McMurray, J.P. Carney, J.H. Petrini and J.A. Tainer The Rad50 zinc-hook is a structure joining Mre11 complexes in DNA recombination and repair, Nature 418 (2002) 562-566.

[206] M. de Jager, J. van Noort, D.C. van Gent, C. Dekker, R. Kanaar and C. Wyman Human Rad50/Mre11 is a flexible complex that can tether DNA ends, Mol Cell 8 (2001) 1129-1135.

[207] V.M. Blinov, E.V. Koonin, A.E. Gorbalenya, A.V. Kaliman and V.M. Kryukov Two early genes of bacteriophage T5 encode proteins containing an NTP-binding sequence motif and probably involved in DNA replication, recombination and repair, FEBS Lett 252 (1989) 47-52.

[208] A.E. Gorbalenya and E.V. Koonin Superfamily of UvrA-related NTP-binding proteins. Implications for rational classification of recombination/repair systems, J Mol Biol 213 (1990) 583-591.

[209] S. Daoudal-Cotterell, M.E. Gallego and C.I. White The plant Rad50-Mre11 protein complex, FEBS Lett 516 (2002) 164-166.

[210] J. Huang and W.S. Dynan Reconstitution of the mammalian DNA double-strand break end-joining reaction reveals a requirement for an Mre11/Rad50/NBS1-containing fraction, Nucleic Acids Res 30 (2002) 667-674.

[211] D. Udayakumar, C.L. Bladen, F.Z. Hudson and W.S. Dynan Distinct pathways of nonhomologous end joining that are differentially regulated by DNA-dependent protein kinase-mediated phosphorylation, J Biol Chem 278 (2003) 41631-41635.

[212] E. Harfst, S. Cooper, S. Neubauer, L. Distel and U. Grawunder Normal V(D)J recombination in cells from patients with Nijmegen breakage syndrome, Mol Immunol 37 (2000) 915-929.

[213] H. Tauchi, S. Matsuura, J. Kobayashi, S. Sakamoto and K. Komatsu Nijmegen breakage syndrome gene, NBS1, and molecular links to factors for genome stability, Oncogene 21 (2002) 8967-8980.

[214] S. Matsuura, J. Kobayashi, H. Tauchi and K. Komatsu Nijmegen breakage syndrome and DNA double strand break repair by NBS1 complex, Adv Biophys 38 (2004) 65-80.

[215] R.B. Painter and B.R. Young Radiosensitivity in ataxia-telangiectasia: a new explanation, Proc Natl Acad Sci U S A 77 (1980) 7315-7317.

[216] J. Bartek, C. Lukas and J. Lukas Checking on DNA damage in S phase, Nat Rev Mol Cell Biol 5 (2004) 792-804.

[217] S. Zhao, Y.C. Weng, S.S. Yuan, Y.T. Lin, H.C. Hsu, S.C. Lin, E. Gerbino, M.H. Song, M.Z. Zdzienicka, R.A. Gatti, J.W. Shay, Y. Ziv, Y. Shiloh and E.Y. Lee Functional link between ataxia-telangiectasia and Nijmegen breakage syndrome gene products, Nature 405 (2000) 473-477.

[218] J.H. Lee, B. Xu, C.H. Lee, J.Y. Ahn, M.S. Song, H. Lee, C.E. Canman, J.S. Lee, M.B. Kastan and D.S. Lim Distinct functions of Nijmegen breakage syndrome in ataxia telangiectasia mutated-dependent responses to DNA damage, Mol Cancer Res 1 (2003) 674-681.

[219] J. Falck, J. Coates and S.P. Jackson Conserved modes of recruitment of ATM, ATR and DNA-PKcs to sites of DNA damage, Nature 434 (2005) 605-611.

[220] K.M. Kironmai and K. Muniyappa Alteration of telomeric sequences and senescence caused by mutations in RAD50 of Saccharomyces cerevisiae, Genes Cells 2 (1997) 443-455.

[221] S.J. Boulton and S.P. Jackson Components of the Ku-dependent non-homologous end-joining pathway are involved in telomeric length maintenance and telomeric silencing, Embo J 17 (1998) 1819-1828.

[222] X. Bi, S.C. Wei and Y.S. Rong Telomere protection without a telomerase; the role of ATM and Mre11 in Drosophila telomere maintenance, Curr Biol 14 (2004) 1348-1353.

[223] L. Ciapponi, G. Cenci, J. Ducau, C. Flores, D. Johnson-Schlitz, M.M. Gorski, W.R. Engels and M. Gatti The Drosophila Mre11/Rad50 complex is required to prevent both telomeric fusion and chromosome breakage, Curr Biol 14 (2004) 1360-1366.

[224] G. Wu, W.H. Lee and P.L. Chen NBS1 and TRF1 colocalize at promyelocytic leukemia bodies during late S/G2 phases in immortalized telomerase-negative cells. Implication of NBS1 in alternative lengthening of telomeres, J Biol Chem 275 (2000) 30618-30622.

[225] W.Q. Jiang, Z.H. Zhong, J.D. Henson, A.A. Neumann, A.C. Chang and R.R. Reddel Suppression of alternative lengthening of telomeres by Sp100-mediated sequestration of the MRE11/RAD50/NBS1 complex, Mol Cell Biol 25 (2005) 2708-2721.

[226] S.J. Boulton and S.P. Jackson Identification of a Saccharomyces cerevisiae Ku80 homologue: roles in DNA double strand break rejoining and in telomeric maintenance, Nucleic Acids Res 24 (1996) 4639-4648.

[227] S.E. Porter, P.W. Greenwell, K.B. Ritchie and T.D. Petes The DNA-binding protein Hdf1p (a putative Ku homologue) is required for maintaining normal telomere length in Saccharomyces cerevisiae, Nucleic Acids Res 24 (1996) 582-585.

[228] H.L. Liber and W.G. Thilly Mutation assay at the thymidine kinase locus in diploid human lymphoblasts, Mutat Res 94 (1982) 467-485.

[229] F. Xia, X. Wang, Y.H. Wang, N.M. Tsang, D.W. Yandell, K.T. Kelsey and H.L. Liber Altered p53 status correlates with differences in sensitivity to radiation-induced mutation and apoptosis in two closely related human lymphoblast lines, Cancer Res 55 (1995) 12-15.

[230] K.A. Mattern, S.J. Swiggers, A.L. Nigg, B. Lowenberg, A.B. Houtsmuller and J.M. Zijlmans Dynamics of protein binding to telomeres in living cells: implications for telomere structure and function, Mol Cell Biol 24 (2004) 5587-5594.

[231] P. Mari, B.I. Florea, S.P. Persengiev, N.S. Verkaik, H.T. Bruggenwirth, M. Modesti, G. Giglia-Mari, K. Bezstarosti, J.A.A. Demmers, T.M. Luider, A.B. Houtsmuller and D.C. Van Gent Dynamic assembly of end-joining complexes requires interaction between Ku70/80 and XRCC4 Proc Natl Acad Sci U S A 103 (2006) 18597-18602.

[232] J.A. Aten, J. Stap, P.M. Krawczyk, C.H. van Oven, R.A. Hoebe, J. Essers and R. Kanaar Dynamics of DNA double-strand breaks revealed by clustering of damaged chromosome domains, Science 303 (2004) 92-95.

[233] A.D. Dymnikov, D.J. Brenner, G. Johnson and G. Randers-Pehrson Rev. Sci. Instrum. 71 (2000) 1646-1650.

[234] G. Randers-Pehrson, C.R. Geard, G. Johnson, C.D. Elliston and D.J. Brenner The Columbia University single-ion microbeam, Radiat Res 156 (2001) 210-214.

[235] T.W. Ridler and S. Calvard Picture thresholding using an iterative selection method, IEEE Trans Syst Man Cybern 8 (1978) 630-632.

[236] A. Zotter, M.S. Luijsterburg, D.O. Warmerdam, S. Ibrahim, A. Nigg, W.A. van Cappellen, J.H. Hoeijmakers, R. van Driel, W. Vermeulen and A.B. Houtsmuller Recruitment of the nucleotide excision repair endonuclease XPG to sites of UV-induced dna damage depends on functional TFIIH, Mol Cell Biol 26 (2006) 8868-8879.

[237] M.J. Mone, T. Bernas, C. Dinant, F.A. Goedvree, E.M. Manders, M. Volker, A.B. Houtsmuller, J.H. Hoeijmakers, W. Vermeulen and R. van Driel In vivo dynamics of chromatin-associated complex formation in mammalian nucleotide excision repair, Proc Natl Acad Sci U S A 101 (2004) 15933-15937.

[238] M. Muftuoglu, H.K. Wong, S.Z. Imam, D.M. Wilson, 3rd, V.A. Bohr and P.L. Opresko Telomere repeat binding factor 2 interacts with base excision repair proteins and stimulates DNA synthesis by DNA polymerase beta, Cancer Res 66 (2006) 113-124.

[239] P. Munoz, R. Blanco, J.M. Flores and M.A. Blasco XPF nuclease-dependent telomere loss and increased DNA damage in mice overexpressing TRF2 result in premature aging and cancer, Nat Genet 37 (2005) 1063-1071.

[240] C.L. Limoli and J.F. Ward A new method for introducing double-strand breaks into cellular DNA, Radiat Res 134 (1993) 160-169.

[241] E.P. Rogakou, C. Boon, C. Redon and W.M. Bonner Megabase chromatin domains involved in DNA double-strand breaks in vivo, J Cell Biol 146 (1999) 905-916.

[242] C. Lukas, J. Bartek and J. Lukas Imaging of protein movement induced by chromosomal breakage: tiny 'local' lesions pose great 'global' challenges, Chromosoma 114 (2005) 146-154.

[243] J.S. Bedford and W.C. Dewey Radiation Research Society. 1952-2002. Historical and current highlights in radiation biology: has anything important been learned by irradiating cells?, Radiat Res 158 (2002) 251-291.

[244] C. Lukas, J. Falck, J. Bartkova, J. Bartek and J. Lukas Distinct spatiotemporal dynamics of mammalian checkpoint regulators induced by DNA damage, Nat Cell Biol 5 (2003) 255-260.

[245] R.J. Michelson, S. Rosenstein and T. Weinert A telomeric repeat sequence adjacent to a DNA double-stranded break produces an anticheckpoint, Genes Dev 19 (2005) 2546-2559.

[246] N.S. Bae and P. Baumann A RAP1/TRF2 complex inhibits nonhomologous end-joining at human telomeric DNA ends, Mol Cell 26 (2007) 323-334.

[247] E.H.a.D. Lane Antibodies: A Laboratory Manual, Cold Spring Harbor Laboratory, Cold Spring Harbor, 1988.

[248] L.G. DeFazio, R.M. Stansel, J.D. Griffith and G. Chu Synapsis of DNA ends by DNA-dependent protein kinase, Embo J 21 (2002) 3192-3200.

[249] S. Zhang, P. Hemmerich and F. Grosse Nucleolar localization of the human telomeric repeat binding factor 2 (TRF2), J Cell Sci 117 (2004) 3935-3945.

[250] M. Martin, A. Genesca, L. Latre, I. Jaco, G.E. Taccioli, J. Egozcue, M.A. Blasco, G. Iliakis and L. Tusell Postreplicative joining of DNA double-strand breaks causes genomic instability in DNA-PKcs-deficient mouse embryonic fibroblasts, Cancer Res 65 (2005) 10223-10232.

[251] J.B. Storer, T.J. Mitchell and R.J. Fry Extrapolation of the relative risk of radiogenic neoplasms across mouse strains and to man, Radiat Res 114 (1988) 331-353.

[252] R.L. Ullrich, N.D. Bowles, L.C. Satterfield and C.M. Davis Strain-dependent susceptibility to radiation-induced mammary cancer is a result of differences in epithelial cell sensitivity to transformation, Radiat Res 146 (1996) 353-355.

[253] B. Ponnaiya, M.N. Cornforth and R.L. Ullrich Radiation-induced chromosomal instability in BALB/c and C57BL/6 mice: the difference is as clear as black and white, Radiat Res 147 (1997) 121-125.

[254] R. Okayasu, K. Suetomi, Y. Yu, A. Silver, J.S. Bedford, R. Cox and R.L. Ullrich A deficiency in DNA repair and DNA-PKcs expression in the radiosensitive BALB/c mouse, Cancer Res 60 (2000) 4342-4345.

[255] R.S. Maser, K.K. Wong, E. Sahin, H. Xia, M. Naylor, H.M. Hedberg, S.E. Artandi and R.A. DePinho DNA-dependent protein kinase catalytic subunit is not required for dysfunctional telomere fusion and checkpoint response in the telomerase-deficient mouse, Mol Cell Biol 27 (2007) 2253-2265.

[256] D. Hockemeyer, J.P. Daniels, H. Takai and T. de Lange Recent expansion of the telomeric complex in rodents: Two distinct POT1 proteins protect mouse telomeres, Cell 126 (2006) 63-77.

[257] L. Wu, A.S. Multani, H. He, W. Cosme-Blanco, Y. Deng, J.M. Deng, O. Bachilo, S. Pathak, H. Tahara, S.M. Bailey, Y. Deng, R.R. Behringer and S. Chang Pot1

deficiency initiates DNA damage checkpoint activation and aberrant homologous recombination at telomeres, Cell 126 (2006) 49-62.

[258] J.M. Zijlmans, U.M. Martens, S.S. Poon, A.K. Raap, H.J. Tanke, R.K. Ward and P.M. Lansdorp Telomeres in the mouse have large inter-chromosomal variations in the number of T2AG3 repeats, Proc Natl Acad Sci U S A 94 (1997) 7423-7428.

[259] S.J. Veuger, N.J. Curtin, C.J. Richardson, G.C. Smith and B.W. Durkacz Radiosensitization and DNA repair inhibition by the combined use of novel inhibitors of DNA-dependent protein kinase and poly(ADP-ribose) polymerase-1, Cancer Res 63 (2003) 6008-6015.

[260] S. Burma, B.P. Chen, M. Murphy, A. Kurimasa and D.J. Chen ATM phosphorylates histone H2AX in response to DNA double-strand breaks, J Biol Chem 276 (2001) 42462-42467.

[261] Q. Zhang, E.S. Williams, K.F. Askin, Y. Peng, J.S. Bedford, H.L. Liber and S.M. Bailey Suppression of DNA-PK by RNAi has different quantitative effects on telomere dysfunction and mutagenesis in human lymphoblasts treated with gamma rays or HZE particles, Radiat Res 164 (2005) 497-504.

[262] S. Zhao, W. Renthal and E.Y. Lee Functional analysis of FHA and BRCT domains of NBS1 in chromatin association and DNA damage responses, Nucleic Acids Res 30 (2002) 4815-4822.

[263] N. Assenmacher and K.P. Hopfner MRE11/RAD50/NBS1: complex activities, Chromosoma 113 (2004) 157-166.

[264] C.J. Bakkenist and M.B. Kastan Initiating cellular stress responses, Cell 118 (2004) 9-17.

[265] T. Uziel, Y. Lerenthal, L. Moyal, Y. Andegeko, L. Mittelman and Y. Shiloh Requirement of the MRN complex for ATM activation by DNA damage, Embo J 22 (2003) 5612-5621.

[266] Y. Zhang, J. Zhou and C.U. Lim The role of NBS1 in DNA double strand break repair, telomere stability, and cell cycle checkpoint control, Cell Res 16 (2006) 45-54.

[267] Y. Zhang, C.U. Lim, E.S. Williams, J. Zhou, Q. Zhang, M.H. Fox, S.M. Bailey and H.L. Liber NBS1 knockdown by small interfering RNA increases ionizing radiation mutagenesis and telomere association in human cells, Cancer Res 65 (2005) 5544-5553.

[268] T.K. Pandita, S. Pathak and C.R. Geard Chromosome end associations, telomeres and telomerase activity in ataxia telangiectasia cells, Cytogenet Cell Genet 71 (1995) 86-93.

[269] T.L. Kojis, R.A. Gatti and R.S. Sparkes The cytogenetics of ataxia telangiectasia, Cancer Genet Cytogenet 56 (1991) 143-156.

[270] B.R. Williams, O.K. Mirzoeva, W.F. Morgan, J. Lin, W. Dunnick and J.H. Petrini A murine model of Nijmegen breakage syndrome, Curr Biol 12 (2002) 648-653.

[271] Y. Bai and J.P. Murnane Telomere instability in a human tumor cell line expressing NBS1 with mutations at sites phosphorylated by ATM, Mol Cancer Res 1 (2003) 1058-1069.

[272] P. Slijepcevic The role of DNA damage response proteins at telomeres--an "integrative" model, DNA Repair (Amst) 5 (2006) 1299-1306.

[273] I. Dionne and R.J. Wellinger Processing of telomeric DNA ends requires the passage of a replication fork, Nucleic Acids Res 26 (1998) 5365-5371.

[274] K.M. Miller, O. Rog and J.P. Cooper Semi-conservative DNA replication through telomeres requires Taz1, Nature 440 (2006) 824-828.

[275] R. Ohki and F. Ishikawa Telomere-bound TRF1 and TRF2 stall the replication fork at telomeric repeats, Nucleic Acids Res 32 (2004) 1627-1637.

[276] M.D. Evans and M.S. Cooke Factors contributing to the outcome of oxidative damage to nucleic acids, Bioessays 26 (2004) 533-542.

[277] V. Lundblad and J.W. Szostak A mutant with a defect in telomere elongation leads to senescence in yeast, Cell 57 (1989) 633-643.

[278] R.K. Pandita, G.G. Sharma, A. Laszlo, K.M. Hopkins, S. Davey, M. Chakhparonian, A. Gupta, R.J. Wellinger, J. Zhang, S.N. Powell, J.L. Roti Roti, H.B. Lieberman and T.K. Pandita Mammalian Rad9 plays a role in telomere stability, S- and G2-phase-specific cell survival, and homologous recombinational repair, Mol Cell Biol 26 (2006) 1850-1864.

[279] N. Tuteja, R. Tuteja, A. Ochem, P. Taneja, N.W. Huang, A. Simoncsits, S. Susic, K. Rahman, L. Marusic, J. Chen and et al. Human DNA helicase II: a novel DNA unwinding enzyme identified as the Ku autoantigen, Embo J 13 (1994) 4991-5001.

[280] H.L. Hsu, D. Gilley, E.H. Blackburn and D.J. Chen Ku is associated with the telomere in mammals, Proc Natl Acad Sci U S A 96 (1999) 12454-12458.

[281] E. Van Dyck, A.Z. Stasiak, A. Stasiak and S.C. West Visualization of recombination intermediates produced by RAD52-mediated single-strand annealing, EMBO Rep 2 (2001) 905-909.

[282] J. Drouet, P. Frit, C. Delteil, J.P. de Villartay, B. Salles and P. Calsou Interplay between Ku, Artemis, and the DNA-dependent protein kinase catalytic subunit at DNA ends, J Biol Chem 281 (2006) 27784-27793.

[283] C. Lenain, S. Bauwens, S. Amiard, M. Brunori, M.J. Giraud-Panis and E. Gilson The Apollo 5' exonuclease functions together with TRF2 to protect telomeres from DNA repair, Curr Biol 16 (2006) 1303-1310.

[284] M. van Overbeek and T. de Lange Apollo, an Artemis-related nuclease, interacts with TRF2 and protects human telomeres in S phase, Curr Biol 16 (2006) 1295-1302.

[285] D. Ristic, M. Modesti, R. Kanaar and C. Wyman Rad52 and Ku bind to different DNA structures produced early in double-strand break repair, Nucleic Acids Res 31 (2003) 5229-5237.

List of Abbreviations

Abbreviation	Meaning
ALT	alternative lengthening of telomere
Am	Americium
APB	ALT-associated PML bodies
ATM	ataxia telangiectasia mutated protein
ATR	ATM rad3-related
BER	base excision repair
Bp	basepair (unit of measure)
BRCA1	breast cancer protein 1
BRCT	breast cancer C-terminal domain
BrdU	bromodeoxyuridine
CCD	charge-coupled device
CO-FISH	chromosome orientation-fluorescence in situ hybridization
DAPI	4',6'-Diamidino-2-Phenylindole
DDB2	DNA damage binding protein 2
D-loop	displacement loop
DNA-PK	DNA-dependent protein kinase
DNA-PKcs	The catalytic subunit of the DNA-dependent protein kinase
DSB	double strand breaks
FBS	fetal bovine serum
FEN1	flap structure-specific nuclease protein 1
FHA	fork head associated domain
FISH	fluorescence in situ hybridization
FITC	fluorescein isothiocyanate
GFP	green fluorescent protein
HDF	human dermal fibroblasts
HR	homologous recombination
IR	ionizing radiation
IRF3	interferon regulatory factor 3
IRIF	ionizing radiation induced foci
kBq	kiloBecquerel (unit of measure)
keV	kilo electron volt (unit of measure)
MDC1	mediator of damage checkpoint protein 1
MDM2	mouse double minute protein 2
MF	mammary fibroblast
MRN	MRE11/RAD50/NBS1 complex
NBN	Murine homolog to NBS1
NBS	Nijmegen breakage syndrome
NBS1	Nijmegen Breakage syndrome protein 1
NER	nucleotide excision repair
NHEJ	non-homologous end-joining
PI-3	phosphotidylinositol 3
PIKK	PI-3-kinase like kinase

PML	promyelocytic leukemia
Abbreviation	**Meaning**
PNA	peptide nucleic acid
Polβ	DNA polymerase β
POT1	Protection of telomere 1
Rap1	repressor activator protein 1
RDS	radiation-resistant DNA synthesis
RNAi	RNA interference
RPA	replication protein A
RT	room temperature
SCID	severe combined immunodeficiency
Ser	Serine
siRNA	short interfering RNA
SMC	structural maintenance of chromosome
SQ	serine-glutamine motif
SSB	single-strand break
TA	telomere associations
TEBP	telomere end-binding protein
TERC	telomerase RNA component
TERT	telomerase reverse transcriptase
Thr	Threonine
TIN2	TRF1 interacting nuclear protein 2
T-loop	Telomere Loops
TPP1	compiled from former protein names TINT1, PTOP, PIP1
TQ	threonine-glutamine motif
TRF1	Telomere Repeat binding factor 1
TRF2	Telomere repeat binding factor 2
UV	ultraviolet
XLF	XRCC4-like factor
XPC	xeroderma pigmentosum C
XRCC4	X-ray complementing Chinese hamster 4
γ-H2AX	phosphorylated from of variant histone H2AX